An Open Access Journal Available Online

# *Covenant Journal of Engineering Technology (CJET)*

**Vol. 1 No. 2, September 2018 (Special Edition)**

**Publication of the College of Engineering,**
**Covenant University, Canaanland.**

**Editor-in-Chief**: Dr. Olugbenga Omotosho
editorcjet@covenantuniversity.edu.ng

**Managing Editor**: Edwin O. Agbaike
me@covenantuniversity.edu.ng

*Website: http//Journal.covenantuniversity.edu.ng/cjet/*

**ISSN:** Print xxxx-xxxx
Online xxxx-xxxx

Published by Covenant University Journals,
Covenant University, Canaanland, Km 10, Idiroko Road,
P.M.B. 1023, Ota, Ogun State, Nigeria

Printed by Covenant University Press

**Articles**

**Covenant Journal of Engineering Technology (CJET) Vol. 1, No. 2, Sept. 2018**

An Open Access Journal Available Online

# Finite Element Analysis of Displacement and Von-Mises Stress in Cylindrical Liquified Petroleum Gas Pressure Tank

**C.U. Ugochukwu[1*], O.O. Oluwole[1], K.M. Odunfa[1]**

[1]Department of Mechanical Engineering,
University of Ibadan, Ibadan Nigeria.

***Abstract*:** Increase in demand of liquefied petroleum gas (LPG) has led to development of LPG facilities throughout the world. The limitation of ASME standard in the design of pressure vessels and reoccurring cases of gas plant, gas cylinder explosions led to this research. In this research, finite element method was used to investigate the displacements, deflections and Von-Mises stresses in a cylindrical liquefied petroleum gas pressure tank with respect to plate thickness at different operating pressures and ambient conditions. A cylindrical pressure tank made of ASTM A516 Grade 70 with thickness; 2mm, 5mm, 10mm, 20mm and 30mm was selected for the analysis with plain strain condition assumptions. ANSYS was used to generate the mesh model of the liquefied petroleum gas pressure tank and conduct the finite element analysis. The displacement, deflection and Von-Mises stress showed an inverse relationship with the tank section shell thickness while varying the LPG pressure; 0.5MPa at $20^0$C, 0.91MPa at $40^0$C and 1.55MPa at $60^0$C respectively. It was also observed that the factor of safety showed a linear relationship with increasing shell thickness. For each operating pressure, a minimum shell thickness was deduced. This minimum thickness was at a Von-Mises stress which falls below the materials yield stress and allowable stress. Therefore, the vessel will not fail once operated at or above the minimum pressure tank shell thickness. The effect of weldment along the seams of vessel was not carried out in this research work. Sharp edges are stress raisers, also there is possibility of stress been developed at the inlet and exhaust valves of the pressure tank. The effect of stress at this points on the vessel were not considered for this research work.

***Key-words***— LPG, ANSYS, Finite Element Method, Von-Mises Stress.

## 1. Introduction

Liquefied petroleum gas (LPG) is a derivative of two large energy industries: natural gas processing and crude oil refining. Worldwide, natural gas processing is a source of approximately 60%, while crude oil refining contributes 40% of LPG produced (Foramfera, 2016). The main components of liquefied petroleum gas are propane and butane. LPG is colourless and odourless, but commercially odorized with ethyl mercaptan so that it can be detected when it has reached one-fifth the concentration needed for an explosion [2].

The Nigeria LNG Limited has reserved 250,000 metric tonnes per annum for the domestic market with a projection of 3 million metric tonnes per annum within five years [3]. Due to the growing demand for LPG, companies are rapidly developing facilities across the LPG value chain.

Liquefied Petroleum Gas is stored in pressure vessels. These containers are either cylindrical or spherical. While cylindrical vessel has ease of manufacture, spherical vessel has distinct advantage of less floor area coverage and high-pressure capability [4]. Despite these advantages of spherical vessels, the complexity of design limits their effective utilization. As the size of spherical vessels increases, high pressure is developed towards the base of the sphere. Hence, LPG is often stored, transported and distributed in cylindrical pressure vessels. The head of the vessel is of various kind of configuration which includes; flanged, torisherical, ellipsoidal and hemispherical [5]. When a pressure vessel is under load, stress is developed on the walls of the container. A number of stress theories, also called "yield criteria," are available for describing the effects of combined stresses [6]. A material will yield or fails when it Von-mises stress is at a critical value which is known as the yield strength. The yield criterion is compared with experimental values to know if failure will occur.

The American Society of Mechanical Engineers (ASME) provides codes and simple formulas that regulate the design and construction of pressure vessels [7]. ASME standard is a generalization of simple formulas and has limitation in terms of specifying the actual fluid content on the pressure vessel. It does not put into consideration several actions or combination of actions such as local loads, seismic load, wind loads and external pressure in its design formula [8]. Therefore, what is needed is design by analysis which requires creativity and action of the designer.

There has been reoccurring cases of gas plants, cylinder explosions across Nigeria, particularly in the LPG domain either during transit, storage or during domestic use [9]. Therefore, there is need to give careful attention to LPG pressure tanks in line with design.

The finite element method is a useful numerical method utilized in solving many engineering problems. Finite element works by breaking down or discretizing a real object/system into a smaller number of finite, well defined sub-structures (element) which can be represented by simple equations [10]. Each of these elements has nodal points, subjected to finite degrees of freedom. The

mathematical model developed is formed by assembling all individual elements. The behavior of each element is then used to analyze the performance of the whole system. In applying FEM to any engineering problem, one needs to understand the following: the physical behavior of the system (strength, heat transfer etc.), the performance (safety, weakness), the accuracy of the FEM in comparison to the analytical method [11]. ANSYS is finite element software which allows for visualization of the effect of loads and other boundary conditions on the model been analyzed for easy understanding which does not involve

Writing or interpretation of codes. The results of the analysis can easily be visualized and utilized by local designers/engineers who are not experts in finite element analysis. An ANSYS result, when validated is in harmony with order finite element computational platforms [12, 13].

## 2. Methodology

ANSYS workbench version 14 finite element computational platform was used in this work.

### 2.1 Assumptions

- Plain strain condition
- The material selected is homogeneous and isotropic.
- Uniform internal pressure.

The work involved two stages

a. validation of the computational platform to be used
b. Use of 3D finite element model to perform Von-mises stress analysis and displacement in liquefied petroleum gas pressure tanThe work of Oluwole and Emagbetere (2013) was used as bases for validation since similar finite element software (Matlab) was used.

### 2.2 Finite Element Modeling

Finite element analysis was utilized in this research. The theory of plate elasticity and plate bending was used. When the thickness is small in comparison with other dimensions, the vessels is referred to as membranes and the associated stresses resulting from the contained pressure are called membrane stresses. These membrane stresses are average tension or compression stresses. They are assumed to be uniform across the vessel wall and act tangentially to its surface. The membrane or wall is assumed to offer no resistance to bending. When the wall offers resistance to bending, bending stresses occur in addition to membrane stresses [4].

Membrane element.

$$P = \frac{F}{A} \quad (1)$$

therefore, $F = PA$

where, P is the pressure acting on the inner wall, A is the area, F is the traction force acting on the plate surface.

In order to develop the stiffness matrix and calculate displacements in x and y direction, theory of Elasticity is used [14, 15]. Equilibrium equation in terms of stress is given as;

$$\frac{\partial \sigma_x}{\partial x} + \frac{\partial \tau_{xy}}{\partial y} + f_x = 0 \quad (2)$$

$$\frac{\partial \tau xy}{\partial x} + \frac{\partial \sigma_y}{\partial y} + f_y = 0 \quad (3)$$

where $f_x$ and $f_y$ are body forces $\sigma_x$ and $\sigma_y$ are stress components. The constitutive equation (relating stress to strain) is given as

$$\{\sigma\} = [D]\{\epsilon\} \quad (4)$$

where $\{\sigma\} = \{\sigma_x\ \sigma_y\ \tau_{xy}\}^T$ denotes the stress and $\{\epsilon\} = \{\epsilon_x\ \epsilon_y\ \gamma_{xy}\}^T$ is the strain

If equation (2) and (3) is multiplied with weight function, we have

$$\int_\Omega \begin{Bmatrix} \omega_1\left(\frac{\partial \sigma_x}{\partial x} + \frac{\partial \tau_{xy}}{\partial y}\right) \\ \omega_2\left(\frac{\partial \tau_{xy}}{\partial x} + \frac{\partial \sigma_y}{\partial y}\right) \end{Bmatrix} d\Omega + \int_\Omega \begin{Bmatrix} \omega_1 f_x \\ \omega_2 f_y \end{Bmatrix} d\Omega - \int_{\Gamma e} \begin{Bmatrix} \omega_1 \Phi_x \\ \omega_2 \Phi_y \end{Bmatrix} d\Gamma = 0 \quad (5)$$

The term in the second integral is the body force which is assumed to be zero. While the term in third integral is the traction force which in this case is the force F due to the applied pressure, therefore,

$$F = PA = \int_{\Gamma e} \begin{Bmatrix} \omega_1 \Phi_x \\ \omega_2 \Phi_y \end{Bmatrix} d\Gamma \quad (6)$$

Simplifying equation (5) yields

$$\int_\Omega \begin{bmatrix} \frac{\partial \omega_1}{\partial x} & 0 & \frac{\partial \omega_1}{\partial y} \\ 0 & \frac{\partial \omega_2}{\partial y} & \frac{\partial \omega_2}{\partial x} \end{bmatrix} \begin{Bmatrix} \sigma_x \\ \sigma_y \\ \tau_{xy} \end{Bmatrix} d\Omega = PA \quad (7)$$

Combining equation (4) into (7) gives,

$$\int_\Omega \begin{bmatrix} \frac{\partial \omega_1}{\partial x} & 0 & \frac{\partial \omega_1}{\partial y} \\ 0 & \frac{\partial \omega_2}{\partial y} & \frac{\partial \omega_2}{\partial x} \end{bmatrix} [D] \begin{Bmatrix} \epsilon_x \\ \epsilon_y \\ \tau_{xy} \end{Bmatrix} d\Omega = PA \quad (8)$$

on further simplification the stiffness matrix is given as;

$$[K^e] = \int_{\Omega e} [B]^T [D][B] d\Omega = [B]^T [D][B] A \quad (9)$$

where [Ke] = [Km] is the element membrane stiffness matrix, [D] is the elasticity matrix and [B] is the strain matrix.

*Bending element*. For the bending element, we use a three noded plate bending element. Theory of classical plate bending is used [14,16].The displacement function w is assumed to be;

$$\omega(x,y) = a_1 + a_2 x + a_3 y + a_4 x^2 + a_5 xy + a_6 y^2 + a_7 x^3 + a_8 (x^2 y + xy^2) + a_9 y^3 = [X]\{a\} \quad (10)$$

where

$$[X] = [1\ x\ y\ x^2\ xy\ y^2\ x^3\ (x^2y + xy^2)\ y^3] \quad (11)$$

$$\{a\} = \{a_1\ a_2\ a_3\ a_4\ a_5\ a_6\ a_7\ a_8\ a_9\}^T \quad (12)$$

Differentiating [X] with respect to x and y gives a 9 x 9 matrix for the three nodes.

Further differentiation per node yields

$$[L] = \begin{bmatrix} 0 & 0 & 0 & 2 & 0 & 0 & 6x & 2y & 0 \\ 0 & 0 & 0 & 0 & 0 & 2 & 0 & 2x & 6y \\ 0 & 0 & 0 & 0 & 2 & 0 & 0 & 4(x+y) & 0 \end{bmatrix} \quad (13)$$

The bending element stiffness matrix $[K_b]$ is given as;

$$[K_b] = [\ddot{X}]^{-T} \int_{\Omega e} [L]^T [D][L]\, d\Omega [\ddot{X}]^{-1} \quad (14)$$

Total element stiffness matrix**.** In order to get the total element (system) stiffness matrix [K], we combine stiffness matrix of the membrane element $[K_m]$ and bending element [Kb] ;

$$[K] = [K_m] + [K_b] \quad (15)$$

The combination takes the following form

$$\begin{bmatrix} K_m & 0 \\ 0 & K_b \end{bmatrix}$$

The finite element equation is expressed as

$$[K]\{U\} = \{F\} \quad (16)$$

where {F} is the applied force, {U} is the displacement.

### 2.3 Von-Mises Stress

For the Von-mises stress to be calculated analytical, there are three principal stresses which are;

σ1 = Principal stress = Longitudinal (axial)stress

σ2 = Principal stress = Circumferential (hoop) stress

σ3 = Radial stress = 0. No stress in z-direction that will lead to displacement or elongation.

Von-mises stress

$$= \sqrt{\sigma_1^2 - \sigma_1\sigma_2 + \sigma_2^2} \quad (17)$$

$$\sigma 2 = \frac{Pr}{2t} \quad (18)$$

$$\sigma 1 = \frac{Pr}{t} \quad (19)$$

p = internal pressure

r = radius of cylinder

t = plate thickness

### 2.4 Factor of Safety (FOS)

The material already has a factor of safety of 3.5, therefore, for each simulation carried out per tank plate thickness, the factor of safety is calculated to determined safety of the vessel at that operating pressure. For this research work, the factor of safety is calculated as follows:

$$FOS = \frac{\text{Material minimum tensile strength}}{\text{Material Allowable stress}} \quad (20)$$

Material Allowable stress = Finite element Analysis Von-Mises Stress (equivalent stress developed during simulation with ANSYS static structural)

## 3. Validation of the Finite Element Computational Platform

Finite element analysis of displacement and Von-mises stress in pressure vessel has already been done with a case study in petroleum road tankers. The tank content is diesel (AGO), with a loading pressure of 14480 N/m2 The analysis was done using Matlab programming. This work did not consider the effect of increasing pressure at elevated temperature on the tank plate thickness. Also the contour plotting are line plots and requires interpretation of written codes to visualize the effects of loads and other boundary conditions. To validate this work, ANSYS static structural was used with the same material properties and simulation parameters as used in Matlab.

### 3.1 Parameters Used for Validation

Length of tanker = 485 cm

Vertical axis of tanker = 180 cm

Horizontal axis of tanker = 244 cm

Thickness of tanker = 0.2 cm

Poison ratio = 0.3

Loading pressure = 14480 N/m2

Material of construction = A516M Grade 70

Specified minimum yield stress = 25 × 107 N/m2

Maximum allowable stress = 13.8 × 107 N/m2

Elastic modulus = 200 × 109 N/m2

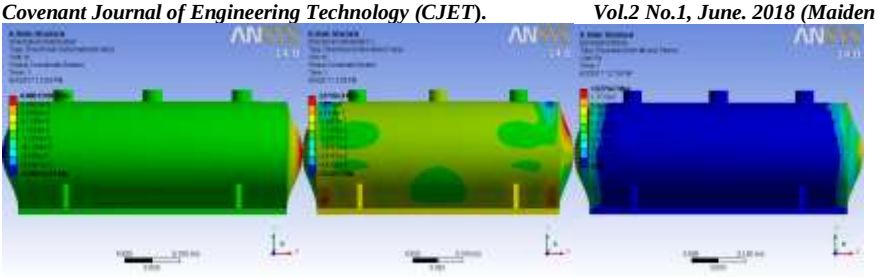

(a) (b) (c)

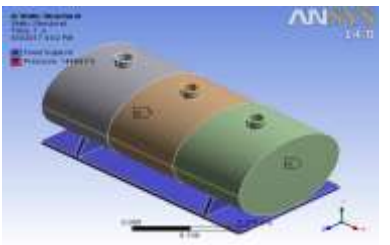

(d)

**Fig. 1** ANSYS Static Structural Validation for Diesel Tanker (a) Displacement in x-axis (b) Displacement in y-axis (c) Von-Mises Stress. (d) Tank model before simulation

Figure 1 above shows that the Von-Mises stress is tensile in nature, causing the elliptical section of the tank to bulge out. Areas in the contour plotting shown in red are areas where the Von-mises stress is mostly felt, hence these areas will experience more displacements. The result in comparism with Matlab is shown in the table below.

**Table 1** Camparism of Matlab generated result with ANSYS Static Structural for validation of a diesel tanker.

| FEA Application | Displacement in x-axis (m) | Displacement in y-axis (m) | FEAVon-Mises Stress $N/m^2$ | ASME Von-Mises Stress $N/m^2$ |
|---|---|---|---|---|
| Matlab Program | $5.2201x10^{-9}$ | $1.4789x10^{-7}$ | $5.4318x10^{6}$ | $7.6494x10^{6}$ |
| ANSYS Static Structural | $9.6507x10^{-5}$ | $2.0716x10^{-6}$ | $6.425x10^{6}$ | $7.6494x10^{6}$ |

As shown in the table above, the result of the Matlab program is much identical to that of ANSYS Static Structural. In fact, the FEA Von-Mises Stress of ANSYS Static Structural is in close range with the ASME Von-Mises stress that is the analytical Von-mises. Having validated the result, the research work proceeded with the application of ANSYS Static Structural for the finite element analysis of liquefied petroleum gas pressure tank model.

3.2 Development of the LPG Cylindrical Pressure Tank Model for Simulation

In order to reduce computational complexities, the LPG tank model was made simple. The cylindrical pressure tank model (Fig. 2) was developed into different thicknesses: 2mm, 5mm, 10mm, 20mm and 30mm using Solidworks. Each of this model was imported into ANSYS static structural analysis system independently and the simulation was carried out in this sequence; Analysis system (static structural), Engineering Data, Geometry, Model, Setup and Solution**.**

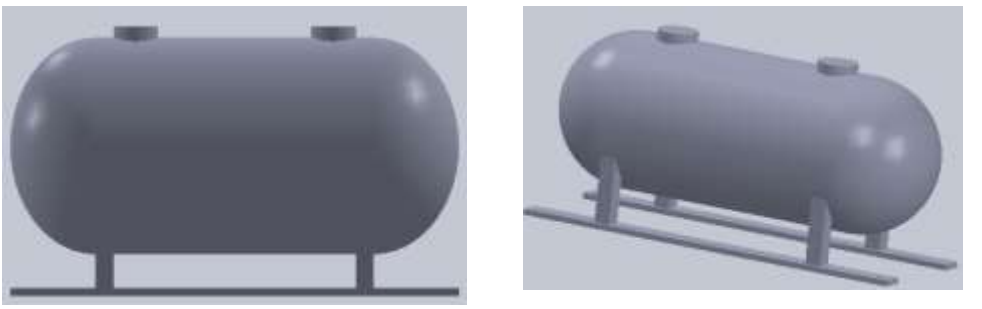

(a) (b)

**Fig. 2** Views of the Model of the LPG Pressure Tank

### 3.3 Statics Analysis for the LPG Tank

This involves application of finite element analysis include meshing, boundary conditions and the material properties specification etc.

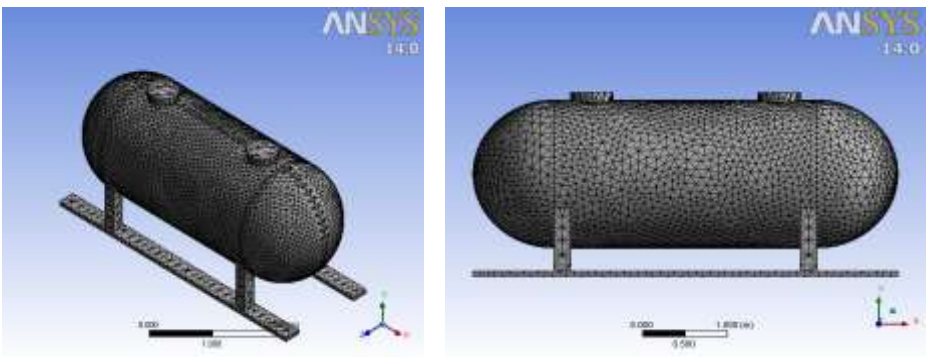


(a) (b)

**Fig. 3** meshing at (a) 2mm plate thickness and (b) 10mm plate thickness

Meshing: Meshing is critical to any modeling and simulation work. For the LPG tank, the mesh size chosen was fine mesh and the smoothing was medium. This was done to influence the accuracy and the computing speed. As plate thickness increases, number of nodes and elements increases. Figure 3 is a view of the different kinds of mesh utilized in this work.

Boundary condition: In this part of the simulation, the boundary conditions are specified. The internal pressure applied are 0.5MPa, 0.91MPa and 1.55MPa each at different plate thickness and ambient temperature: $20^0$C, $40^0$C and $60^0$C

respectively. The base of the vessel is fixed to a support (dirichlet boundary condition).There are two in-plane displacement u and v in x and y directions and one deflection w in z-direction.

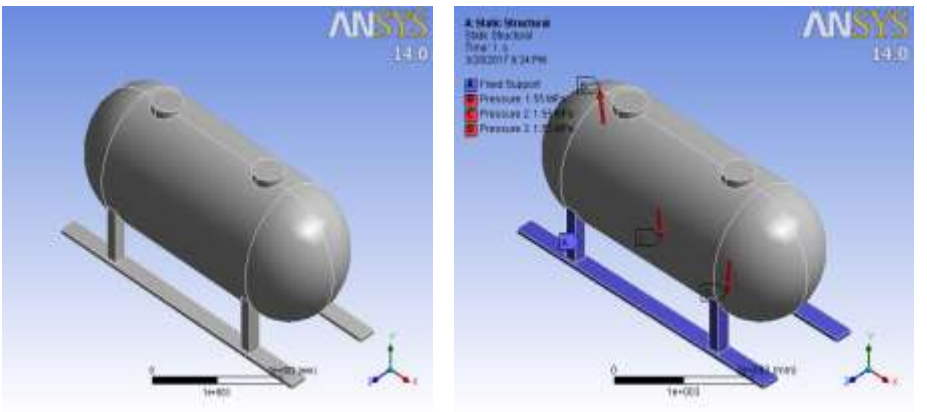


(a) (b)

**Fig. 4** (a) Tank model imported to ANSYS Static Structural (b) Application of boundary condition

### 3.4 Tank Parameters for Analysis

Length of tank = 495cm
Internal diameter = 190cm
Diameter of head = 95cm
Plate thickness = 2mm, 5mm, 10mm, 20mm and 30mm. (These range of thickness are in line with ASME SECTION VIII DIVISION 1 PART ULT).
Tank material: ASTM A516 Grade 70
Material allowable stress = 138MN/$m^2$
Material minimum yield stress = 260MN/$m^2$
Material minimum tensile strength= 485MPa
Modulus of elasticity = 200GN/$m^2$
Material factor of safety = 3.5

## 4. Simulation of the Liquefied Petroleum Gas Pressure Tank

The simulation was carried out in stages as highlighted below:

### 4.1 Simulation at $60^0$C, 1.55MPa (Case 1)

The tank parameters for analysis are as stated above. Each cylindrical LPG pressure tank model of thickness: 2mm, 5mm, 10mm and 30mm was subjected to same internal pressure and temperature.

LPG Temperature = $60^0$C
Internal pressure = 1.55MPa

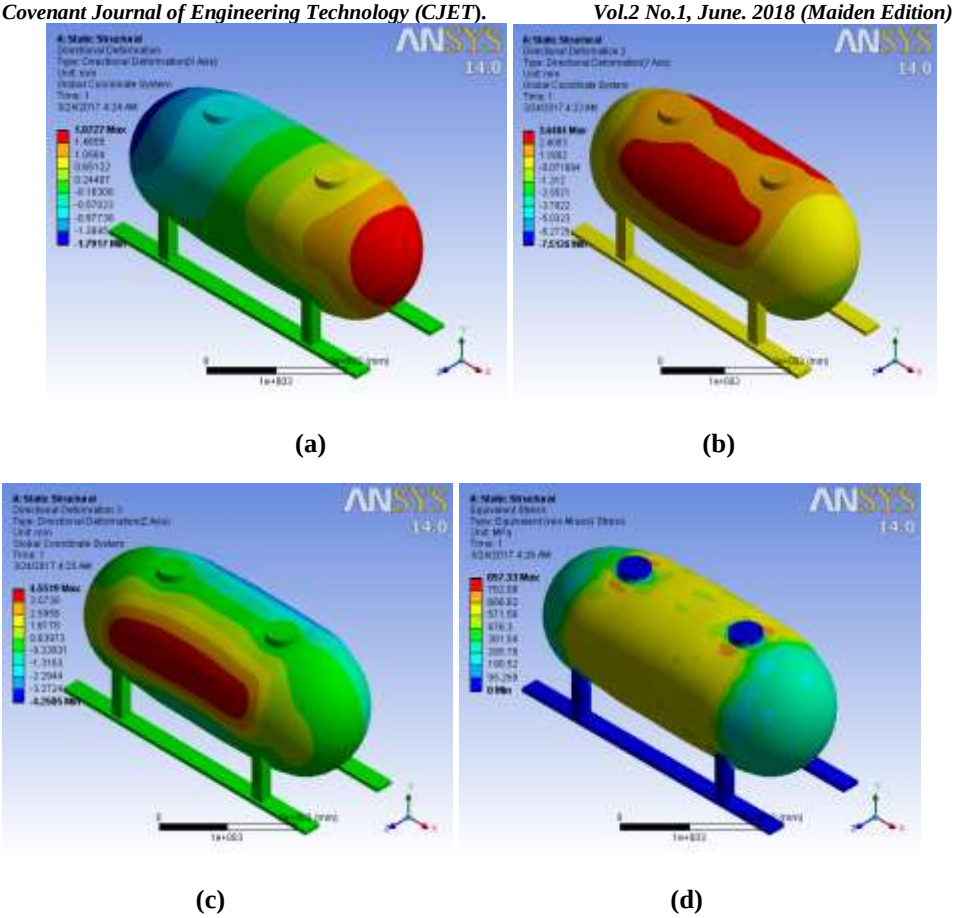


**Fig. 5** Application of 1.55MPa at $60^0$C to 2mm tank model thickness (a) displacement in x-axis (b) displacement in y-axis (c) deflection (d) Von-Mises stress

### 4.2 Results and Discussion as Presented in Case 1

Results. Figure 5 (a) and (b) shows the displacement in x and y direction. The contour plotting in red are areas where the displacement is more pronounced. This is similar to the deflection as shown in Fig. 5 (c). ANSYS Von-mises stress causes the head of the tank to enlarge/bulge out and the deformation of the cylindrical section as shown in Figure. 5 (d). Table 2 shows the displacement and deflection at different plate thicknesses. As plate thickness increases, displacement in x and y direction and deflection in z decreases. This is pictorially illustrated in Figure. 6, Figure 7 and Figure. 8. Also, the Von-mises stress converges to zero as the plate thickness increases as seen in Figure. 9. Table 3 shows the variation in Factor of safety, at different ASME and FEA stresses and plate thicknesses.

**Table 2**. Displacements and deflection at different plate thickness for cylindrical LPG pressure tank at 1.55MPa, $60^0$C

| PLATE THICKNESS (mm) | DISPLACEMENT IN X-AXIS (mm) | DISPLACEMENT IN Y-AXIS (mm) | DEFLECTION (Z-AXIS) (mm) |
|---|---|---|---|
| 2 | 1.87270 | 3.64840 | 4.55190 |
| 5 | 0.79979 | 1.27340 | 2.36770 |
| 10 | 0.39974 | 0.61834 | 1.12540 |
| 20 | 0.19751 | 0.34636 | 0.49299 |
| 30 | 0.12950 | 0.24184 | 0.28865 |

**Table 3** ASME stress, FEA stress and Factor of Safety at different plate thickness for LPG at 1.55MPa, $60^0$C

| PLATE THICKNESS (mm) | FEA Von-Mises/Stress developed (MPa) | ASME Von-Mises stress (MPa) | (FEA) Factor of Safety |
|---|---|---|---|
| 2 | 857.33 | 637.61 | 0.57 |
| 5 | 401.02 | 254.00 | 1.21 |
| 10 | 208.71 | 127.00 | 2.32 |
| 20 | 102.91 | 63.77 | 4.71 |
| 30 | 64.34 | 42.50 | 7.54 |

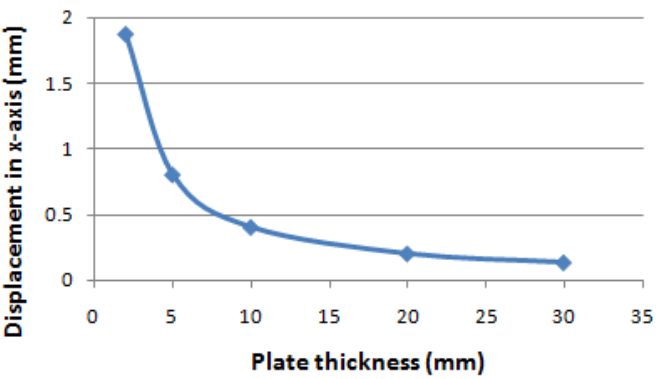


**Fig. 6** In plane displacement in x-axis versus thickness at 1.55MPa, $60^0$C

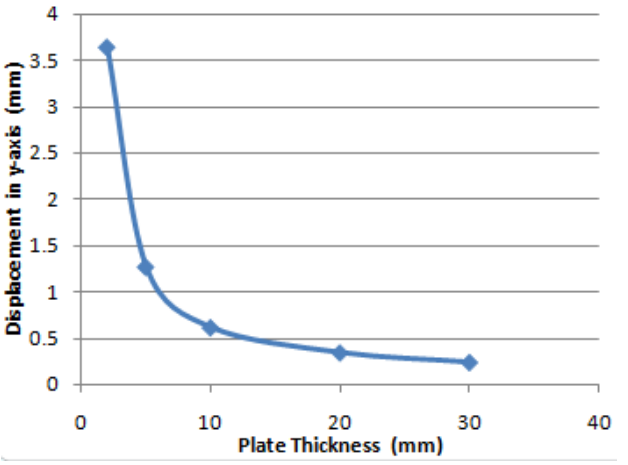


**Fig. 7** In plane displacement in y-axis versus thickness at 1.55MPa, $60^0$C

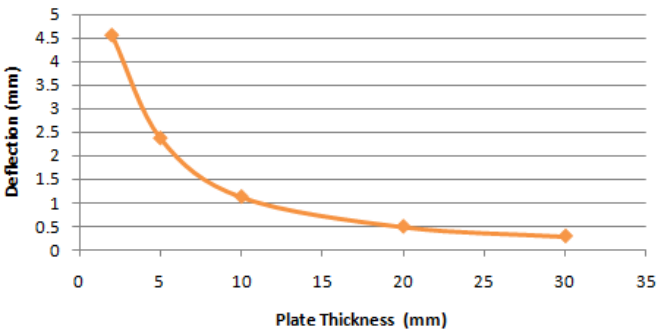


**Fig. 8** Deflection versus thickness at 1.55MPa, $60^0$C

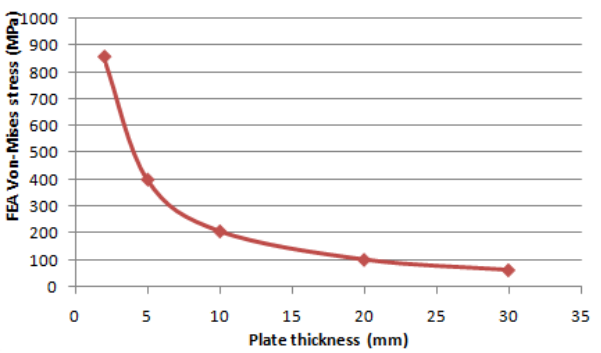


**Fig. 9** FEA Von-Mises Stress (stress developed)Versus thickness at 1.55MPa, $60^0$C

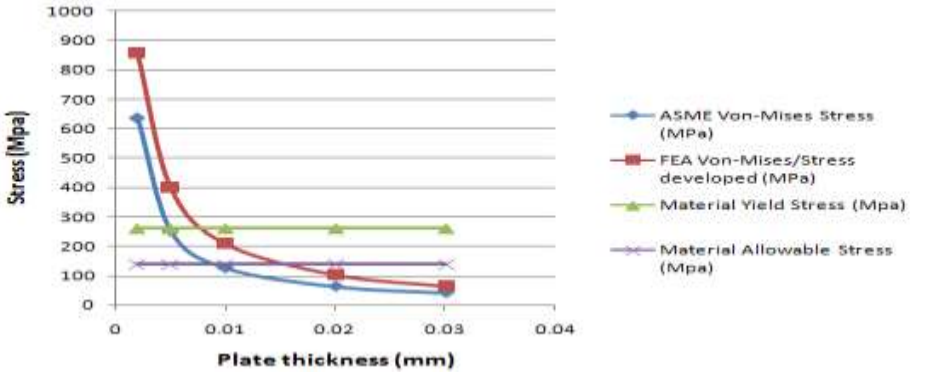


**Fig. 10** Comparing FEA Von-Mises (stress developed) at 1.55MPa, with ASME Von-Mises stress, Material yield stress and Allowable stress.

Discussion of Results as Presented in Case 1. Increasing the LPG pressure tank plate thickness decreases the displacement, deflection and Von-mises stress as presented in Fig. 6, 7, 8 and 9. The plate material (ASTM A516 Grade 70) of the LPG tank already have a factor of safety of 3.5. For the range of thicknesses considered as shown in Table 3, 10mm thickness and below will cause catastrophic failure if the LPG pressure tank is to operate at 1.55MPa and $60^0$C since there factor of safety is less than 3.5 (material's factor of safety). At 20mm thickness and above, the tank material will not yield (failure will not occur) since this range of thickness offers factor of safety greater than 3.5. Considering Fig.10, the graph of material allowable stress intersects the graph of FEA Von- mises stress (stress developed) at about 15mm. Therefore, 15mm could be taking as the minimum plate thickness for LPG pressure tank operating at 1.55MPa and $60^0$C. Since the vessel material is isotropic in nature, increasing plate thickness will keep the hoop stress/circumferential stress below the material yield stress, therefore, it will be twice as strong in the axial direction. The major disadvantage is the increase in weight of the vessel.

### 4.3 Simulation at $20^0$C, 0.5MPa (Case 2)

For cylindrical LPG pressure tank model of thickness: 2mm, 5mm, 10mm and 30mm each subjected to same internal pressure and temperature

LPG Temperature = $20^0$C

Internal pressure = 0.5MPa

The tank parameters for analysis are the same as in case 1and 2 except the temperature and LPG pressure.

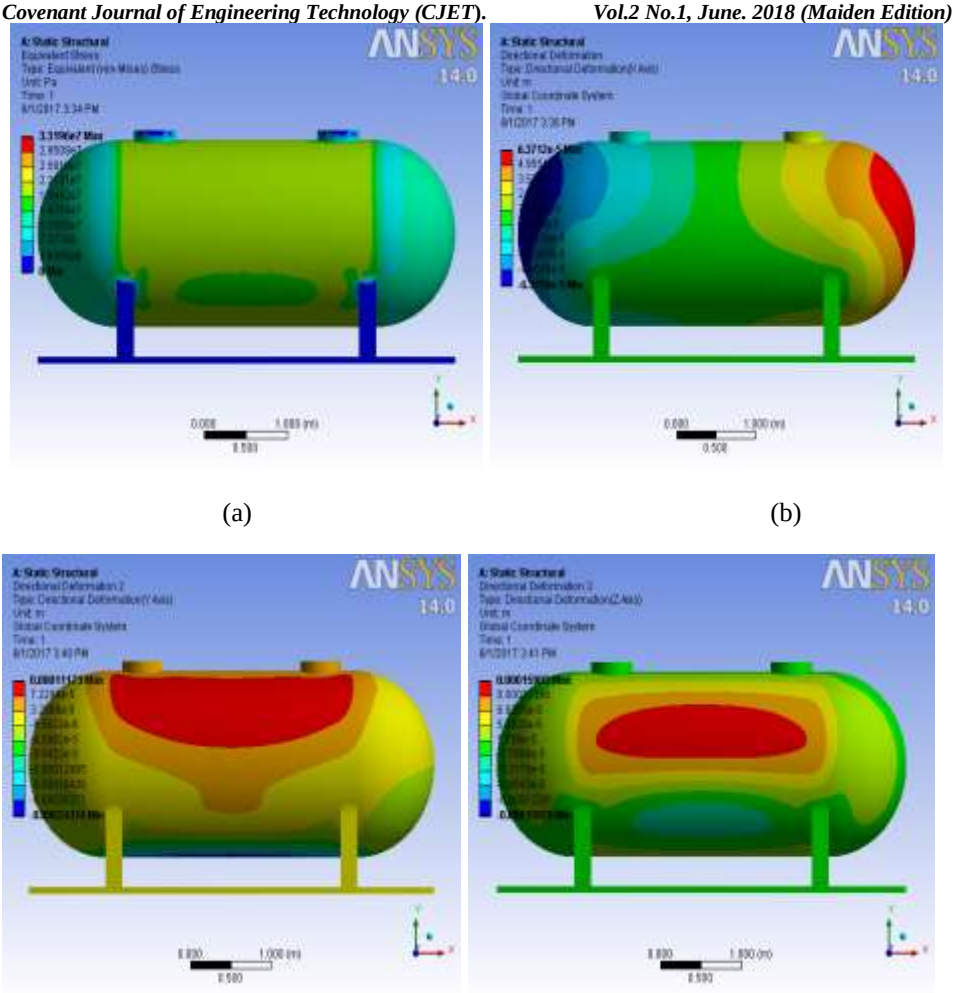

(a) (b)

(c) (d)

**Fig. 11** Application of 0.5MPa at $20^0$C , 10mm thickness (a) Von-Mises stress (b) displacement in x-axis (c)displacement in y-axis (d) deflection (z-axis).

### 4.4 Results and Discussion as Presented in Case 2

*Results*. Figure 11 shows the ANSYS static structural contour plots of the LPG pressure tank at 0.5MPa and $20^0$C. Figure 11 (b) and (c) shows the displacement in x and y direction while (d) shows the deflection in z direction. Plots in red are area where the biaxial state stress is mostly felt. These results are presented in tabular form as shown in Table 6. Graphical presentation of these results is similar to Fig. 6,7 and 8. Table7 follow the same trend as presented in Table 3 of case 1.

**Table 6** Displacements and deflections at different plate thickness for cylindrical LPG pressure tank at 0.5MPa, $20^0$C

| PLATE THICKNESS (mm) | DISPLACEMENT IN X-AXIS (mm) | DISPLACEMENT IN Y-AXIS (mm) | DEFLECTION (Z-AXIS) (mm) |
|---|---|---|---|
| 2 | 0.604060 | 1.176200 | 1.467600 |
| 5 | 0.258000 | 0.410780 | 0.763770 |
| 10 | 0.063712 | 0.111730 | 0.159030 |
| 30 | 0.041815 | 0.077964 | 0.092854 |

**Table:7** ASME Stress, FEA stress and Factor of Safety at different plate thickness for LPG at 0.5MPa, $20^0$C

| PLATE THICKNESS (mm) | FEA Von-Mises/Stress developed (MPa) | ASME Von-Mises stress (MPa) | (FEA) Factor of Safety |
|---|---|---|---|
| 2 | 276.61 | 205.68 | 1.75 |
| 5 | 129.36 | 82.28 | 3.75 |
| 10 | 33.196 | 41.14 | 14.61 |
| 30 | 20.722 | 13.71 | 23.41 |

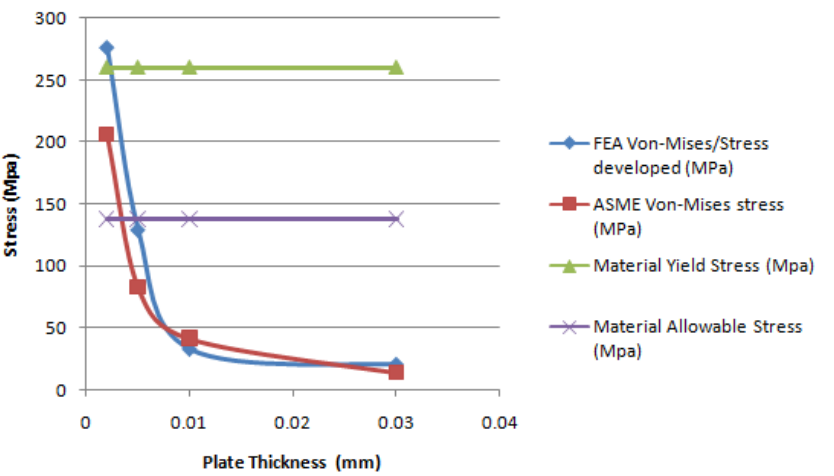


**Fig. 12** Comparing FEA Von-Mises (stress developed) at 0.5MPa with ASME Von-Mises stress, Material yield stress and Allowable stress.

Discussion of results as presented in simulation case 2. Displacement, deflection, Von-mises stress and the factor of safety follow the same trend as simulation case 1. The FEA Von-mises stress that is the stress developed shows some correlation with the ASME Von-mises stress. In Table 6, the deflections are more than displacement values since the hoop stresses often results to bending of the vessel plate material. Considering Table 7, at 5mm thickness, the finite element factor of safety (3.75) is greater than the material's factor of safety (3.5). Also, this is illustrated graphically in Figure 12 in which the graph of

material allowable stress intersets the graph of FEA Von-mises stress at 5mm. Therefore, it can said that at LPG pressure of 0.5MPa and ambient temperature of $20^0$C, the minimum plate thickness recommended is 5mm.

### 4.5 Simulation at $40^0$C, 0.91MPa (Case 3)

The same range of thickness was maintained (2mm, 5mm, 10mm, 20mm and 30mm), tank material properties remains the same but operating temperature and pressure was changed.

LPG Temperature = $40^0$C
Internal pressure = 0.91MPa

**Table 4** Displacements and deflection at different plate thickness for cylindrical LPG pressure tank at 0.91MPa, $40^0$C

| PLATE THICKNESS (mm) | DISPLACEMENT IN X-AXIS (mm) | DISPLACEMENT IN Y-AXIS (mm) | DEFLECTION (Z-AXIS) (mm) |
|---|---|---|---|
| 2 | 1.099400 | 2.14060 | 2.67100 |
| 5 | 0.470400 | 0.74904 | 1.39510 |
| 10 | 0.234690 | 0.36303 | 0.66072 |
| 20 | 0.115960 | 0.20335 | 0.28944 |
| 30 | 0.076102 | 0.14189 | 0.16899 |

**Table 5** ASME stress, FEA stress and Factor of Safety at different plate thickness for LPG at 0.91MPa, $40^0$C

| PLATE Thickness (mm) | FEA Von-Mises/Stress developed (MPa) | ASME Von-Mises stress (MPa) | (FEA) Factor of Safety |
|---|---|---|---|
| 2 | 503.430 | 374.34 | 0.96 |
| 5 | 235.480 | 149.74 | 2.06 |
| 10 | 122.530 | 74.87 | 3.96 |
| 20 | 60.417 | 37.44 | 8.03 |
| 30 | 37.714 | 24.96 | 12.86 |

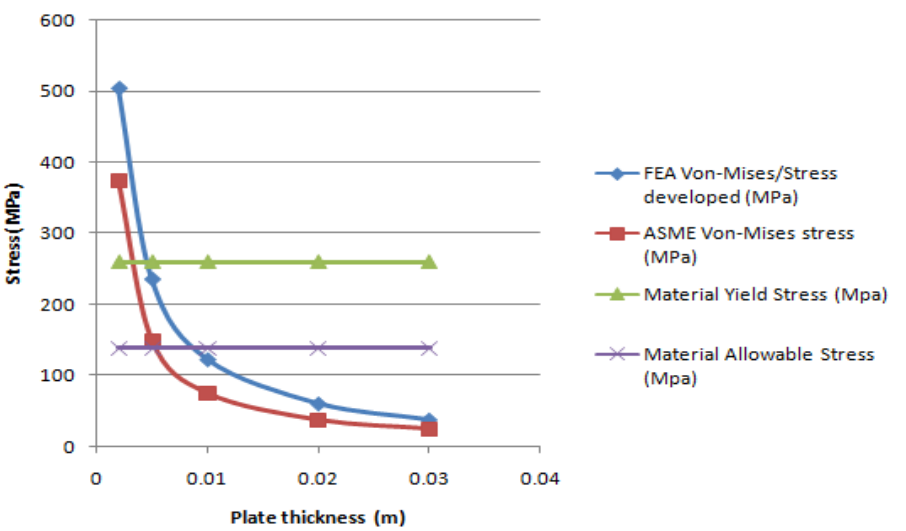

**Fig. 13** Comparing FEA Von-Mises (stress developed) at 0.91MPa with ASME Von-Mises stress, Material yield stress and Allowable stress.

### 4.6 Results and Discussion as Presented in Case 3

Table 4 and 5 follows the trend of case 1 and 2. Figure 13 shows the non linear relationship between stress and plate thickness. It also shows the convergence of finite element Von-mises stress(stress developed) and ASME Von-mises stress. The inverse relationship between thickness and stress is due to the disparity between circumferential stress (hoop stress) and plate thickness. Since the tank material is usually welded, therefore the welded area experience HAZ (heat-affected-zone). As pressure increases, hoop stress builds up in the heat-affected-zone, leading to crack initiation, propagation and material failure. This will occur once the stress developed is above the material allowable stress. For the range of thickness considered, 10mm thickness is taking as the minimum plate thickness at 0.91MPa since it offers factor of safety greater than the material's factor of safety. In Figure 11, the graph of material allowable stress intersects the graph of FEA Von-Mises stress at 10mm thickness showing that failure will not occur at this thickness and above it.

## 5. Conclusion

The Von-Mises stress and displacement in the Liquefied petroleum gas (LPG) pressure tank under different pressure distribution and ambient condition has been obtained using the finite element method. As temperature increases, LPG pressure increases, hence, there is need to design the pressure tank in such a way that the thickness will accommodate the rise in pressure. This will yield better results and reduce the risk of an explosion. For the different pressure range considered: 0.5MPa, 0.91MPa and 1.55MPa, the Von-Mises stress decreases with increasing plate thickness. A minimum plate thickness was deduced for each pressure range: 5mm thickness for 0.5MPa, 10mm thickness for 0.91MPa and 15mm thickness for 1.55MPa. At this minimum plate thickness, the Von-Mises stresses were found to be lower than the tank material allowable stress ($138MN/m^2$). The finite element Von-mises stress developed during simulation were in the same range with the ASME Von-mises. The range of thickness and stress are in compliance with ASME section VIII division 1 part ULT. The vessel material ASTM A516 Grade 70 already has a factor of safety of 3.5; therefore, design consideration should include material's yield and allowable stress and factor of safety greater than 3.5. For this research work, there are different possible scenarios. Once the boundary condition changes, the result will change, therefore, each should be treated as a case study. The effect of weldment along the seams of the vessel was not carried out in this work.

## References

[1] Foraminifera Market Research. Liquefied Petroleum Gas Bulk Storage and Marketing in Nigeria; How Viable? Retrieved February 10th 2017 from

http://www.foramfera.com/liquefied- petroleum-gas-bulk-storage-and-marketing-in-nigeria-how-viable/. (2017)

[2] Bruce G. The Smell of Danger. Chemmatters. Journal of American Chemical Society.Retrieved February 2nd 2017 from http://brucegoldfarb.com/clips/GoldfarbPropane.pdf. (1988).

[3] Abdul-Kadir K. A. Domestic LPG Market Growth-Infrastructural Challenges and Opportunities. Retrieved 02/02/17 from http://nigerialpgas.com/downloads/Domestic_LPG_Market_Growth_Infrastructural_Challenges_and_Opportunities.p df. (2016).

[4] Dennis R.M. Pressure Vessel Design Manual: Illustrated Procedures for Solving Major Pressure Vessel Design

Problems, New York: Gulf Professional Publishing. pp. 10-109. (2004).

[5] Dražan K., Ivan S., Antun S., Željko I. and Darko D. Stress Analyses of Cylindrical Vessel with Changeable Head Geometry. Scientific Bulletin, Series C, Volume XXIII, Fascicle: Mechanics, Tribology, Machine Manufacturing Technology. ISSN 1224-3264. (2009).

[6] Adeyefa O. and Oluwole. O. Finite Element Modeling of Variable Membrane Thickness for FieldnFabricated Spherical (LNG) Pressure Vessels. http://www.scirp.org/journal/eng. (2013).

[7] ASME. ASME Boiler and Pressure Vessel Codes. The American Society of Mechanical Engineers, New york. Library of Congress Catalog Card Number 56-3934. (2004).

[8] Oluwole O and Emagbetere E. Finite Element Analysis of In-plane Displacements and Von-Mises Stresses in Ellipsoidal and Circular Cylindrical Petroleum Tankers. (http://www.scirp.org/journal/eng). (2013).

[9] Awoyinfa S. Two killed, seven injured in Ogun gas plant explosion. Punch Newspapaer Nigeria. punchng.com/two-killed-seven-injured-ogun-gas-plant-explosion/. (2017).

[10] Richard G.B. Advance Strength and Applied Stress Analysis. Second edition. McGraw hill publishing companies Inc. (1999).

[11] Adeyefa O.A. Finite Element Analysis of Double-Jacked Field-Fabricated Spherical Liquefied Natural Gas (LNG) Pressure Vessels. Ph.D. Thesis, University of Ibadan (2015).

[12] Jorge R.M., Helder S.W. and Carlos A.C. Stress Analysis on Vessel/Nozzle Intersections With/Without Pad Reinforcement for Cylindrical Pressure Vessels. Proc. of 19th Int Congress of Mech. Engineering, Brasília, DF. (2007).

[13] Morrish K. and Shankar K.M. Comparative Stress Analysis of Elliptical and Cylindrical Pressure Vessels With and

Without Autofrettage Consideration Using Finite Element Method. Int. J. Adv. Engg. Res. Studies/IV/II/, pp. 189-195 (2015).

[14] Young W.K. and Hyochoong B. Finite Element Method Using Mathlab, New York: CRC Press, pp. 307- 373. (1997).

[15] Timoshenko T. and Goodier J. Theory of Elasticity, New York: McGraw Hill Books Company Inc., pp. 255-257.(1951)

[16] Zienkiewicz O.C. and Taylor R.L. The Finite Element Method, Oxford: Butterworth-Heinemann, vol. 2, pp. 111-210. (2000).

**Covenant Journal of Engineering Technology (CJET) Vol. 1, No. 2, Sept. 2018**

An Open Access Journal Available Online

# Solid State Fermentation of Orange Pomace for Bioethanol Production

**U. Musa[1], I. A. Mohammed[1], S. M. Munnir[1], M.U.Garba[1], A.F. Abdulhamid[2] & E.P Uduak [1]**

[1]Chemical Engineering Department,
Federal University of Technology, Minna, Nigeria.
[2] Engineering Department,
National Agency for Science and Engineering Infrastructure,
Abuja, Nigeria.

***Abstract***: This study is aimed at studying the effect of process variables on solid state fermentation of orange pomace for bioethanol production using *Saccharomyces cerevisiae.* The effect of substrate concentrations (100 - 350 g), fermentation period (24 - 72 hours) and inoculum amount (2.0 - 4.5 g) on solid state fermentation of orange pomace for bioethanol production was investigated. Characterization of the resulting bioethanol was carried out to determine its fuel properties (viscosity, flash point, density, refractive index, specific gravity, pH and boiling point). Experimental results revealed increase in the process variables (substrate concentration, fermentation period and inoculum amount) led to a corresponding increase in bioethanol yield until an optimum condition was reached (substrate loading of 200 g, pH of 4.5, fermentation temperature of 35°C, inoculum amount of 3 g and fermentation period of 72 hours) after which a decline in yield was observed. The maximum ethanol yield of 32.32 % v/v was obtained at these condition. Characterization of the bioethanol sample showed that the ethanol has satisfactory fuel properties that establishes its suitability as an alternative renewable fuel that can be blended with gasoline.

***KEY WORDS*:** Bioethanol, biomass, fermentation, fuel, orange pomace, solid state

## 1.0 Introduction

Alternative sustainable energy derived from biomass are presently considered as promising and attractive energy source when compared to fossil derived fuels.

Cellulosic bioethanol obtained from biomass fermentation is a renewable and environmentally friendly alternative fuel to petroleum gasoline [1]. It is presently the most commonly used liquid biofuel. Bioethanol has negligible contribution to global warming in comparison to petroleum gasoline [2]. Bioethanol is produced via microbial fermentation and distillation of the ethanoic wash from fermented biomass-extracted sugars. It can be used as a liquid fuel in automobile engines, either wholly or blended with petroleum gasoline [3]. Brazil and USA are the two major producers of ethanol, these two countries accounts for 62 % of the world production. First generation feedstocks (starch and sugar) are mainly used for this bioethanol production in these parts of the world [4]. The use of first generation feedstock is unfit for bioethanol production because starch and sugar feedstocks are basis for human and animal nutrition hence there will be problems on ethical concerns and favourable economics. It is based on this fact that second generation feedstocks (non-food feedstock's) are used for bioethanol. Second generation feedstocks consist of locally available and abundant agricultural waste [5]. Lignocellulose biomass is considered as second generation feedstocks. It is an ideal feedstock for biofuel production because it does not compete with food resources, reduces carbon dioxide emission by about 75% in comparison to fossil derived fuels [6].

Fruit pomaces are viable raw materials for bioethanol synthesis. Pomaces differs significantly from wood (hardwood or softwood). Woody materials are known to be naturally harsh and require thorough pretreatment before fermentation. Pomaces contains very high amount of easily accessible fermentable sugar content. These characteristics make pomaces suitable for all varieties of fermentation media [5].

Solid state fermentation (SSF) is an attractive technology for producing higher yield of bioethanol as compared to submerged liquid fermentation. In this process the microorganisms strive well due to the enabling environment similar to its natural habitat thereby resulting into higher metabolic activities [7]. Solid-state fermentation involves the process of microbial growth and product formation on solid particles in the absence (or near absence) of water; however, the substrate is known to contain sufficient moisture to permit microbial growth and metabolism [8]. Solid state fermentation results into higher bioethanol yields and better product characteristics in comparison with submerged fermentation which is characterized by the cultivation of the microorganisms in a liquid medium. Another great advantage of solid state fermentation over submerged fermentation is the lower capital and operating costs due to the utilization of low cost agricultural and agro-industrial wastes as substrates. The low water volume used in solid state fermentation process has also a large impact on the economy of the process mainly because of the smaller fermenter-size, the more reduced the downstream processing, stirring and sterilization costs [9 – 10]. In solid state fermentation the

microorganisms grow on a moist solid with little or no free water, although the capillary water may be present. Solid state fermentation process is best used for fungi and microorganisms requiring less moisture content; hence this process can also be used for fermentation process involving organisms (bacteria) requiring high water activity [11]. Different researches have reported the solid state fermentation of different fruit pomaces; banana peels [12], sweet potatoes [13], carob pods [14], grape and sugar beet pomaces [15], rice bran [6] for bioethanol production. There are little or no documented literatures on the production of bioethanol from orange pomace.

Orange peel waste (OPW) is the solid residue of orange juice production. Orange peel is an excellent example of a wasted resource. It consists of peels, membranes, cores, juice sacs and seeds which are rich source of pectin, appreciable quantity of cellulose, and soluble sugars. Orange peels is usually available in large quantity as it constitute over 50% of the processed fruits. It can be easily fermented to produce produces ethanol at a temperature between 25 and 35°C [16]. Its commercial uses are limited and its disposal is of great concern from the environmental point of view. The aim of this work is to study the effect of process variables on the solid state fermentation of orange pomace for bioethanol production and also the characterization of the bioethanol to determine its relevant fuel properties.

## 2.0 Materials and Method

The orange pomace was obtained from Minna, washed in order to remove dirt and sand. Sodium hydroxide, yeast (*saccharomyces cerevisiae*), glucose and peptone were all of analytical grade.

### 2.1 Test for sugar content (brix) in the orange pomace

This was done with the aid of a hand held refractometer, to ensure that the glucose content in the substrate will be suitable or appropriate for saccharification and fermentation. The pomace collected was pulverized into pulp with the aid of a blender; this was pressed to extort the juice from the pulp. The lens of the refractometer was then cleaned with a cotton wool to guarantee a clean lens surface, after which little drops of the juice was added to the refractometer and it was closed. The sugar content was recorded from the micro-gauge as soon as a sharp colour was observed.

### 2.2 Pretreatment of the orange pomace

All the glassware were washed and autoclave for 1hr at a temperature of 121°C for sterilization. To a 500 ml conical flask, 150 g of the pulverized pomace was weighed. 30 ml of 4.0% sodium hydroxide buffer in the ratio (5:1) was used for pretreatment for 2 hr to make cellulose more accessible for enzyme activity [17].

### 2.3 Preparation of the culture media

The yeast (*saccharomyces cerevisiae*) was used for fermentation of the substrate sugar was cultivated for 2 days (48 hrs) before commencing the experiment. 20 g and 10 g of glucose and peptone respectively were diluted in 1L of

distilled water and untainted for 20 minutes at a temperature of 121℃ to produce 100 ml of glucose-yeast-peptone (GYP) medium in a conical flask. 5 ml suspension of the yeast strain (*Saccharomyces cerevisaie*) was introduced in to the prepared culture media. This was incubated at room temperature on a rotary shaker at a speed of 200 rpm for 48hr (2days) before injection into fermentation medium [17].

### 2.4 Solid State Fermentation

The prepared yeast (*Saccharomyces cerevisiae*) was introduced into the pretreated samples in the conical flasks and covered with foil paper. The mixer was charged into an incubator and allowed to ferment for different fermentation period between 24 and 72 hours and at a constant temperature of 35°C. The resulting ethanol liquor was boiled off via a distillation column apparatus for an hour at 79.5℃. There after the yield of ethanol was deduced by calculating the specific gravity of the ethanol obtained and the resulting value is used to deduce the ethanol concentration.

## 3.0 Result and Discussion

### 3.1 Orange Pomace Analysis

The sugar brix was determined with the aid of a refractometer and it was recorded as. The Fehling solution test for reducing sugar was carried out on the substrate. The colour of the substrate changed from bright yellow to red, this indicated the presence of reducing sugar in the sample.

### 3.2 Effect of Process Variables on Bioethanol Yield.

*Effect of fermentation period on bioethanol yield.*

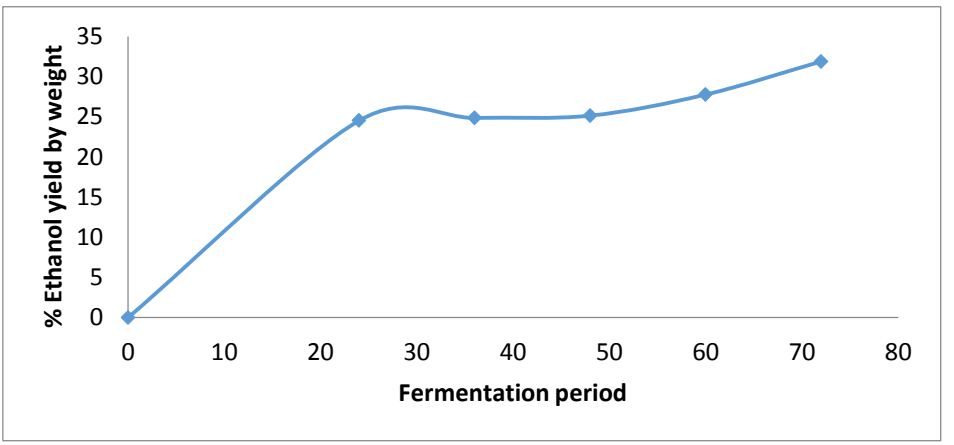


**Fig. 1** Effect of fermentation period on ethanol yield

The effect of fermentation period on ethanol yield was carried out between the fermentation period of 24 to 72 hours, at a constant temperature (35 °C), constant substrate loading (150 g), constant yeast strain or concentration of yeast (3.0g). From Figure 3.1, it was observed that there was a corresponding increase in the percentage yield of the bioethanol yield as the fermentation period increased from 24 to 72 hours. Optimum yield of 31.87 % (w/w) of

bioethanol was obtained at a fermentation period of 72 hours (3 days). The increase in bioethanol yield with time was attributed the appreciable contact between the enzyme and the hydrolyzed sugar. This result was in accordance with the result of Kanokphorn *et al*. [18] who reported the fermentation of leaf waste for bioethanol production.

*Effect of substrate loading on bioethanol yield*

The effect of substrate loading (100 to 350 g) on ethanol yield was carried out at a constant temperature of 35 $^{o}$C, optimum fermentation period of 72 hours and constant inoculum amount (3 g).

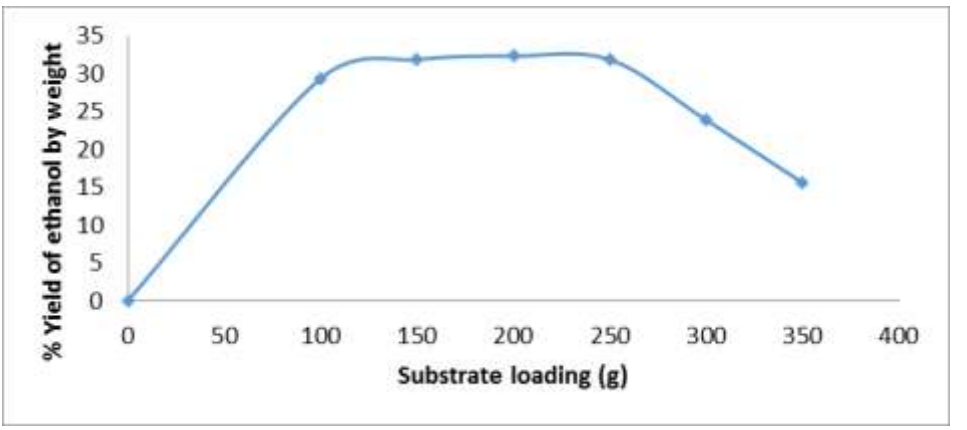


**Fig. 2** Effect of substrate loading on bioethanol yield

From on Figure 2 it was observed that bioethanol yield increased significantly as the substrate loading increased from 0 to 100 g. However as the substrate loading increased from 100 – 250g the bioethanol yield was gradual until a maximum yield of 32.32 % (w/w). Subsequently the yield decreased drastically as the substrate loading increased beyond 250 g. Higher substrate loading prevents the ethanol fermentation because the yeast cannot sufficiently act on all the substrate since the inoculum amount is constant (3 g). Another reason for the decrease in ethanol yield is the accumulation of high concentration of ethanol and by products which changes the broth pH [19].

*Effect of inoculum amount on bioethanol yield*

The effect of inoculum amount (2.0 to 4.5 g) on ethanol yield was carried out at a constant temperature of 35 $^{o}$C, constant substrate amount of 150 g, constant pH of 4.5 and constant fermentation period of 72 hours.

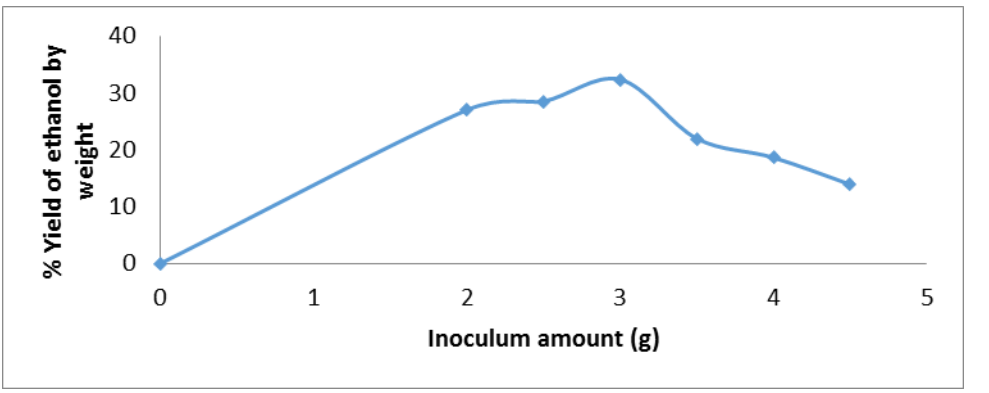


**Fig. 3** Effect of inoculum amount on ethanol yield

The percentage yield of bioethanol increased as the inoculum amount increased from 0 to 3 g. there was a decrease in the percentage of bioethanol produced as the inoculum amount increased from 3.5 to 4.5 g. The optimum yield of 32.32 % (w/w) bioethanol was obtained when 3.0 g of inoculum was used. The result is in conformity to the study of Neelakandan and Usharani [20].

### 3.3 Bioethanol Characterization

The appearance of the ethanol sample after filtration and distillation was clear and colourless. The boiling point of the ethanol sample obtained from this study was 79.20°C which is slightly higher than the boiling point of standard ethanol (78.5°C). The higher value obtained in this work may be due to the presence of impurities in the ethanol sample produced.

**Table 1** Properties of Bioethanol Produced

| **Property** | ***Standard ethanol** | **Orange Pomace ethanol sample** |
|---|---|---|
| Appearance | Clears colourless | Clear colourless |
| Boiling point (°C) | 78.50 | 79.20 |
| Density (g/cm$^{3)}$ | 0.789 | 0.795 |
| Specific gravity | 0.789 | 0.795 |
| Viscosity (cP) | 1.20 | 1.25 |
| Solubility | Miscible | Miscible |
| Flammability | Flammable | Flammable |
| Refractive index | 1.360 | 1.334 |
| Flash point (°C) | 12.8 | 12 |
| pH | 7.0 | 6.94 |

*(Source: Walker, [20])

The density of the sample was 0.795 g/cm$^3$ which shows close proximity to the density of the standard ethanol sample. Viscosity is the resistance of a fluid to flow or the property of fluid that resists the force tending to cause the fluid to flow. The viscosity of the ethanol sample was determined to be 1.25 cP. The solubility is a direct measurement of

hydrophobicity or the tendency of water to exclude a substance from solution. Solubility is the maximum concentration which an aqueous solution can tolerate before the onset of phase separation. The ethanol sample was completely miscible with water. This result was in agreement with reported literature [20]. The bioethanol sample produced burns with blue flame when ignited. The flash point of 12 $^{o}$C obtained in this study shows close proximity 12.8$^{o}$C reported for standard ethanol. The pH of the bioethanol sample was 6.94 indicating that the bioethanol sample is neutral and this corresponds with the pH of standard ethanol.

## 4.0 Conclusion

The study has attempted and succeeded in reporting for the very first time the potential of a typical Nigerian orange pomaces for bioethanol production via solid state fermentation. Optimum yield of 32.32 % (w/w) was obtained at a temperature of 35 $^{o}$C, pH of 4.5, substrate loading of 150 g, inoculum amount of 3 g and fermentation period 72 hours. Properties of bioethanol produced were satisfactorily in agreement with standard specification.

## References


[1] Shen, F., Zeng, Y., Deng, S., Liu, R., "Bioethanol production from sweet sorghum stalk juice with immobilized yeast", *Procedia Environmental Sciences*, 11, 782–789, (2011).

[2] Kim T. H and Kim T. H., "Overview of technical barriers and implementation of cellulosic ethanol in the U.S. ", *Energy*, 66, pp. 13-19, (2014).

[3] Graeme, M. Walker. "*Bioethanol: Science and Technology of fuel alcohol*". University of Abertay Dundee, Scotland, pp. 8- 11, (2010).

[4] Kim, S and Dale, B.E., "Global Potential Bioethanol Production from Wasted Crops and Crop Residues". *Biomass and Bioenergy*2, pp, 361-375, (2004).

[5] Ucuncu, C., "Chemical Consumption Analysis of Agro Industrial Waste and their Potential Usage in Bioethanol Production", M.Sc Thesis Submitted to the Graduate School of Engineering and Sciences of Ġzmir Institute of Technology, 1-93, (2011).

[6] Canabarro , N.I., Alessio, C., Foletto , E.L., Kuhn , R.C., Priamo, W.L., Marcio A. Mazutti, M.A., "Ethanol production by solid-state saccharification and fermentation in a packed-bed bioreactor" , *Renewable Energy*, 102 ,pp. 9-14, (2017)

[7] Manpreet, S., Sawray, S., Sachin, D., Pankaj, S., Banerjee, U.C., "Influence of Process Parameters on the Production of Metabolites in Solid State Fermentation". *Malaysian Journal of Microbiology*, 2, pp. 1-9, (2005).

[8] Pandey, A., "Solid State Fermentation". *Biochemical Engineering Journal*, 13, pp. 81-84, (2003).

[9] Holker, U and Lenz, J., "Biotechnology Advantages of Laboratory Scale Solid State Fermentation with Fungi",

*Applied Microbiology*, 8, pp. 175-186, (2004).

[10] Nigam, P.S., Gupta, N., Anthawal, A., "Pretreatment of Agro Industrial Residues". *Biotechnology for Agro Industrial Residue Utilization*, 14, pp. 13-23, (2009).

[11] Thomas, L., Larroche, C and Pandey, A., "Current developments in solid-state fermentation. Fermentation", *Biochemical Engineering Journal*, 81 pp. 146 – 161, (2013)

[12] Manikandan, K., Saravana, V., Viruthagiri, T., "Kinectic Studies on Ethanol Production from Banana Peel Wastes using Mutant Strain". *Indian Journal of Biotechnology*, 7, pp. 83-88, (2008).

[13] Manas, R.S., Mishra, J., Thatoi, H., "Bioethanol from Sweet Potatoes Flour in Solid State Fermentation". *Brazilian Archives of Biotechnology*, (56), pp. 4-7, (2013).

[14] Mazaheri, D., Shojaosadati, S.A., Mousavi, S.M., Hejazi, P., Saharkhiz, S., "Bioethanol Production from Carob Pods by Solid-State Fermentation with *Zymomonas Mobilis*", *Applied Energy*, 99, pp. 372–378, (2012)

[15] Rodrı´guez, L.A., Toro, M.E., Vazquez, F., Correa-Daneri, M.L., Gouiric, S.C., Vallejo, M.D., "Bioethanol production from by solid-state fermentation", *International Journal of Hydrogen Energy*, 35 (2010) pp. 5914–5917.

[16] Reena, D (2016) Biofuel from waste: A review, International Journal of Recent Advances in Engineering & Technology (IJRAET) V-4 I-1

[17] Mishra, J., Deepesh, K., Sumeru, K.V and Manoj, S., "A comparative study of ethanol production from various agro residues by using *Saccharomyces cerevisiae and Candida albicans*". *Journal of Yeast and Fungi Research*, 3, pp. 12-17, (2012).

18] Kanokphorn, S., Rokeyoh, S., Chompoonuch, W., "Conversion of Leaf Waste to Sugar and Ethanol by SHF and SSF USING Cellulase from *Cellulomonas* Sp.". *International Journal of Advanced Biotechnology and Research*, 2, pp. 345-349, (2011).

[19] Lin, Y., Zhang, W., Li, C., Sakaribara, K., Tanaka, S., Kong, C., "Factors Affecting Ethanol Fermentation Using Saccharomyces *Cerevisiae*".. *Biomass and Bioenergy*, 42, pp. 1-5, (2012).

[20] Neelakandan, T., Usharin, G., "Optimization and Production of Bioethanol from Cashew Apple Juice Using Immobilized Yeast Cells by Saccharomyces Cerevisiae". *Journal of Scientific Research*, 4, pp. 85-89, (2009).

[21] Walter, A., Rosilo-Calle, F., Dotzan, P., Piacente, E., Borges da Cunha, K., "Perspective on Fuel Ethanol Consumption and Trade". *Biomass and Bioenergy*, 32, 730-748, (2010).

[20] Neelakandan, T., Usharin, G., "Optimization and Production

of Bioethanol from Cashew Apple Juice Using Immobilized Yeast Cells by Saccharomyces Cerevisiae". *Journal of Scientific Research*, 4, pp. 85-89, (2009).

[21] Walter, A., Rosilo-Calle, F., Dotzan, P., Piacente, E., Borges da Cunha, K., "Perspective on Fuel Ethanol Consumption and Trade". *Biomass and Bioenergy*, 32, 730-748, (2010).

**Covenant Journal of Engineering Technology (CJET) Vol. 1, No. 2, Sept. 2018**

An Open Access Journal Available Online

# Effect of Curing Water Qualities on Compressive Strength of Concrete

**O.A. Dauda[1], J.O. Akinmusuru[2], A.M. Dauda[3], O.S.I. Fayomi[4] & T.O. Durotoye[5]**

[1]Department of Civil Engineering, Covenant University, Canaanland, Ota, Nigeria
[2]Department of Civil Engineering, Covenant University, Canaanland, Ota, Nigeria
[3]Department of Civil Engineering, Covenant University, Ota, Ogun State, Nigeria
[4]Department of Mechanical Engineering, Covenant University, Ota, Ogun State, Nigeria
[5]Department of Civil Engineering, Covenant University, Ota, Ogun State, Nigeria
4sheun@gmail.com;
joseph.akinmusuru@covenantuniversity.edu.ng

***Abstract***: The strength development and durability of concrete can be influenced by the quality of water used for curing the concrete. Consequently, this study was aimed at investigating the effect of contaminating the water for curing concrete on its compressive strength. Raw (tap) water and a water cement ratio of 0.6 were used in the production of the concrete cubes of 50 mm x 50 mm x 50 mm. The concrete samples produced were cured in raw water and water contaminated with varying percentages (25, 50 and 100%) of wastewater collected from a wastewater stabilisation pond. Chemical analysis was carried out to determine the pH, total dissolved solids (TDS), chloride, hardness, alkalinity, salinity, temperature and conductivity of the wastewater. The results of chemical analysis showed that these parameters are higher in the wastewater samples than in the raw water samples. The compressive strength of the concrete cubes were determined after 1, 3, 7, 14, 28, 60 and 90 days of curing.

The compressive strength of concrete samples immersed in raw water, shows there was a progressive decrease in the strengths of the samples immersed in contaminated water as the percentage of the wastewater increased. Therefore, it is recommended that concrete that will be in contact with wastewater or sewage-polluted water should have been cured in uncontaminated water that gives assurance of maximum strength development. for the compressive strength of concrete cured in raw water, for 28 days the compressive strength of concrete in 25% waste $H_2O$ + 75% raw$H_2O$, 50% waste $H_2O$ + 50% raw$H_2O$ and 100% wastewater content decrease by 12.35%, 25.44%, 35.74% respectively.

***Key Words***: Concrete; Compressive Strength; Waste Water; Qualities.

## 1. Introduction

Bio deterioration refers to undesirable changes in a material, According to the Webster's dictionary, Microbial Corrosion of concrete structures is the gradual destruction or undermining of concrete by microbes or microorganisms (Al-Jabri1ab, 2011).

The strength and durability of concrete is reduced due to the presence of chemical impurities in water (Nikhil, 2014). The quality of water used in curing concrete plays a vital role on the strength of the concrete. In this work, the researcher is trying to figure out the effect of wastewater on the compressive strength of concrete cubes and hydraulic structures such as bridges, septic tanks etc. Since quality of water affects the strength, it is necessary for us to go into the purity and quality of water. Structures sited close to septic tanks, slow moving water prone to pollution should be specially designed bearing in mind the destructive and microbial effects on their intended functionality (Ata, 2014). Hydration and gain in strength of fresh concrete is negatively impacted microbial actions (Mahasneh, 2014).

Corrosion is the result of a series of chemical, physical and (micro) biological processes leading to the deterioration of materials such as steel and stone. It is a world-wide problem with great societal and economic consequences.

Concrete is one of the strongest construction materials applied in centuries all over the world. Concrete structures belong to these usually considered as indestructible because of their longer service life as compared with the most constructional products.

However, they can get destroyed for a variety of reasons including the material limitations, poor quality design and construction practices, as well as the hard exposure conditions.

Many architectural and other buildings structures undergo bio deterioration when exposed to contact with soil, water, sewage, as well as food, agricultural products and waste materials. By living organisms. They form specific communities that interact in many different ways with mineral materials and their external environment. This complex phenomenon occurs in conjunction with many physical and chemical destructive processes. Thus, it is difficult to distinguish an extent of the damage caused by biotic factors from that resulting from abiotic ones.

Corrosion due to the activities of micro-organisms is referred to as

microbial corrosion. These organisms are involved in the corrosion process by the virtue of their growth and metabolic actions and their presence often provide concentration cells in the structure where they are present, whereby some areas in the structure are anodic to the rest. These bacteria are therefore classified into two- those that require oxygen in the metabolic and growth processes often referred to as aerobic bacteria and those that carry out their activities in the absence of oxygen often referred to as anaerobic. These bacteria are active in stagnant water mainly at bottom of tanks, the soil, freshwater, seawater and air.

This Research aim is to investigate the effect of microbial corrosion on concrete structures in other to attain this, the specific objectives are to:

1. determine and evaluate the effects of waste water on Compressive strength of concrete

## 2. Methodology

For compressive strength test of concrete cubes, standard cubical moulds of size 50mmx50mmx50mm were used in line with the specifications i.e. w/c ratio of 0.60. Fifty sets of cubes were prepared for each trial by mixing with raw water, and tested for 1, 3, 7, 14, 28, 2months, 3months of curing with different waste water percentage mixes. The following four combinations were made in achieving various compressive strengths of the concrete:

- 100% raw water
- 100% waste water
- 50% waste water + 50% raw water.
- 25% waste water + 75% raw water.

### 2.1 Materials

**Materials used**

i. Cement-The cement used in this investigation is Ordinary Portland Cement (OPC) with specific gravity of 3.15

ii. Fine aggregate- This consisted of locally available river sand which is free from impurities, the size of which is less than 4.75 mm with specific gravity of 2.64 and absorption value of 1%.

iii. The waste water was collected from sewage treatment plant located at Covenant University, km 10, Idiroko, road, Ota, Ogun state and the raw water was collected at the tap of civil engineering building in the same university

Table 2.1: Physical Properties of Waste Water

PHYSICAL TEST OF WASTE WEATER RESULTS

| DESCRIPTION | PARAMETERS | 1DAY | 3DAYS | 7DAYS | 14DAYS | 28DAYS | 2MONTHS | 3MONTHS |
|---|---|---|---|---|---|---|---|---|
| 25% wasteH$_2$0 +75%Clean H$_2$O concrete | PH | 8.74 | 13.46 | 11.51 | 11.32 | 11.64 | 11.6 | 11.54 |
| | Temperature | 28.1$^0$c | 27.3$^0$c | 27.7$^0$c | 27.0$^0$c | 27.5$^0$c | 28.2$^0$c | 29.9$^0$c |
| | Conductivity | 68.0M$_s$ | 3.61M$_s$ | 4.510M$_s$ | 4.87M$_s$ | 1812$^\mu$s | 1520$^\mu$s | 1057$^\mu$s |
| | TDS | 484ppm | 2.54ppm | 3.19ppm | 3.44ppm | 1.28ppm | 2.51ppm | 748ppm |
| | Salinity | 36.8ppm | 2.05ppm | 2.62ppm | 2.77ppm | 1.03ppm | 2.5ppm | 571ppm |
| 25% wasteH$_2$0 +75%Clean H$_2$O Reinforcement | PH | 8.74 | 9.81 | 8.05 | 4.65 | 7.46 | 8.54 | 10.54 |
| | Temperature | 28.1$^0$c | 26.2$^0$c | 27.2$^0$c | 26.7$^0$c | 27.3$^0$c | 27.7$^0$c | 28.6$^0$c |
| | Conductivity | 68.0M$_s$ | 260$^\mu$s | 250$^\mu$s | 338$^\mu$s | 446$^\mu$s | 350$^\mu$s | 246$^\mu$s |
| | TDS | 484ppm | 185ppm | 178ppm | 262ppm | 316ppm | 280ppm | 172ppm |
| | Salinity | 36.8ppm | 140ppm | 133ppm | 235ppm | 238ppm | 210ppm | 172ppm |
| 50% wasteH$_2$0 +50%Clean H$_2$O Concrete | PH | 8.74 | 13.45 | 11.4 | 11.43 | 11.49 | 11.45 | 11.44 |
| | Temperature | 27.8$^0$c | 27.2$^0$c | 27.7$^0$c | 26.7$^0$c | 27.3$^0$c | 27.8$^0$c | 28.8$^0$c |
| | Conductivity | 511$^\mu$s | 4.27M$_s$ | 4.88M$_s$ | 5.91M$_s$ | 6.25M$_s$ | 6.50M$_s$ | 6.65M$_s$ |
| | TDS | 363ppm | 2.98ppm | 3.38ppm | 4.17ppm | 4.50ppm | 4.55ppm | 4.68ppm |
| | Salinity | 273ppm | 2.42ppm | 2.68ppm | 3.33ppm | 2.73ppm | 3.1ppm | 3.98ppm |
| 50% wasteH$_2$0 +50%Clean H$_2$O Reinforcement | PH | 8.74 | 9.41 | 7.53 | 4.08 | 7.75 | 8.3 | 9.47 |
| | Temperature | 27.8$^0$c | 26.1$^0$c | 27.1$^0$c | 26.8$^0$c | 27.2$^0$c | 27.7$^0$c | 28.8$^0$c |
| | Conductivity | 511$^\mu$s | 330$^\mu$s | 342$^\mu$s | 407$^\mu$s | 254$^\mu$s | 220$^\mu$s | 202$^\mu$s |
| | TDS | 363ppm | 236ppm | 237ppm | 560ppm | 179ppm | 156ppm | 143ppm |
| | Salinity | 273ppm | 174ppm | 177ppm | 446ppm | 134ppm | 120ppm | 109ppm |
| 100% wasteH$_2$0 Concrete | PH | 8.74 | 13.46 | 11.51 | 11.32 | 11.64 | 11.6 | 11.54 |
| | Temperature | 27.8$^0$c | 27.3$^0$c | 27.5$^0$c | 26.9$^0$c | 27.4$^0$c | 27.1$^0$c | 28.8$^0$c |
| | Conductivity | 511$^\mu$s | 4.40M$_s$ | 5.310M$_s$ | 6.58M$_s$ | 6.91M$_s$ | 6.71M$_s$ | 6.52M$_s$ |
| | TDS | 363ppm | 2.94ppm | 3.84ppm | 4.75ppm | 4.91ppm | 4.71ppm | 4.59ppm |
| | Salinity | 273ppm | 2.17ppm | 3.03ppm | 4.01ppm | 4.11ppm | 4.0ppm | 3.9ppm |
| 100% wasteH$_2$0 Reinforcement | PH | 8.74 | 9.37 | 7.58 | 4.95 | 7.6 | 7.8 | 8.81 |
| | Temperature | 27.8$^0$c | 26.1$^0$c | 27.8$^0$c | 26.8$^0$c | 27.1$^0$c | 27.6$^0$c | 28.9$^0$c |
| | Conductivity | 511$^\mu$s | 465$^\mu$s | 510$^\mu$s | 606$^\mu$s | 379$^\mu$s | 210$^\mu$s | 103.6$^\mu$s |
| | TDS | 363ppm | 357ppm | 358ppm | 443ppm | 269ppm | 160ppm | 73.6ppm |
| | Salinity | 273ppm | 269ppm | 269ppm | 382ppm | 201ppm | 110ppm | 59.5ppm |
| 100% Clean H$_2$O Concrete | PH | 8.74 | 13.54 | 11.41 | 10.74 | 11.6 | 11.6 | 11.65 |
| | Temperature | 27.8$^0$c | 27.2$^0$c | 27.7$^0$c | 27.0$^0$c | 27.2$^0$c | 27.8$^0$c | 28.9$^0$c |
| | Conductivity | 511$^\mu$s | 4.23M$_s$ | 4.44M$_s$ | 5.95M$_s$ | 6.28M$_s$ | 6.8M$_s$ | 7.0M$_s$ |
| | TDS | 363ppm | 2.95ppm | 3.06ppm | 4.12ppm | 4.39ppm | 4.58ppm | 4.97ppm |
| | Salinity | 273ppm | 2.36ppm | 2.49ppm | 3.51ppm | 3.72ppm | 4.01ppm | 4.22ppm |
| 100% Clean H$_2$O Reinforcement | PH | 8.74 | 9.82 | 7.98 | 3.72 | 8.08 | 8.28 | 8.46 |
| | Temperature | 27.8$^0$c | 26.1$^0$c | 27.1$^0$c | 26.9$^0$c | 27.1$^0$c | 27.7$^0$c | 28.9$^0$c |
| | Conductivity | 511$^\mu$s | 87.5$^\mu$s | 97.8$^\mu$s | 224$^\mu$s | 100.4$^\mu$s | 234$^\mu$s | 272$^\mu$s |
| | TDS | 363ppm | 63.4ppm | 69.2ppm | 347ppm | 71.5ppm | 151ppm | 193ppm |
| | Salinity | 273ppm | 51.2ppm | 55.6ppm | 305ppm | 57.1ppm | 110ppm | 145ppm |

### 2.3. Compression Test

Compression test is the most common test conducted on hardened concrete, partly because it is an easy test to perform, and partly because most of the desirable characteristic properties of concrete are qualitatively related to its compressive strength.( Rakesh A. M and S.K. Dubey 2014).

The compression test is carried out on specimens cubical or in cylindrical shapes. Prism is sometime used, but it is not common in our country.

The cube specimen is of the size 50x50x50 mm.

The 1,3, 7, 14,28 days, 60 days and 90 days cubes (50mm x 50mm x50mm) were collected from their curing environment. The curing location was the same for each of the specimen which was cured from various quality of water. The specimen, which were removed from the water bath, were keep aside for drying until they were ready for testing. Two cubes from each set were taken for testing of 1 day concrete. After this then two cubes were taken for testing 3days concrete. Two cubes was taken for testing 7days concrete from the different curing water. Same was done for 14days, 28days, 60 days and 90 days two cubes was taken from the various curing water.

This Compression testing Machine was used on the first day, third day, seventh day, fourteenth day, twenty eight day, 60 days and 90 days cured concrete specimens. For each test day, the cubes were placed in the loading apparatus, and the load was actuated at a controlled loading rate. Once the specimen reached its critical load, one of the load indicators needle recorded the exact failure point.

## 3. Results and Discussion

### 3.1 Results

The effects of wastewater on the compressive strength of concrete cubes are shown in Table 4.1, and graphically illustrated in Fig. 4.1. The variation of the different percentages of wastewater on the compressive strength of concrete cubes are shown in Fig.4.1, for the 100% raw water, the compressive strength increases with the curing periods, for the 100% wastewater, the compressive strength increased up to the 28days and started decreasing from 60 days, for the 25% wastewater and 75% raw water, the compressive strength increases with the curing periods, for 50% wastewater and 50% raw water, the compressive strength increases with the curing periods.

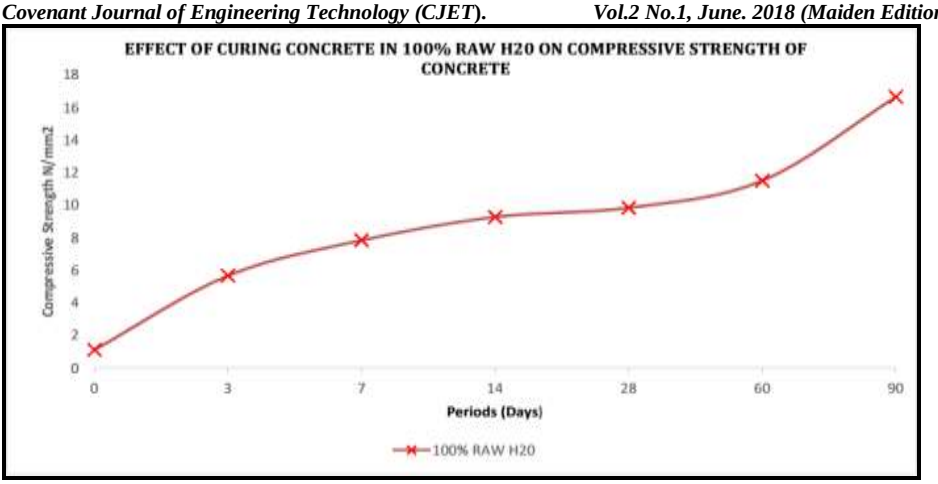


Figure 1: Effects of curing concrete in 100% raw h20.

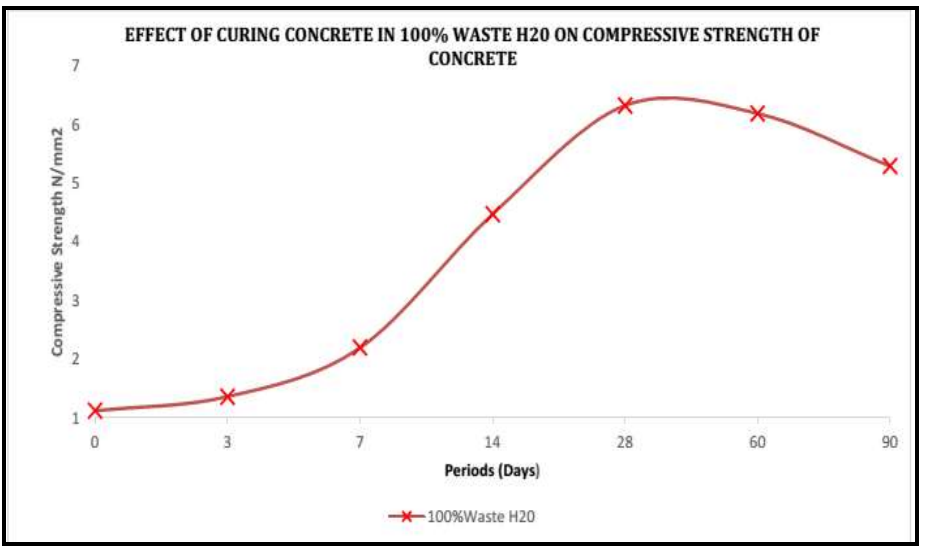


**Figure 2: Effects of curing concrete in 100% waste h20.**

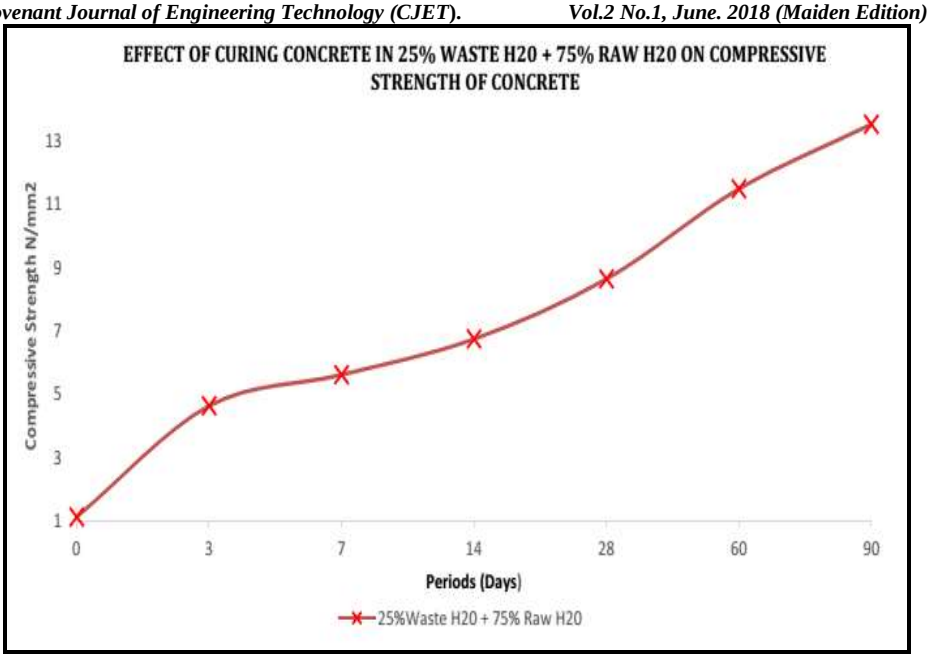


Figure 3: Effects of curing concrete in 25% waste $H_20$ +75% raw $H_20$.

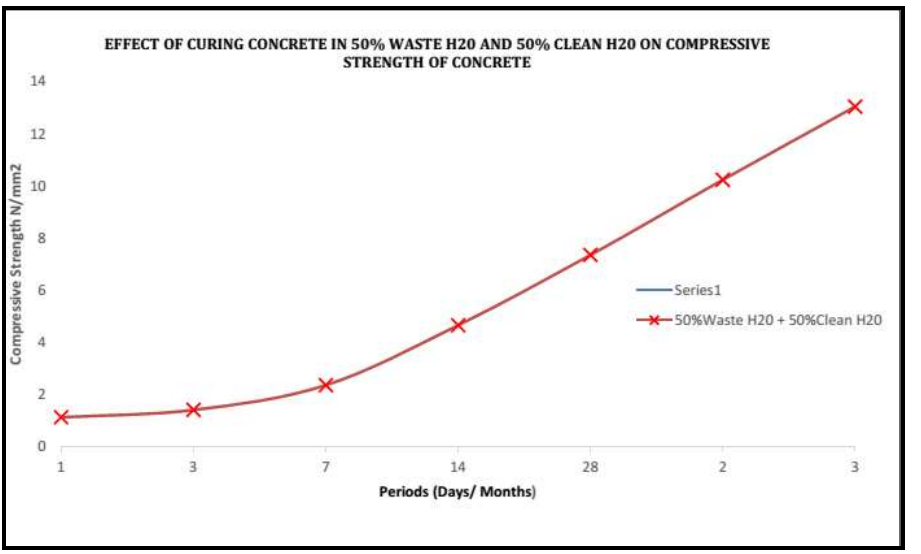


Figure **Error! No text of specified style in document.**: Effects of curing concrete in 50% waste $H_20$ + 50% raw $H_20$.

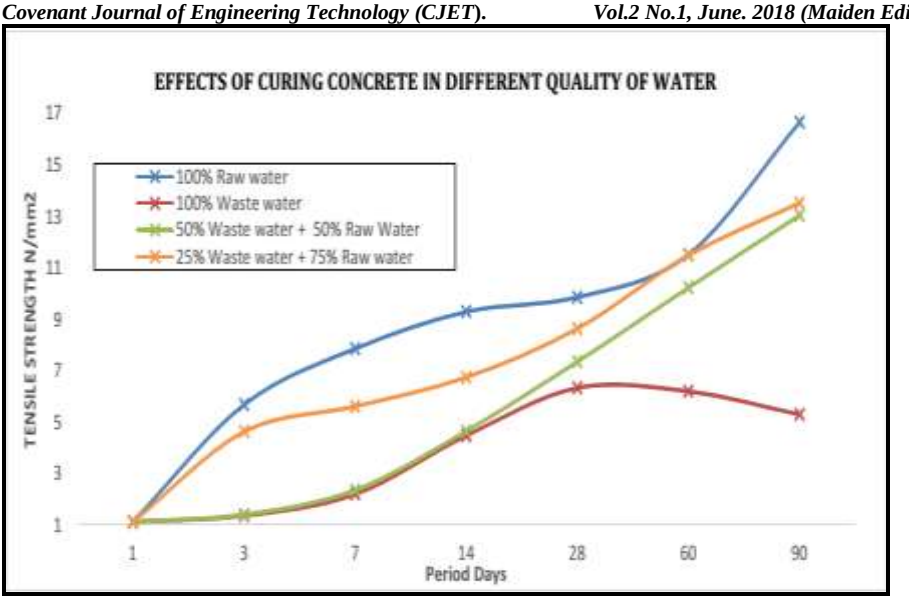


Figure 5: Effects of Curing Water On Compressive Strength Of Concrete.

### 3.2. Discussion

From the study, effects of different percentages of wastewater on the concrete cubes has the effect of increasing the compressive strength for the curing periods for 100% wastewater up to the 28$^{th}$ days and started decreasing from the 60$^{th}$ day up unto to the 90$^{th}$ day, while the steel immersed in 25% wastewater+ 75% raw water had the effect of increasing the compressive strength for the curing periods for up to the 90$^{th}$day, the steel immersed in 50% wastewater+ 50% raw water, the compressive strength increased for the curing periods for up to 90$^{th}$ day, For the 100% raw water, the compressive strength increases with curing periods up to the 90$^{th}$ day.

Table 2 shows the extent of increase (% increase) of the effect of wastewater on the compressive strength of concrete. Similarly,

On curing of the 100% wastewater for 3days, the compressive strength was 1.364N/mm$^2$, a rate of increase percentage of 21.35% from the initial strength for 0day (1.124N/mm$^2$), on curing of the 100% wastewater for 7days, the compressive strength was 2.20N/mm$^2$, a rapid rate of increase percentage from 21.35% to 95.73%, the increase continues to the 28$^{th}$ day with an increase percentage of 463.7%, however, there was a rate of decrease on the 60$^{th}$ day, from 463.7% to 451.60% and from 451.60% to 371.53% on the 90$^{th}$ day..

On curing of the 50% wastewater + 50% Raw water for 3days, the compressive strength was 1.404N/mm$^2$, a rate of increase percentage of 24.91% from the initial strength for 0day (1.124N/mm$^2$), on curing of the 50% wastewater + 50% raw water for 7days, the compressive strength was 2.356N/mm$^2$, a rapid rate of increase percentage from 24.91% to 109.61%, the increasing continues up to the 90$^{th}$ day with an increase percentage of 1060.85%.

On curing of the 25% wastewater + 75% raw water for 3days, the compressive strength was

4.636N/mm$^2$, a rate of increase percentage of 312.46% from the initial strength for 0day (1.124N/mm$^2$), on curing of the 25% wastewater + 75% raw water for 7days, the compressive strength was 5.616N/mm$^2$, a rate of increase percentage from 312.46% to 399.64%, the increase continues up to the 90$^{th}$ day with an increase percentage of 1103.91%.

For the 100% raw water, which serve as a control there was a rapid rate of increase percentage of 1383.27% up to the 90$^{th}$ day. The compressive strength of concrete samples cured in raw water progressively increased until maximum strength was attained.

## 4. Results and Analysis

Table 2 present the relation between curing time and the compressive strength of concrete Cubes cured in different water types.

Table 4.1: Percentage difference in strength with curing period of concrete

| Period of curing (days) | 1 | 3 | 7 | 14 | 28 | 60 | 90 |
|---|---|---|---|---|---|---|---|
| 100% Raw water Compressive strength (N/mm$^2$) | 1.124 | 5.684 | 7.86 | 9.296 | 9.86 | 11.52 | 16.672 |
| % Increase | - | 405.69 | 599.29 | 727.05 | 924.01 | 924.91 | 1383.27 |
| 100% wastewater Compressive strength (N/mm$^2$) | 1.124 | 1.364 | 2.2 | 4.48 | 6.336 | 6.2 | 5.3 |
| % Increase | - | 21.35 | 95.73 | 298.58 | 463.7 | 451.60 | 371.53 |
| 50% wastewater + 50% Raw water Compressive strength (N/mm$^2$) | 1.124 | 1.404 | 2.356 | 4.656 | 7.352 | 10.24 | 13.048 |
| % Increase | - | 24.91 | 109.61 | 314.23 | 554.09 | 811.03 | 1060.85 |
| 25% wastewater + 75% Raw water Compressive strength (N/mm$^2$) | 1.124 | 4.636 | 5.616 | 6.748 | 8.642 | 11.496 | 13.532 |
| % Increase | - | 312.46 | 399.64 | 500.36 | 672.81 | 922.78 | 1103.91 |

## 5. Conclusion

From the results obtained, the following conclusions were drawn:

Relative to the compressive strength of concrete cured in raw water, for 28 days the compressive strength of concrete in 25% waste $H_2O$ + 75% raw$H_2O$, 50% waste $H_2O$ + 50% raw$H_2O$ and 100% wastewater content decrease by 12.35%, 25.44%, 35.74% respectively.

From the study, different percentages of wastewater on the concrete cubes has the effect of increasing the compressive strength for the curing periods for 100% wastewater up to the 28$^{th}$ day. Then started decreasing from 60 days onwards, There is an

increasing compressive strength for all the curing periods studied for 25% wastewater+ 75% raw water up to the 90 days, There is an increasing compressive strength for all the curing periods for 50% wastewater+ 50% raw water up to the 90 days write up. For the 100% raw water, the compressive strength increased with curing periods throughout.

**Acknowledgement**

The success associated with the accomplishment of this task would be incomplete without acknowledging the department of Civil Engineering, Covenant University, Ota, Ogun State. Under whose constant support and encouragement this paper has been accomplished flawlessly.

**References**

1. Amann RI, Krumholz L, and Stahl DA, (1990). Fluorescent - Olignonucleotide probing of whole cells for determinative, phylogenetic and environmental studies in microbiology. *Journal of Bacteriology* , 762-770.
2. Ata, O. (. (2014). Effects of different Sources of water on Concrete strength, A case study of Ile-Ife. *Else and Environmental Research*, Vol 6,No 3.450-463.
3. Aviam O, Bar-Nes G, Zeiri Y, and Sivan A, (2004). Accelerated biodegradation of cement by sulfur-oxidizing bacteria as a bioassay for evaluating immobilization of low-level radioactive waste. Applied Environmental Microbiology. 70:6031-6036.
4. Ayakumar S and Saravanane R, (. (2010). JBiodeterioration of Coastal Concrete Structures by Marine Green Algae. . *International Journal of Civil Engineering.*, 8:352-261.
5. Bassam Z. Mahasneh, (. (2014). Assessment of Replacing Wastewater and Treated Water with Tap Water in Making Concrete Mix. *Electronic Journal of Geotechnical Engineering.*, Vol. 19.
6. Bastidas-Arteaga E, Sánchez-Silva M, Chateauneuf A, and Ribas- Silva M,(2008). A newly isolated fungus participates in the corrosion of concrete sewer pipes. . *Water Science Technology*, 31:263-271
7. Bastidas-Arteaga E, (. B. (2008 & 2004). Cement paste alteration by liquid manure organic acids: chemical and mineralogical characterization. *Cement Concrete Resource. 34:*, 1823- 1835.
8. Bastidas-Arteaga E, S.-S. M.-S. (2008). Coupled reliability model of biodeterioration, chloride ingress and cracking for reinforced concrete structures. *Structural Safety.*, 30:110-129.
9. Bertron A, Escadeillas G, and Duchesne J, (2004) Cement paste alteration by liquid

manure organic acids: chemical and mineralogical characterization. Cement Concrete Resource. 34:1823-1835

**10.** Cho K and Mori T (1995). A newly isolated fungus participates in the corrosion of concrete sewer pipes. Water Science Technology. 31:263-71

**11.** Cwalina B, (2008) (The role of cracks. Cement Concrete Comp.32:101-109). Biodeterioration of concrete. Water repellent surface impregnation for extension of service of reinforced concrete structures in marine environment. *Arch Civil Engineering Environment.* , 4:133-140.

**12.** Dai JG, Akira Y, Wittmann FH, Yokota H, and Zhang P, (2010). Water repellent surface impregnation for extension of service of reinforced concrete structures in marine environments: The role of cracks. Cement Concrete Comp. 32:101-109.

**13.** Domingo JWS, Revetta RP, Iker B, Gomez-Alvarez V, Garcia J, Sullivan J, and Weast J, (2011). Molecular survey of concrete sewer biofilm microbial communities.. Biofoluing., 27:993- 1001.

**14.** Ede AN, and Agbede JO,(2015). Use of coconut husk fibre for improved compressive and flexural strength of concrete. International Journal of Scientific and Engineering Research. 1:968-974.

**15.** Gaylarde C, R.-S. M. (2003). Microbial impact on building materials: an overview. *Material Structure*, 36:342-352.

**16.** Gu JD, F. T. (1998). Biodeterioration of concrete by the fungus Fusarium. . *International Biodeterioration Biodegradation.*, 41:101-109.

**17.** Javaherdashti. R, a. S. (2006). Evaluation of sessile microorganisms in pipelines and cooling towers of some Iranian industries. *Journal of Material Engineering Performance*, 15:5-8.

**18.** Jayakumar S and Saravanane R, (2010). Biodeterioration of Coastal Concrete Structures by Marine Green Algae. International Journal of Civil Engineering. 8:352

**19.** K. S. AL-Jabri1ab, (2011). Effect of using Wastewater on the Properties of High Strength Concrete, Department of Civil and Architectural Engineering,. *The twelfth East Asia - PacificConference on Structural Engineering and ConstructionSultan Qaboos University* (pp. 370-376). Oman. : Elseveir Sciencedirect Procedia Engineering, .

**20.** Lahav O, L. Y. (2004). Modeling hydrogen sulphide emission rates in gravity sewage collection systems. . . *Journal of*

*Environmental Engineering,* 11:1382-1389.

**21.** *Mori T, Nonaka T, Tazak K, Koga M, Hikosaka Y, and Nota S, (1992). Interactions of nutrients, moisture, and pH on microbial corrosionof concrete sewer pipes. Water Resource. 26:29-37.*

**22.** Nica D, D. J. (2000). Isolation and characterization of microorganisms involved in the biodeterioration of concrete in sewers. . *International Biodeterioration Biodegradation.* , 46:61-68.

**23.** Nikhil. T.R, (2014). Impact of Water Quality on Strength Properties of Concrete. . *Indian Journal of applied Research.*, Vol.4 issue7.

**24.** Oyenuga V.O, (. (2001). *Simplified Reinforced Concrete Design, 2nd Edition.* Lagos: Asros Publishers.

**25.** Raheem A/A, B. G. (2013). Establishing threshold level for gravel inclusion in concrete production. *Innovative Systems Design and Engineering.* ., 4:25-30.

**26.** Ramkar A.P. and Ansari U.S (2016). (2016). Effect of Treated Waste Water on Strength of Concrete. IOSR. *Journal of Mechanical and Civil Engineering,*, Vol 13, Issue 6, Pp 41-45.

**27.** Ribas-Silva M,(1995). Study of biological degradation applied to concrete. *Proc, Transactions of 13th International Conference on Structural Mechanics in Reactor Technology* (pp. Pp327-332.). University of Federal do Rio Grande do Sul, Porto Alegre,: Brazil.

**28.** Rose A.H, (. (1981). Microbial Biodeterioration. Economic Microbiology. *Academic Press*, (pp. Pp35-80.). London.

**29.** *Sanchez-Silva M and Rosowsky D, (2008). Biodeterioration of construction materials: state of the art and future challenges. . Journal of Material and Civil Engineering., 20: 352-365.*

**30.** *Sand W, (1987). Importance of hydrogen sulfide, thiosulfate, and methylmercaptan for growth of Thiobacilli during simulation of concrete corrosion. Applied Environmental Microbiology. 53:1645-1648.*

**31.** Satoh H, Odagiri M, Ito T. and Okabe S ,(2009). Microbial community structures and in situ sulfate-reducing and sulfur-oxidizing activities in biofilms developed on mortar specimens in a corroded sewer system. Water Resources. 43:4729-4739.

**32.** Videla HA, and Herrera,L. (2005). Microbiologically influenced corrosion: looking to the future. . *International Microbiology.*, 8:169–180.

**33.** Warscheid T, and Braams. J. (2000). Biodeterioration of

stone: a review. . *International Biodeterioration Biodegradation.* , 46: 343–368.

**34.** Wendler E, (. ,. (1997). New materials and approaches for the conservation of stone, Saving our Cultural Heritage: TWiley, New York. . *he Conservation of Historic Stone Structures.* , Pp181-196.

**35.** Yilmaz K, (2010). A study on the effect of fly ash and silica fume substituted cement paste and mortars. . *Science Resource Essays.* , 5:990- 998.

**36.** Zhang L, 2. a. (2008,& 2011). *Advanced concrete technology, 1st Edition,.* New Jersey:: John Wiley & Sons, Inc.

**37.** Zhang L, S. P. (2008). Chemical and biological technologies for hydrogen sulfide emission control in sewer systems: A review. *Water Resource.*, . 42:1-12.

**38.** Zongjin L, (2011). Advanced concrete technology, 1st Edition, New Jersey: John Wiley & Sons, Inc.

**39.** Zuo R, (. (2007). Biofilms: strategies for metal corrosion inhibition employing microorganisms. *Applied Microbiology Biotechnology*. , 76: 1245–1253.

**Covenant Journal of Engineering Technology (CJET) Vol. 1, No. 2, Sept. 2018**

An Open Access Journal Available Online

# Theme: Renewable Energy and Sustainability Experimental and Numerical Study of Drying of Moringa Oleifera Leaves

**O. S. Olaoye[*1], A. Alausa[2] & O. Onihale[3]**

[1,2,3]Department of Mechanical Engineering,
Ladoke Akintola University of Technology,
Ogbomoso, P.M.B. 4000, Oyo State, Nigeria

*osolaoye@lautech.edu.ng, 08038645736

***Abstract***: Drying is a preservation technique to reduce the water content of the food product to a safe level and to minimize biochemical reactions of the degradation and also to increase the shelf life of the product. Moringa being an agricultural product of high chemical, nutritional and medical use is susceptible to degradation due to relatively high moisture content. Moringa leaf is sensitive to sunlight, therefore, forced convection drying method with two types of air velocities (2.2 and 1.2 m/s) was employed in its drying. A batch of moringa leaves of 200g by mass having an initial moisture content of 83% wet basis was dried to desired 14% wet basis moisture content at average temperature of 40oC. Drying chamber and ambient temperatures, relative humidity, air flow velocity and rate of weight reduction were measured. The experimental and model results were statistically validated. Also numerical modeling of heat and mass transfer that occurred in the drying process was done using COMSOL Multiphysics 4.3b that uses finite element approach. It took between 10 and 12 hours to dry moringa leaves to the desired moisture content at drying air velocity 2.2 m/s and 1.2 m/s respectively. The results predicted from the modelling when compared with the experimental data have a considerably agreement.

***Keywords***: Drying, Solar dryer, Heat and mass transfer, Modeling, COMSOL Multiphysics

## 1. Introduction

Drying has been used from ancient times to preserve food products. Open-air drying is the most commonly used technique, especially in tropical and subtropical regions.

The most common way to do this is to place the leaves on a mat, floors etc. and leave it in the open to dry. Drying of moringa leaves is a preservation activity done by farmers and herbal practitioners. It also affects the quality, nutritional values and the potency level of the leaves when exposed to the direct sunlight (Amedorme, et al., 2013 and Mujumdar, 2007). This process takes a long time and makes the leaves subjected to attack by the weather, animals and insects. However, because of the sensitivity of the leaves to direct sunlight, an indirect type of solar dryer was employed in this study. Thus, if the drying time can be reduced, the quality of dried product will be improved. Therefore, there is the need for an alternative drying methods such as those based on solar energy. The use of a solar dryer for drying can never be overestimated. In drying, many parameters influence the drying process and to be experimenting for optimizing of all these parameters may be costly (Curcio, 2006). Kumar et al (2012) considered variable properties of the material while simulation heat and mass transfer during drying using multiphysics. COMSOl was used to predict temperature and moisture distribution inside the food during drying. Hence a good drying model is essential for optimizing this process using computer simulation. Computer simulation is a powerful tool for achieving measurement of changes in temperature and moisture during dehydration process. Simulation results and information of drying kinetics of herbs material such as time, temperature, moisture content distributions, as well as theoretical approaches to moisture movement, is very essential for the prevention of quality degradation and for the achievement of fast and effective drying. Such information will be very useful to optimize production processes of herbs dried. The increasing development of computer program had a great impact on the quality evaluation of agricultural products (Rajibul and Norma, 2010).The objective of this study is to study the drying process of moringa using both experiment and numerical methods. The model consist of coupled heat conduction and mass diffusion equations which were solved using finite element method through the use of COMSOL Multiphysics 4.3

## 2. Method

### 2.1 Design considerations and features

The solar dryer was designed using locally sourced materials so as to reduce cost, increase ease of maintenance and operation. It consists of a heat collector which harnessed the radiation from the sun, an absorber which absorbed and saved the energy for use by the dryer, a drying chamber, three drying racks and a fan which transferred the heat to the drying chamber resulting in a forced convection. The dryer was an indirect solar dryer. The advantage of this is the protection of the leaves from loss of nutrients due to direct exposure to sunlight. The exploded view of the dryer showing its parts and materials used is shown in Figure 1.

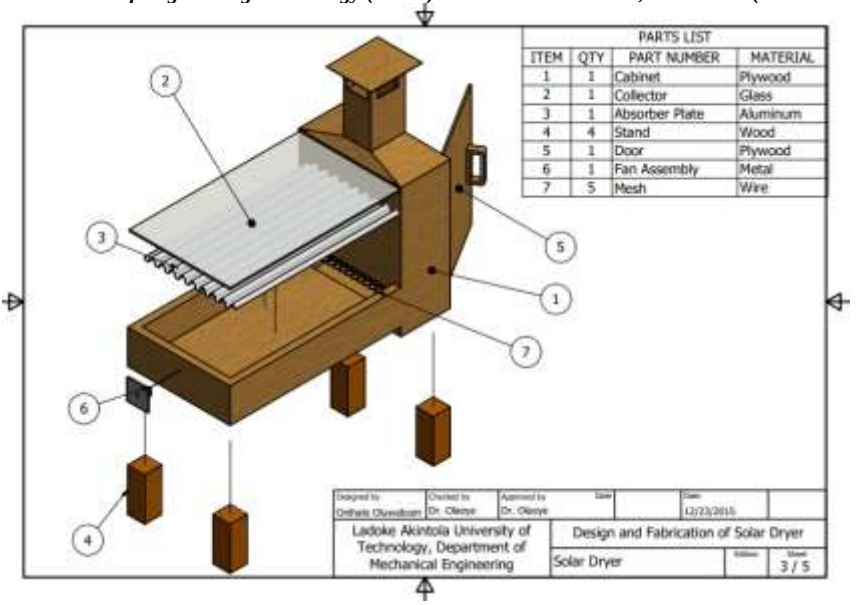


Fig 1: Schematic diagram of the dryer

### 2.2. Design equations

According to Amedorme, et al., (2013), the following equations were used in the design of the dryer.

The efficiency of the dryer was obtained using the following equations

$$\eta_d = \frac{ML}{I_c A_c} \qquad (1)$$

Area of the drying rack obtained by the following equations

$$A_{rac} = \frac{M_p}{P_{gr} h_L \varepsilon (1 - \varepsilon_v)} \qquad (2)$$

Applying Bernouli's equation between the relevant sections of the dryer and sampling the results leads to height of the drying chamber

$$H = \frac{\Delta P_T}{g\left(\frac{1}{T_a} - \frac{1}{T_o}\right)\frac{P_a}{R}} \qquad (3)$$

According to Bolaji (2005), the height difference between the inlet air and exhaust of a forced convention should not exceed 1200 mm with collector area less than 10

Chimney height, h$c$ = 1.2 – (0.75 + 0.1) = 0.35$m$ (4)

### 2.3. Solar Dryer Dimensions

The heat absorber (inner box) of the solar air heater was constructed using 2mm thick aluminum plate, painted black, and was mounted in an outer box built from well-seasoned odum and plywood. The space between the inner box and outer box was filled with foam material of about 40mm thickness and thermal conductivity of 0.043Wm-1K-1.

The solar collector assembly consisted of air flow channel enclosed by transparent cover (glazing). The glazing was a single layer of 4mm thick transparent glass sheet; it had a surface area of 1000mm by 600mm and of transmittance above 0.7 for wave lengths in the rage 0.2–2.0μm. One end of the solar collector had an air inlet vent of area 0.0457m2, it was

fitted with fan to provide the forced convection, and the other end is opened to the drying chamber.

An outlet channel was fitted with chimney. Access door to the drying chamber was provided at the side of the cabinet. Drying trays was contained inside the drying chamber and constructed from a double layer of fine wire mesh with a fairly open structure to allow drying air to pass through the moringa leaves. The flat-plate solar collector was tilted and oriented in such a way that it will receive maximum solar radiation during the desired season of use. It was inclined at 18.13o according to Ogbomoso Latitude (8.13o) the angle of inclination must be 10o more than the local geographical latitude for best all year performance (Bolaji, 2005). The capacity of the dryer is 200g of moringa leaves.

**2.4. Experimental procedure**

Fresh moringaoleifera leaves were obtained from farms in Ogbomoso, South Western Nigeria. They were sorted, washed and dried using the dryer. During the drying process, the temperature of the absorber, collector, drying chamber and air leaving the chimney were measured and recorded at a time interval of 20 minutes. Also, the mass of the product was measured and recorded every hour so as to track the rate at which moisture was reduced and obtain a moisture profile for the drying process. The thermal properties of moringa were obtained at different room temperature (27.43 , 27.15 and 26.85 ) using KD-2 pro thermal analyzer. The experiment was done three times and the average results were recorded. The solar radiation at the time of the experiment was measured using solar power meter (LT Spm – 1116SD). The experiment was carried out for an average of 2 days before obtaining a dried product.

**2.5. Mathematical Model:**

In developing the model, the following assumptions were made:

(1) Thermophysical properties of the moist material and drying air are constant.

(2) There is negligible shrinkage or deformation of material during drying.

(3) Drying air is distributed uniformly through the dryer

(4) Heat and moisture transfer are one dimensional

(5) No chemical reaction takes place during drying

**2.5.1. Governing equations:**

Drying kinetics can be modeled mathematically based on Fick's law of diffusion. The simulation of various product drying systems involves solving a set of heat and mass transfer equations.

The first drying process is heat transfer to the product from the heating source and the second is mass transfer from the interior of the material to its surface and from the surface to the surrounding air.

Heat transfer equation

$$\rho_s Cp_s \frac{\partial T}{\partial t} + \nabla\left(-k_s \nabla T\right) = Q_s \quad \text{Fagh ri, } \textit{et al.,} \text{ 2010)} \qquad (5)$$

$$\hat{r}^2 \rho_s Cp_s \frac{\partial T}{\partial t} + \frac{\partial}{\partial r}\left(-\frac{1}{R_m{}^2} k_s \hat{r}^2 \frac{\partial T}{\partial r}\right) = \hat{r}^2 Q_s \qquad (6)$$

In a similar manner it is possible to derive equation similar to equation 3.21 for porous media

flow, diffusion-reaction problems and so on.

Mass transfer equation

$$\frac{\partial M}{\partial t} + \nabla(-D\nabla m) = \dot{m}_s^{II}$$

(Faghri, *et al.*, 2010) (7)

$$\hat{r}^2 \frac{\partial M}{\partial t} + \frac{\partial}{\partial \hat{r}}\left(-\frac{1}{R_m{}^2}\nabla \hat{r}^2 \frac{\partial M}{\partial r}\right) = \hat{r}^2 \dot{m}_s^{II} \quad (8)$$

Due to symmetry about r = 0, there is zero flux through this point meaning $\frac{\partial}{\partial \hat{r}} = 0$

At the surface, $\hat{r} = 1$, a convective heating expression was used with heat transfer coefficient $h_s(W/m^2K)$ for the influx of heat ($W/m^2$): $q_{in} = h_s(T_{air} - T)$ (9)

Initial moisture content, $M_0$= 80%, initial temperature $T_0$= 27°C

Heat transfer boundary conditions:

At open boundary: ($k\nabla T$) = $h_s$ ($T_{air} - T$)

At symmetry and other boundary: ($k\nabla T$) = 0

Mass transfer boundary conditions:

At open boundary: ($D\nabla M$) = $h_m$ ($M_m - M$)

At symmetry and other boundary: ($D\nabla M$) = 0

### 2.5.2 COMSOL Implementation

The 1D time dependent version of the General form PDE equation system was used to implement the heat and mass transfer equation

$$e_a \frac{\partial^2 u}{\partial t^2} + d_a \frac{\partial u}{\partial t} + \nabla.\Gamma = \text{Fin } \Omega, \quad (10)$$

$$n.\Gamma = G - hT\mu \text{ on } \partial\Omega, \quad (11)$$

$$0 = R \text{ on } \partial\Omega. \quad (12)$$

The space coordinate in the model is $\hat{r}$. For typographical reasons $r_h$ was used for "r-hat". Using radial coordinate to rewrite the heat and mass transfer equation and identifying the general form, the following setting shown in Table 1 generates the correct equation;

Table 1: Equations Generated for Comsol Implementation.

| Coefficient | Expression (Temperature) | Expression (Moisture) |
|---|---|---|
| $e_a$ | 0 | 0 |
| $d_a$ | $\hat{r}^2 \rho_s Cp_s$ | $\hat{r}^2$ |
| $\Gamma$ (flux vector) | $-\frac{1}{R_m{}^2} k_s \hat{r}^2 \frac{\partial T}{\partial r}$ | $-\frac{1}{R_m{}^2}\nabla \hat{r}^2 \frac{\partial M}{\partial r}$ |
| F (source term) | 0 | 0 |

Special care was taken when setting the heat flux boundary condition on the moringa leaf surface $h_s$ ($T_{air} - T$) = $k_s \frac{\partial T}{\partial r}$, so G needs to be accordingly compensated.

$$G = \frac{\hat{r}^2}{R_m{}^2} h_s (T_{air} - T) \quad (13)$$

$$G = \frac{\hat{r}^2}{R_m{}^2} h_m (M_m - M) \quad (14)$$

## 3. Results and Discussion:

### 3.1. Thermal Properties Results

The results of thermal properties are presented in Table 2. From the results presented in the table the highest properties were obtained at 27.15°C and can also be seen that temperature affects thermal properties of the moringa.

Table 2: Properties of moringa of obtained experimentally.

| Temperature (°C) | Thermal Conductivity [W/m.K] | Diffusivity [$m^2$/s] | Specific Heat [J/kg.K] | Moisture content [%] |
|---|---|---|---|---|
| **27.43** | 0.506 | 0.162 | 3.130 | 82.876 |
| **27.15** | 0.517 | 0.194 | 2.668 | 82.488 |
| **26.85** | 0.482 | 0.156 | 3.098 | 82.727 |

The moisture profile of the product with time is shown in Fig. 3 for drying at a velocity of 2.2m/s and 1.2m/s. It is evident that moisture content is reduced faster at a higher velocity.

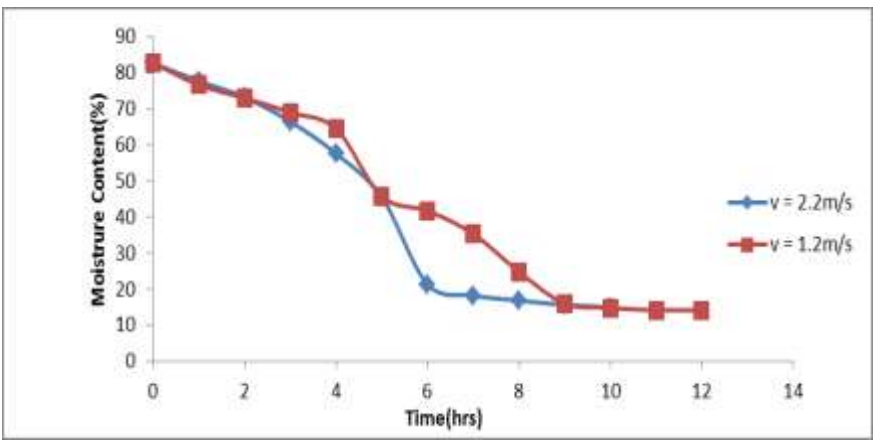


Fig 3: Moisture profile at different velocities (v=2.2m/s and v=1.2m/s).

Figure 4 represents the moisture content with drying time for the three trays in the drying chamber at a velocity of 2.2m/s. It shows that products in tray 3 give off moisture faster than any of the other two trays (moisture reduced up to 65% in about 4 hours). This is because it is the closest to the absorber. The air flowing to it has very low humidity and has the highest temperature, making it possible for moisture to leave at the highest rate. Tray 1 dries moisture faster than tray 2 but not as fast as tray 3. This is because it is the farthest from the absorber but the closest to the chimney opening. Being close to the chimney opening makes it possible for air to leave the tray faster than the rate at which it leaves tray 2.

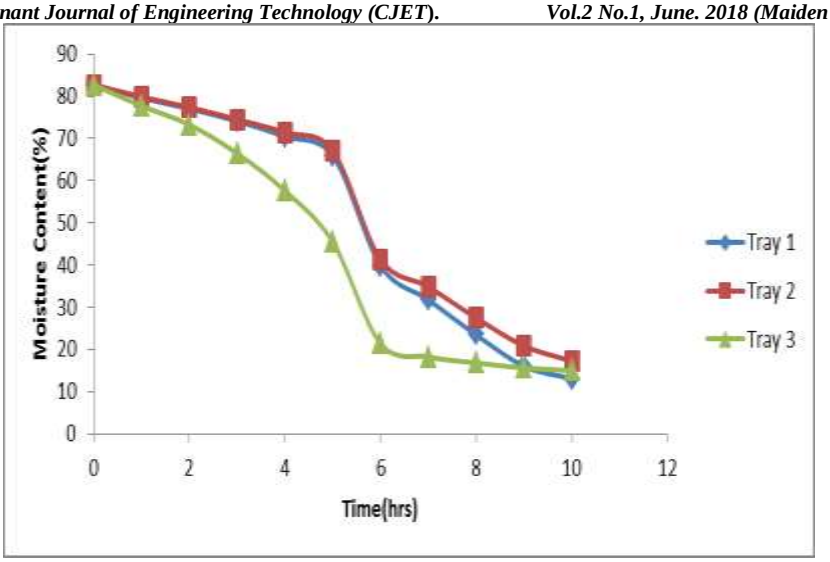


Fig 4: Moisture profile for tray 1, 2 and 3 (for v=2.2m/s)

It is evident from Fig. 5 that a higher velocity leads to a higher temperature of the product. It also results in high rate of increase in temperature. This is due to the fact that heat is diffused faster when the speed at which air is moving is higher. The moisture leaving the product are also transported faster at higher speed, leading to high reduction rate in moisture content and consequent increase in temperature of the product.

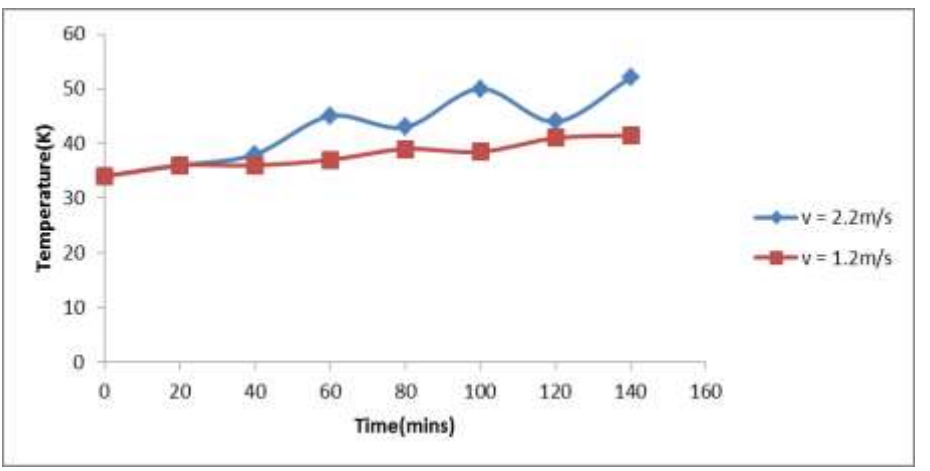


Fig 5: Temperature profile obtained at different velocity (v=2.2m/s and v=1.2m/s).

### 3.2. Comparing Simulated Results with Experimental Results

The temperature evolution of the product is shown in Figs. 6 and 7 for velocity of 2.2m/s and 1.2m/s respectively with a mean drying air temperature of 45°C. It can be seen that the predicted temperatures agreed with those obtained experimentally at some points and

deviated a little at some other points. This may be as a result of certain human factors and challenges incurred during the experimental procedure.

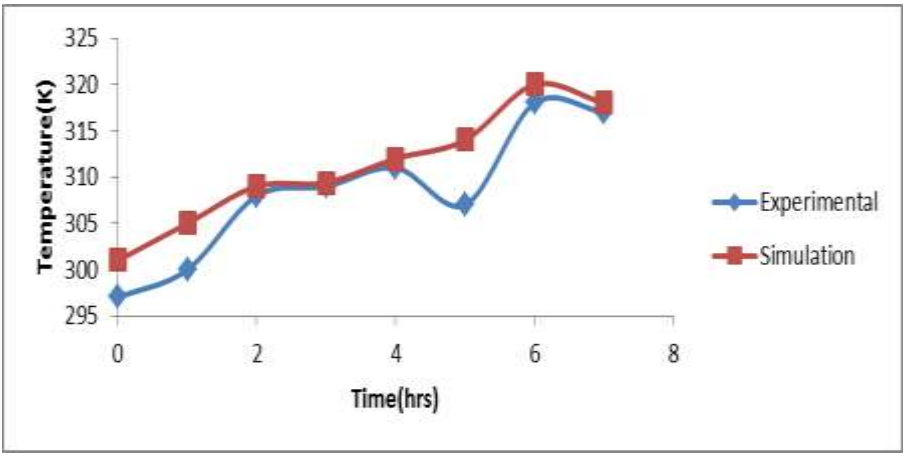


Fig 6: Temperature profile obtained for experimental and simulation procedures (for v=2.2m/s).

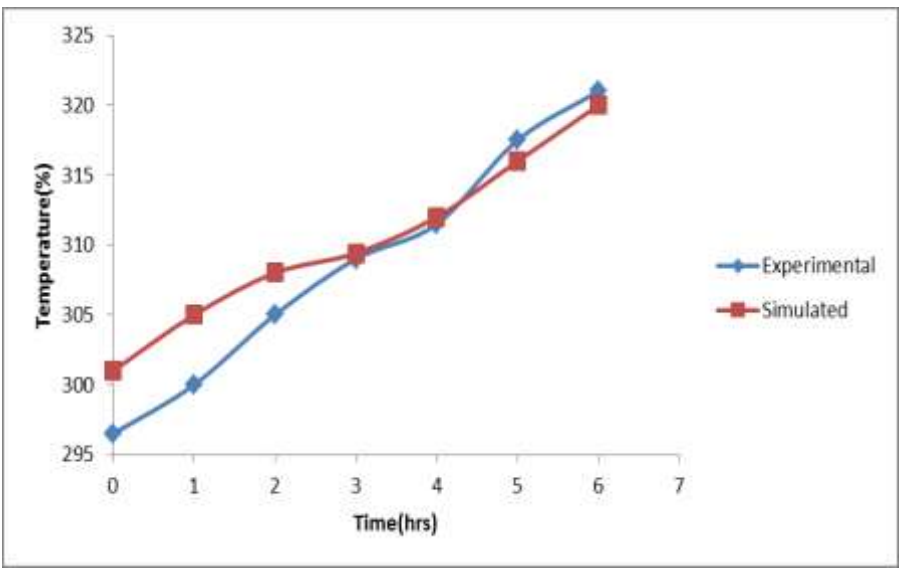


Fig 7: Temperature profile obtained for experimental and simulation procedures (for v=1.2m/s).

The moisture content with drying time is represented in Figs. 8 and 9 for velocity of 2.2m/s and 1.2m/s respectively. It shows that the simulated results and predictions are in accordance with experimental results at a velocity of 2.2m/s.

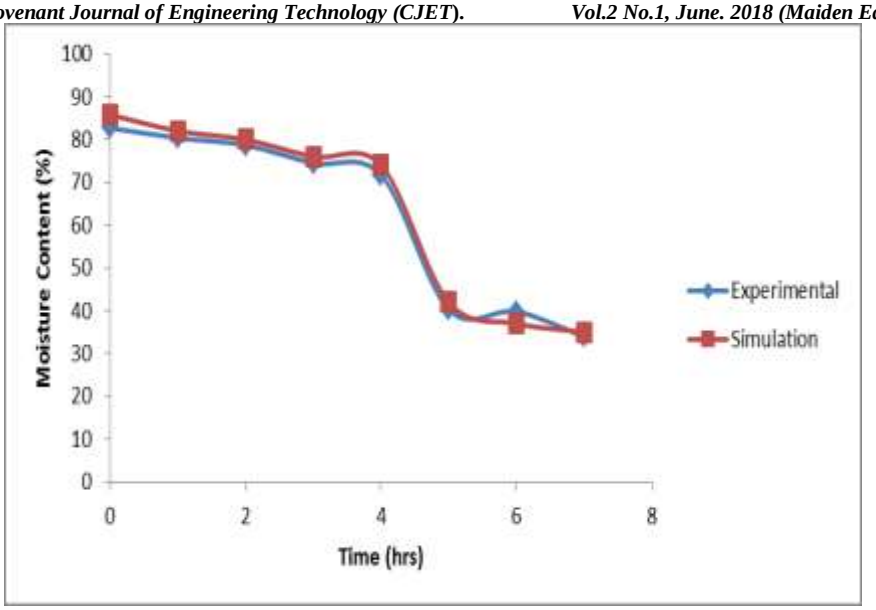


Fig 8: Moisture profile obtained for experimental and simulation procedures (for v=2.2m/s)

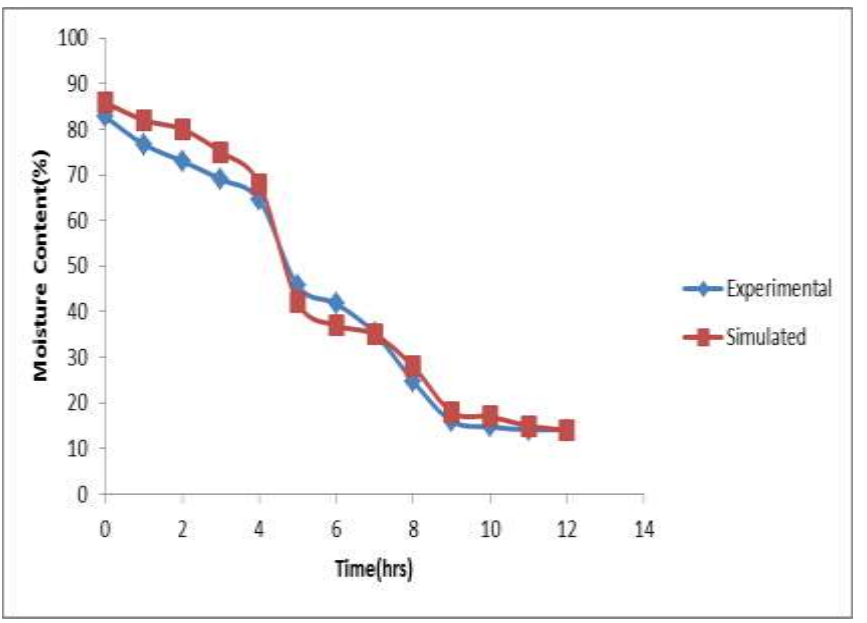


Fig. 9: Moisture profile obtained for experimental and simulation procedures (for v=1.2m/s)

## 4. Conclusion

Moringa leaves were successfully dried using the designed and fabricated dryer. The dried product obtained supports the fact that the solar dryer performs better than open air drying for drying moringa. This is seen in the physical appearance of

the product and the increased rate of drying the leaves. The best product was obtained when performing the drying process at a velocity of 2.2m/s due to the fact that products dried faster and looks better than when performing it at a velocity of 1.2m/s.The simulated and experimental results revealed that the rate of drying is increased at a higher velocity. These results are also similar, which indicates that simulating the drying process can be as effective as performing the experiment with a dryer. Solar dryer was perceived to be an effective equipment for drying leaves.

## 5. Nomenclature

| | |
|---|---|
| $\eta_d$ | Efficiency of the dryer |
| M | Mass of moisture evaporated per second (kg/s) |
| L | Latent heat of evaporation of water (kJ/kg) |
| $I_t$ | Insolation on tilted collector surface (W/$m^2$) |
| $A_c$ | Collector area ($m^2$) |
| $Arac$ | Effective drying rack area |
| $M_p$ | Mass of moringa, |
| $P_{gr}$ | Bulk density of moringa on wet basis, |
| $h_L$ | Depth of drying rack, |
| $\epsilon$ | Crop porosity, |
| $\varepsilon_v$ | Loading bed void fraction, |
| $T_a$ | Temperature of drying air leaving the collector, |
| $\rho_s$ | Density of solid (kg/$m^3$) |
| $Cp_s$ | Heat capacity of solid (J/kgK) |
| $k_s$ | Thermal conductivity of solid (W/mK) |
| $Q_s$ | Internal heat source (W/$m^3$) |
| R | Specific gas constant, |
| $T_0$ | Temperature at collector outlet |
| $T_a$ | Temperature of drying air leaving the collector, |
| g | Acceleration due to gravity |
| H | Height of the drying chamber |
| $P_a$ | Atmospheric pressure |

## 6. References

Amedorme, S., Apodi, J., and Agbezudor, K. (2013). Design and Construction of Forced Convection Indirect Solar Dryer for Drying Moringa Leaves. *Scholars Journal of Engineering and Technology (SJET), 1*(3), 91-97.

Barati, E., and Esfahani, J. (2011). Mathematical modelling of convective drying: Lumped temperature and spatially distributed moisture in slab Energy. *36*(4), 2294-2301.

Bolaji, B., and Olalusi, A, Department of Mechanical Engineering, Univerisity of Agriculture, Abeokuta, Ogun State, Nigeria, (2005).

Bolaji, B,O., (2005). Performance evaluation of a simple solar dryer for food preservation. Proc. 6th Ann. Engin. Conf. of School of Engineering and Engineering Technology, Minna, Nigeria, pp. 8-13.

Curcio, S. (2006). A FEM analysis of transport phenomena occuring during vegetables drying. *Proceeding of the COMSOL Conference.* Milano

Faghri, A., Zhang, Y., and Howell, J. (2010). *Advanced Heat and Mass Transfer*. Global Digital Press.

Kumar, C, Karim, A, Saha, S.C, Joardder, M.U.H, Brown, R, and Biwas, D., (2012). Multipysics Modelling of Convective Drying of Food Materials. Proceedings of the Global Engineering, Science and Technology conference, Dhaka, Bangladesh.Mujumdar, A. (2007). *Handbook of Industrial Drying* (2nd Edition ed.). New York: Marcel Dekker.

Rajibul, M., and Norma, A. (2010). Some Numerical Methods for Temperature and Mass Transfer Simulation on the Dehydration of Herbs. *International Journal of Computer and Electrical Engineering, 2*(4), 1793-8163.

**Covenant Journal of Engineering Technology (CJET) Vol. 1, No. 2, Sept. 2018**

An Open Access Journal Available Online

# Waste Cooking Oil Methyl Ester: Transesterification and Evaluation of Corrosion Rates of Aluminium Exposed to Blended Biodiesel and Automotive Gas Oil

**Olusegun D. Samuel [1*], Taofeek A. Yusuf [2]**

[1]Department of Mechanical Engineering,
Federal University of Petroleum Resources,
Effurun, Delta State, Nigeria
[2] Department of Mechanical Engineering,
University of Agriculture,
Markudi, Benue State, Nigeria

***Abstract***: This study investigated the corrosion of aluminum exposed to biodiesel produced from Waste Cooking Oil (WCO) and Automotive Gas Oil (AGO) blends. Response Surface Methodology (RSM) with three level-three factor central composite design was used in investigating the effects of transesterification variables such as reaction time, catalyst amount and oil/methanol molar ratio on the yield of waste cooking oil methyl ester (WCOME). Reaction time between 40 - 80 min., catalyst amount of 0.5 - 1.5% wt. and methanol to oil molar ratio of 4 - 8 were used in the transesterification experiment. Optimization of process variables was done using RSM. The fuel properties of biodiesel at optimum level in terms of density, kinematic viscosity, flash, pour and cloud points and sulphur content were obtained using standard method as described by ASTM. Blends of WCO biodiesel 0, 10, 20, 40 and 100% of AGO were designated as B0, B10, B20, B40 and B100 respectively. Corrosion characteristics of blends on aluminium (Al) were studied by static immersion test at room temperature. Mechanical properties of the Al were investigated before and after corrosion test. Changes in the morphology of coupons were also investigated. The optimization technique predicted WCOME yield of 97.1% at the optimal level of 78 minutes, 5.99, 1.1% wt. for the reaction time, methanol to oil molar ratio and catalyst amount respectively. The fuel properties at the optimal level were within the

limits specified by ASTM D6751 and EN 14214 standards. The ranges of corrosion rates obtained for the blends were 0-0.2830 mpy. The Brinell hardness ranged for the blends were 105.012, 109.177, 133.717, 155.393, 166.803 N/mm$^2$ while the tensile strength for the blends were 371.20, 386.12, 484.62, 495.22 and 592.89 MPa for B0, B10, B15, B20, B40 and B100 respectively. As the percentage of biodiesel in the blends increased, crack and pits on the morphology of the coupons become pronounced. The blend B10 was detected to perform close to B0 with respect to the Brinell hardness and tensile strength.

***Key Words*:** Biodiesel, Corrosion, Hardness, Tensile Strength, Optimization

## 1. Introduction

Geometrical demand and the escalating price of fossil diesel coupled with environmental degradation have propelled researchers to seek for renewable energy sources that are sustainable and environmental friendly [1, 2]. Owing to the technical advantages associated with biodiesel, it has been preferred to other biofuels such as biogas, solid fuel and bio-ethanol. Biodiesel has gained wider acceptance due to its inherent lubricity, higher cetane, superior flash point, biodegradability, higher cetane number, reduced toxicity and reduced exhaust emissions [3]. However, biodiesel has been linked with degradation of elastomers and corrosion of automotive parts when exposed to renewable fuel [4]. The key parts of vehicular diesel engine such as cylinder head, piston, connecting rod and cylinder sleeves are made of aluminum and they are always in contact with fuel [5]. Sing et al. [5] further stressed that corrosion of aluminum is aggravated either by the impurities in biodiesel or the deterioration of biodiesel. Chew et al. [6] emphasized that the degradation can be attributed to changes in simulated environments such as nature of the fuel, acid content, water and hygroscopic environments. Corrosion of biodiesels produced from lipid feedstocks such as jatropha oil, palm oil, sunflower oil and rapeseed oil with aluminum and other metals have been investigated by researchers [2, 6-8]. Their results indicated that corrosiveness of the biodiesel is higher than diesel. Reports abound on the corrosion studies of lipid feedstock oils afore-mentioned in the literature; however, no work has been reported on the corrosion of light alloy automotive parts exposed to optimized biodiesel from waste cooking oil and its blends. In spite of colossal consequence occasioned by metallic interactions with the alternative fuels, information regarding the spectrum of biodiesel-diesel will provide insight information for effective planning and feasibility tendency to reduce the menace of corrosion. The study has not only examined the optimal production condition of methyl ester from waste cooking oil but also investigated the corrosion characteristics of aluminum resulting from the optimal condition and automotive gas oil mixture/diesel blends.

## 2. Materials and Method

### 2.1. Materials and Analysis of Oil

Waste cooking oil (WCO) donated by United African Company,

restaurant in Sango, Lagos State, Nigeria was utilized for the production of biodiesel from the WCO. The chemicals such as methanol, ethanol and KOH were of analytical grade and the fossil diesel employed for blending process was purchased from Jocceco Filling station, Warri, Delta State, Nigeria.

Machining from the bars was coupon of aluminium which is 99% commercially pure (35 mm length x 25 mm breadth x 2 mm thickness) was used as coupon for corrosion assessment.

Analysis of properties of WCO was conducted by determining the physicochemical properties.

### 2.1.1. Adoption of response surface method for methyl ester of WCO

Transesterification of WCO was conducted in a 2 L reactor, equipped with a reflux condenser and a magnetic stirrer. The waste cooking oil methyl ester (WCOME) was produced by an alkaline transesterification and the transesterification protocol was well expounded in [9]. The WCOME was oven dried at 90 $^{o}$C and average yield of WCOME was determined.

Presented in Table 1 is the range of reaction time ($X_1$), molar ratio ($X_2$), and catalyst amount ($X_3$) investigated on the yield of WCOME.

The graphical analysis of the interactions of the transesterification variables versus WCOME were studied using Eq. (1)

$$Y = \emptyset_0 + \emptyset_1 x_1 + \emptyset_2 x_2 + \emptyset_3 x_3 + \emptyset_{12} x_1 x_2 + \emptyset_{13} x_1 x_3 - \emptyset_{23} x_2 x_3 - \emptyset_{11} x_1^2 + \emptyset_{22} x_2^2 \quad (1)$$

where Y is the predicted yield of WCOME (%), $\emptyset_0$ is the intercept, $\emptyset_1$ , $\emptyset_2$ $and$ $\emptyset_3$ linear coefficients, $\emptyset_{12}, \emptyset_{13}$ $and$ $\emptyset_{23}$ are the interactive coefficients, $\emptyset_{11}, \emptyset_{22}$ $and$ $\emptyset_{33}$ are the polynomial coefficients and $x_1$, $x_2$ and $x_3$ are the coded variables.

Table 1 Independent parameters and levels employed for the WCOME

| Independent variable | Ranges and their levels | | | |
|---|---|---|---|---|
| | Symbols | -1 (low) | 0 (medium) | 1 (high) |
| Reaction time (min) | $X_1$ | 40 | 60 | 80 |
| Oil/methanol molar ratio | $X_2$ | 4.0 | 6.0 | 8.0 |
| Catalyst amount (wt.%) | $X_3$ | 0.5 | 1.0 | 1.5 |

### 2.1.2 Waste Cooking Oil Methyl Ester Blends

Detailed properties of WCOME/Automotive Gas Oil blends such as kinematic viscosity, density, sulphur content, boiling point, cetane number cloud point and pour point and acid value of the WCOME synthesized were analyzed following international biodiesel standards.

### 2.1.3 Corrosion Testing of Aluminium in Automotive Gas Oil-WCOME blends

To conduct corrosion testing, aluminium of 35 mm length/25 mm breadth/2 mm thickness were prepared from bar after grinding operation. At the edge of the coupon, a hole of 3.5 mm was drilled. Before immersion, the coupon was dipped in acetone after it had been degreased, polished and weighed. The prepared

coupons were subjected to a static immersion as reported elsewhere [10]. At every 240 hours, the corrosion rate (CR) of the coupon exposed to the fuel types was estimated using the expression stipulated in Eq. (2).

$$CR = \frac{W_L 534}{\rho_{Br} A_{Al} T_e} \quad 1$$

where $W_L, \rho_{Br}, A_{Al}$ and $T_e$ are weight loss (mg), density of aluminium (g/cm$^3$), total surface area (square inch) and exposure duration (hours).

The hardness of the coupon prior and after exposure was determined by the Brinell hardness testing machine situated in the Mechanical workshop, Petroleum Training Institue, Effurun, Delta State, Nigeria and it was determined according to ASTM E10 [11].

Estimation of the ultimate tensile strength (UTS, MPa) for the aluminium after being exposed to the fuel types were done using the expression highlighted in Eq. (3)

$$UTS = 3.4\,BHN \quad 3$$

Before exposing and after immersing the coupon to the fuel types, the morphology of the aluminium was detected by the JCM 100 mini scanning electron microscope (Joel, USA). Moreover, changes in the basic fuel properties such as density, viscosity, total acid number of fuel types before and after being exposure to aluminium were also examined.

## 3. Results and Discussion

### 3.1 Quality of Waste Cooking Oil

The quality of waste cooking oil (WCO) was detected by analyzing the significant properties of WCO and comparing with those of Vietnam waste cooking oil (VWCO), sunflower waste cooking oil (SWCO), Morrocan waste frying oil (MWFO), diesel fuel (B0) and international biodiesel standards, as presented in Table 2.

The acid value (AV) of WCO (0.84 mg KOH/g) was found to be moderate compared to those SWCO (1.83 mg KOH/g) [12] and MWFO (0.98 mg KOH/g) [13]. As a result of low AV of WCO, the oil will not be subjected to the acid pre-treatment. Hence, the WCO was subjected to alkaline transesterification since its AV certified the requirement needed for alkaline transesterification [14-15]. The moisture content of the WCO (0.08 %w/w) certified the norms of EN14214 and ASTM D6751 (0.05 %w/w max) standards. Hence, the ester conversion will not be significantly affected [16]

The viscosity of the WCO (33.17 mm$^2$/s at 40 $^o$C) was found to be extremely high and 9 times higher than that of B0 (3.61 mm$^2$/s at 40 $^o$C). The viscosity of WCO is comparable to those of VWCO (33.47 mm$^2$/s at 40 $^o$C) [17], SWCO (36.6 mm$^2$/s at 40 $^o$C) [12], MWFO (36.3 mm$^2$/s at 40 $^o$C) [13] but higher than those ASTM (1.9-6.0 mm$^2$/s at 40 $^o$C) and EU (3.5-5.0 mm$^2$/s at 40 $^o$C) standards. The higher viscosity of WCO had been reported to limit mixing of oil during transesterification [18].

The density of WCO (931 kg/m$^3$) is comparable with those of SWCO (921.9 kg/m$^3$), MWFO (962 kg/m$^3$) and VWCO (920 kg/m$^3$), as hinted by EL-Gendy et al. [12], Nachid et al. [13] and Phan and Phan [17], respectively but lower than that of B0 (850 kg/m$^3$) and certified the range of EU14214 standard (860-900 kg/m$^3$).

The lower calorific value of WCO (36.20 MJ/kg) was lower than that of B0 (43.79). The higher calorific value of WCO (38.40 MJ/kg) was lower than those of B0 (46.77 MJ/kg) and waste frying oil (45.34 MJ/kg) reported by Al-Hamamre and Yamin [18]. The presence of oxygen content has been attributed to the lower heating values in biodiesel [19].

Table 2 Physicochemical properties of waste cooking oil

| Properties | WCO [a] | VWCO [b] | SWCO [c] | MWFO [d] | BO [a] | ASTM D6751-02 | EU 14214 |
|---|---|---|---|---|---|---|---|
| Acid value (mgKOH/g | 0.84 | 3.64 | 1.85 | 0.98 | NA | 0.50 max | 0.50 max |
| Moisture content wt.% | 0.08 | - | - | ND | 0.02 | 0.05 | 500 max |
| Kinematic viscosity ($mm^2/s$) | 33.17 | 33.47 | 36.6 | 36.3 | 3.61 | 1.9-6.0 | 3.5-5.0 |
| Density ($kg/m^3$) | 931 | 920 | 921.9 | 96.2 | 850 | NS | 860-900 |
| Lower calorific value (MJ/kg) | 36.20 | ND | ND | ND | 43.79 | NS | NS |
| Higher calorific value (MJ/kg) | 38.40 | ND | ND | ND | 46.77 | NS | NS |

a, Present study; b, Phan and Phan [17]; c, EL-Gendy et al. [12]; d, Nachid et al. [13]; ND, Not determined; NS, Not specified.

### 3.2. Transesterification Process

Highlighted in Table 3 is the experimental and predicted value for WCOME yield at the design points and all the three parameters in coded form. The response polynomial obtained to compute the yield of WCOME including all experimental variables is represented by Eq. (4) in terms of coded experimental variables and Eq. (5) in terms of actual experimental variables.

$$Y = 93.18 + 3.80x_1 + 0.63x_2 + 7.35x_3 - 0.77x_1^2 - 5.67x_2^2 - 18.12x_3^2 - 1.70x_1x_2 + 2.14x_1x_3 - 1.51x_2x_3 \quad (4)$$

$$Y = -76.81 + 0.46X_1 + 21.39X_2 + 155.94X_3 - 0.001922X_1^2 - 1.42X_2^2 - 72.50X_3^2 - 0.043X_1X_2 + 0.21X_1X_3 - 1.51X_2X_3 \quad (5)$$

where Y is the yield of waste cooking methyl ester, $x_1$, $x_2$ and $x_3$ are coded experimental values for reaction time ($X_1$), oil/methanol molar ratio ($X_2$) and catalyst amount ($X_3$), respectively.

The graph between the predicted and actual ester yield (%) is presented in Fig. 1. The closeness of the predicted value to the experimental implies that model developed can be employed to correlate the transesterification variables and the WCOME yield.

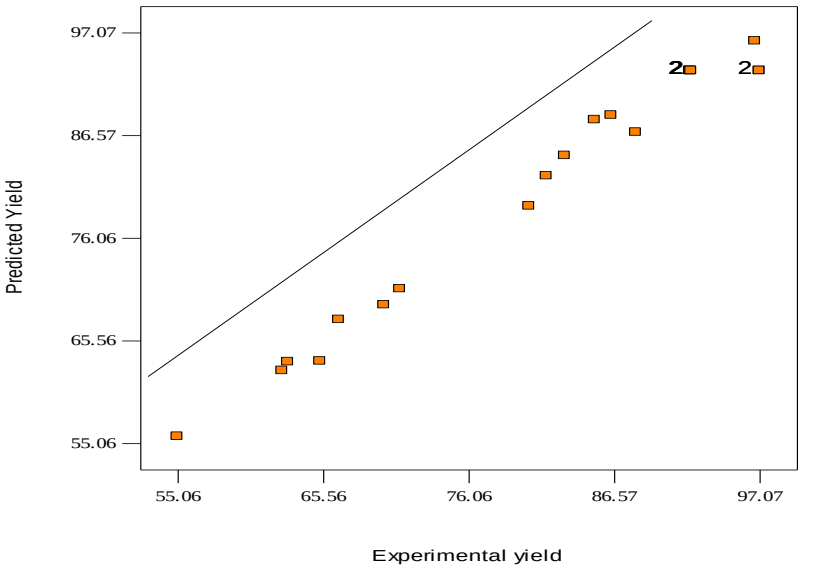


**Fig. 2** Plot of predicted yield versus experimental yield of waste cooking oil methyl ester

**Table 3** Design matrix for the three-factor three level face centered central composite design in coded variables

| | Coded factors | | | Biodiesel Yield (%) | | |
|---|---|---|---|---|---|---|
| | Reaction time (min) | | Methanol to oil molar ratio | Catalyst amount (% w/w) | | |
| Run | $x_1$ | $x_2$ | $x_3$ | Experimental | Predicted | Residual |
| 1 | -1 | -1 | -1 | 55.06 | 55.76 | -0.70 |
| 2 | 1 | -1 | -1 | 62.63 | 62.49 | 0.14 |
| 3 | -1 | 1 | -1 | 65.36 | 63.46 | 1.90 |
| 4 | 1 | 1 | -1 | 63.04 | 63.38 | -0.34 |
| 5 | -1 | -1 | 1 | 69.97 | 69.21 | 0.76 |
| 6 | 1 | -1 | 1 | 83.01 | 84.48 | -1.47 |
| 7 | -1 | 1 | 1 | 71.13 | 70.85 | 0.28 |
| 8 | 1 | 1 | 1 | 80.45 | 79.32 | 1.13 |
| 9 | -1 | 0 | 0 | 86.38 | 88.61 | -2.23 |
| 10 | 1 | 0 | 0 | 96.75 | 96.21 | 0.54 |
| 11 | 0 | -1 | 0 | 88.15 | 86.88 | 1.27 |
| 12 | 0 | 1 | 0 | 85.18 | 88.15 | -2.97 |
| 13 | 0 | 0 | -1 | 66.71 | 67.71 | -1.00 |

| | | | | | | |
|---|---|---|---|---|---|---|
| 14 | 0 | 0 | 1 | 81.71 | 82.40 | -0.69 |
| 15 | 0 | 0 | 0 | 97.07 | 93.18 | 3.89 |
| 16 | 0 | 0 | 0 | 92.04 | 93.18 | -1.14 |
| 17 | 0 | 0 | 0 | 92.04 | 93.18 | -1.14 |
| 18 | 0 | 0 | 0 | 97.07 | 93.18 | 3.89 |
| 19 | 0 | 0 | 0 | 92.13 | 93.18 | -1.05 |
| 20 | 0 | 0 | 0 | 92.13 | 93.18 | -1.05 |

### 3.3 Optimization of Waste Cooking Oil Methyl Ester

The yield of WCOME and the process variables are presented in Fig. 2. It was noticed that WCOME yield increased with an increase in the reaction temperature. Similar observation was also reported by Dwivedi and Sharma [20]. WCOME yield is noticed to increase with the methanol to oil molar ratio beyond stoichiometric ratio (3:1 molar ratio) but decreased beyond molar ratio of 6:1 M.

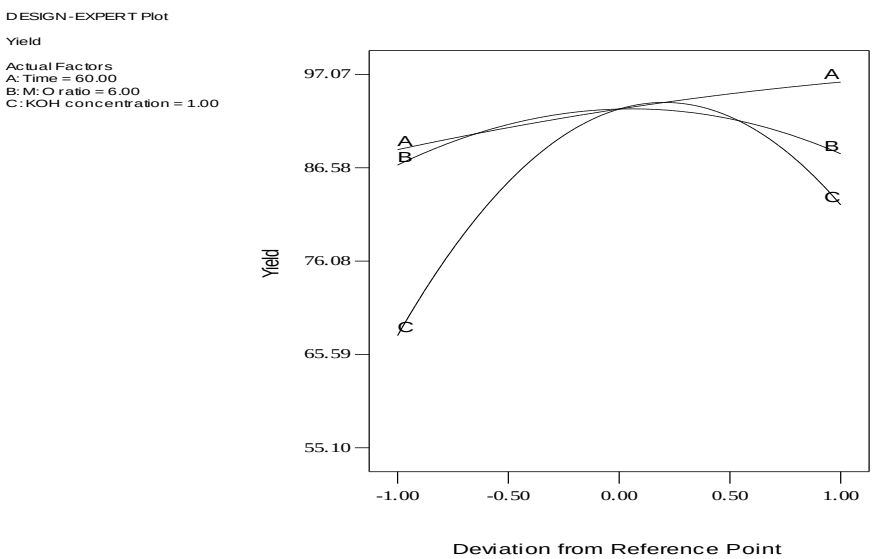


**Fig. 2** Effect of reaction time, molar ratio and catalyst amount on yield of WCOME

### *3.4.* Influence of Transesterification Variables and Optimization of Waste Cooking Oil Methyl Esters

The contour plots and response surface for conversion yield of waste cooking oil methyl ester depending on methanol/oil molar ratio and reaction time (Fig.3a), reaction time and catalyst amount (Fig. 3b) and methanol/oil molar ratio and catalyst amount (Fig.3c), while the third parameter is kept constant at the optimum value are depicted in Fig. 3. The 3D response curve and contour plot of ester yield versus methanol molar ratio and reaction time are shown in Fig. 3a. The WCOME yield of 83.22-93.65% was obtained within the range of 4:1-8:1 M for WCOME as the reaction time was varied from 40 to 80 $^{o}$C. The optimum WCOME

yield (93.65%) was obtained at 6:1 M methanol/oil molar ratio with 60 min reaction time. However, the ester conversion was observed to reduce with a further increased in molar ratio.

As can be observed in Fig. 3b, ester conversion is moderate when the catalyst amount was 0.75 wt.% with the reaction time. There is a decline in WCOME yield when the catalyst amount is increased beyond 1.0 w/w%. The reduction in ester conversion has been linked to the formation of emulsion and gel formation [21]. The highest WCOME yield (93.65%) was attained at a catalyst amount of 1.0 wt.% and reaction time of 60 min.

It was noticed from Fig. 3c that catalyst amount in the range of 0.50-1.50 wt.% and methanol/oil molar ratio of 4:1-8:1 had an ester yield of 83.22-93.65%. In this study, the optimum condition was achieved at 6:1 methanol/oil molar ratio with 1 wt.% of KOH amount.

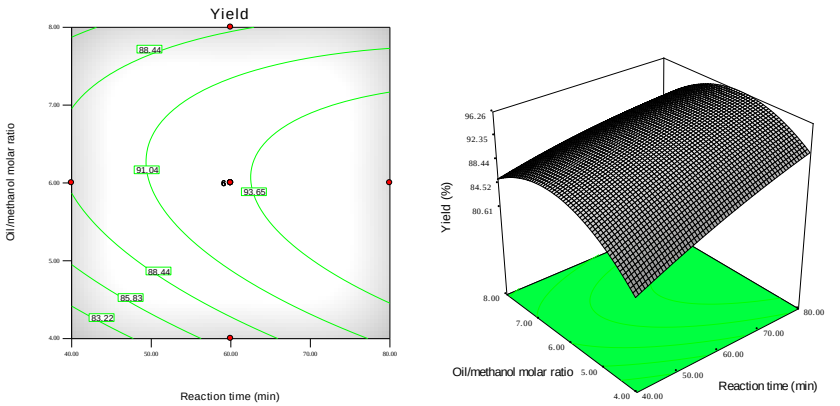


(a)

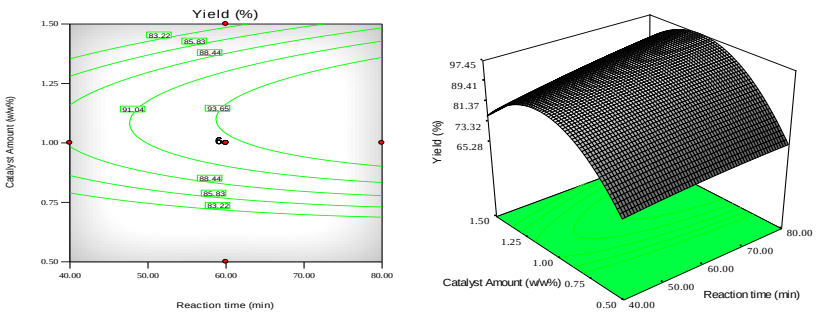


(b)

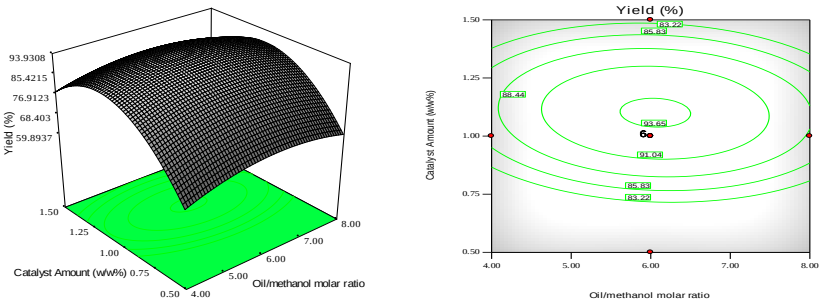


(c)

**Fig. 3** Contour plots and response surface of conversion yield of waste cooking oil methyl ester as a function of (a) methanol/oil molar ratio and reaction time, (b) reaction time and catalyst amount and (c) methanol/oil molar ratio and catalyst amount

### 3.5. Optimization of response parameters

The sets of optimized solutions for optimal production of the WCOME are detailed in Table 4. The reaction time (77.6 minutes), methanol to oil molar ratio (5.99) and catalyst amount (1.11%w/w) with a predicted yield of 97.1% was chosen as the optimized parameters points. After validation, average between the predicted and actual values was found to be 0.03%.

**Table 4** Optimization summary for modified yield response model

| Solution Number | Reaction Time ($X_1$) (min) | Methanol to Oil Molar Ratio ($X_2$) | Catalyst Amount ($X_3$) (% w/w) | Estimated Yield of Waste Cooking Oil Methyl Ester (%) |
|---|---|---|---|---|
| 1 | 77.60 | 5.99 | 1.10 | 97.07* |
| 2 | 77.62 | 5.81 | 1.11 | 97.16 |
| 3 | 77.54 | 5.82 | 1.11 | 97.12 |
| 4 | 77.64 | 6.00 | 1.11 | 97.08 |
| 5 | 77.64 | 5.69 | 1.15 | 97.15 |
| 6 | 78.01 | 5.67 | 1.13 | 97.22 |
| 7 | 79.34 | 5.62 | 1.15 | 97.40 |
| 8 | 79.69 | 6.15 | 1.15 | 97.23 |
| 9 | 77.35 | 5.81 | 1.13 | 97.13 |
| 10 | 79.75 | 6.05 | 1.12 | 97.37 |

* Optimal value selected

Summarized in Table 5 are the properties of produced waste cooking oil methyl ester (WCOME) and its comparison with those Vietnam waste cooking oil methyl Ester (VWCOME), ASTM D6751 and EN 14214 biodiesel standard specifications. The properties of WCOME concurred with those of VCOME and standard specifications. The boiling point (BP) of WCOME (310 $^{o}$C) was higher than that of diesel (290 $^{o}$C) but was not specified by the ASTM D6751 and EN 14214

standards. This indicates that WCOME will not evaporate at low temperature. The high BP of the WCOME has been associated with the absence of volatile compound [22]. The sulphur content of B0 (0.2905 mg) was found to be higher than that of WCOME (0.0071 mg). The finding is in agreement with the report of Bamgboye and Oniya [23]. Fuel of low SC has been associated with a reduction in the environmental pollution during combustion process [24].

**Table 5** Fuel properties of WCOME in comparison with those of VWCOME and European and American Standards

| Property | Unit | Waste Cooking Oil Methyl Ester [a] | ASTM Standard D6751-02 | EU Standard EN14214 | VWCOME [b] | B0 |
|---|---|---|---|---|---|---|
| Density; 15 °C | $kg/m^3$ | 883.34 | NS | 860 – 900 | 880 | 850 |
| Kinematic viscosity; 40 °C | $mm^2/s$ | 4.31 | 1.9 - 6.0 | 3.5 - 5.0 | 4.89 | 3.61 |
| Flash point | °C | 155 | 130 min | 120 min | 120 | 75 |
| Acid value | mg KOH/g | 0.40 | 0.5 max | 0.50 max | 0.43 | - |
| Cloud Point | °C | 2 | Report | - | 3 | -8 [a] |
| Pour Point | °C | -12 | <0 | <0 | 0 | -18 |
| Mid-Boiling point | °C | 310 | | | - | 290 [a] |
| Sulphur Content | mg | 0.0071 | <15.0 | <10.0 | - | 0.2905 |
| Higher Heating value | MJ/kg | 40.07 | - | - | | 46.77 |
| Cetane number | | 61 | 47 | 51 min | - | 48 [a] |

a, Present study; b, Phan and Phan [17]; NS, Not specified.

### 4.5. Characterization of WCOME and its Automotive Gas Oil/Conventional Fuel

Depicted in Figs. 4a-e is the influence of WCOME content on the respective thermophysical properties such as density, kinematic viscosity, flash point, cloud and pour point and sulphur content. Significant improvement in density, kinematic viscosity and flash point (FP) were noticed. Conversely, sulphur content value reduced while cloud point (CP) and pour point (PP) became worsened as the fraction of WCOME advanced in the blends. The higher density of WCOME resulted in more fuel being injected. Fuel of higher viscosity has been remarked to generate good spray across the combustion chamber [18]. In addition, fuel types having higher flash point has been preferred to that of lower FP as it can be properly stored, transported and powered diesel engine without fire hazard [25].

Fuel having lower sulphur content has been remarked to reduce sulphur (VI) oxide if a diesel engine is powered with WCOME [22]. However, WCOME of high CP and PP has been limited for wider utilization in cold and artics regions as they can result in fuel line clogging [26]. In order to reduce the limitation, cold flow improvers have been suggested by researchers [27-31].

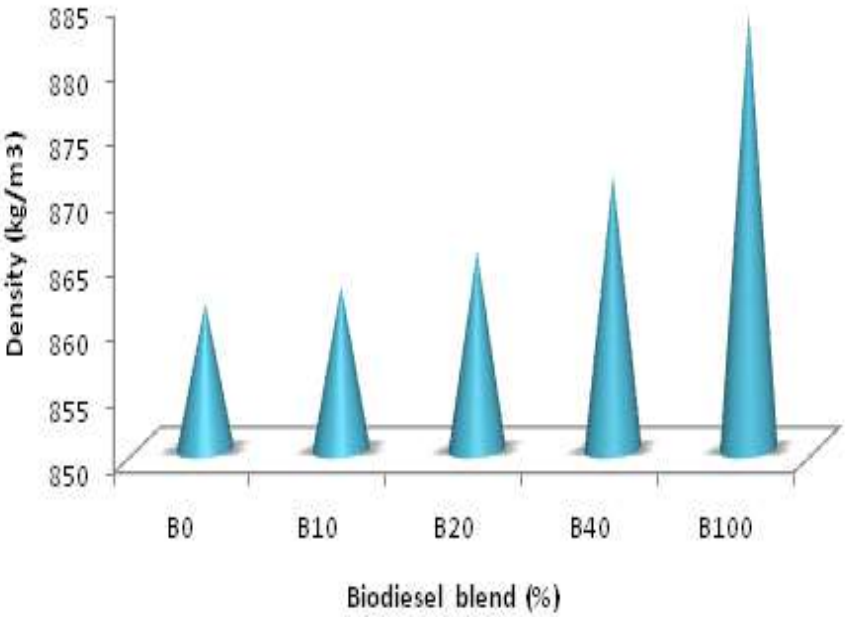


Fig. 4a Variation of density with biodiesel percentage

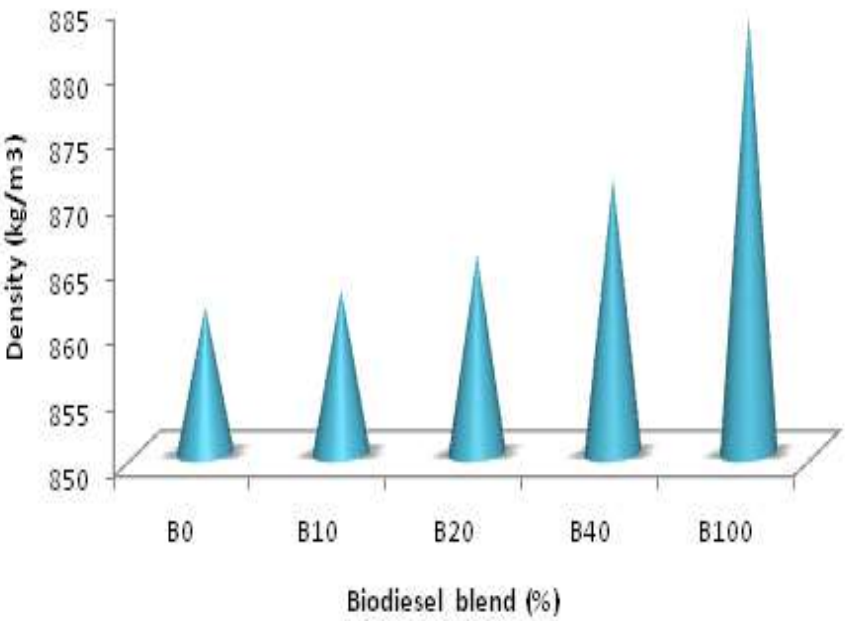


Fig. 4b. Variation of kinematic viscosity with biodiesel percentage

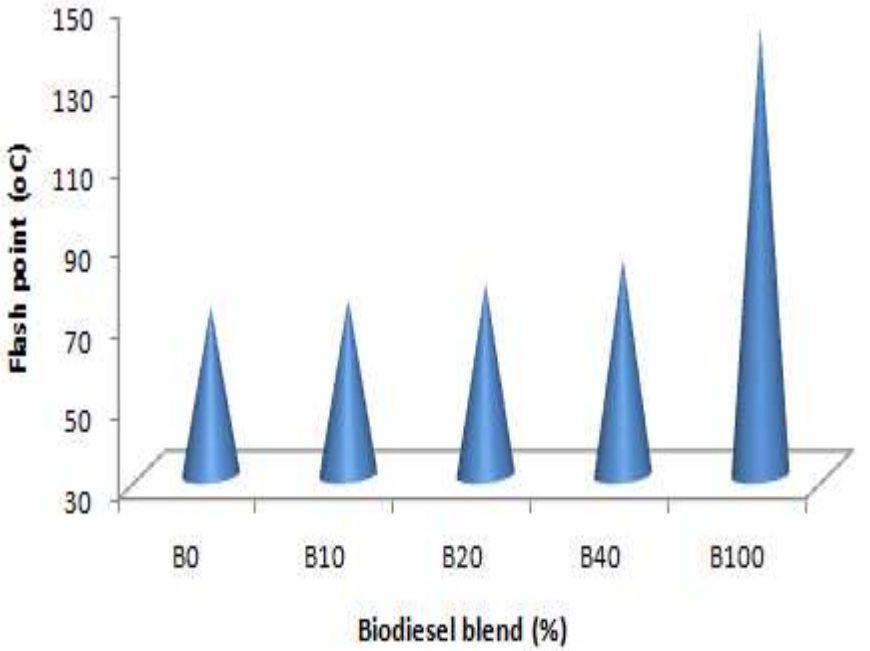


Fig. 4c Variation of flash point with biodiesel percentage

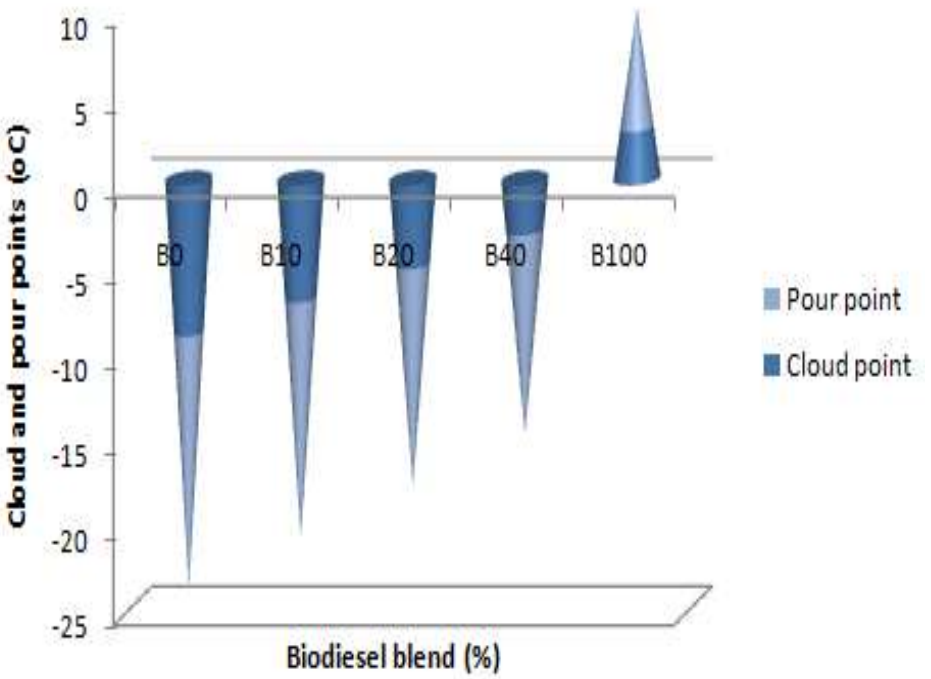


**Fig. 4d** Variation of cloud point and pour point with biodiesel percentage

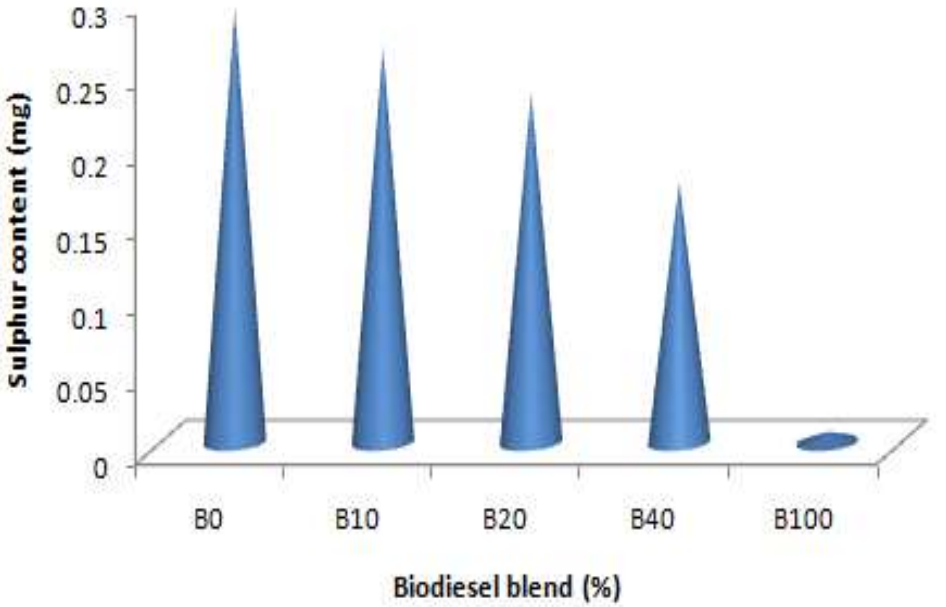


Fig. 4e. Variation of sulphur content with biodiesel percentage

**4.6. Mathematical Relationship Resulted from WCOME-Automotive Gas Oil/Diesel Blends**

Mathematical correlations were developed for the prediction of density, kinematic viscosity, flash point, cloud point, pour point and sulphur content of the fuel types and biodiesel fraction (Table 6). A second–degree equation was found suitable to correlate the variation of densities and WCOME–diesel fuel blends. The coefficient of determinant ($R^2$) from the density regression model shows that over 99.6% of the experimental density is captured in the empirical equation. The second–degree model equation was found adequate to correlate the variation of kinematic viscosity (KV) and WCOME–diesel fuel blends. The high $R^2$ (0.978) indicates that over 97.8% of the actual KV is captured in the empirical equation.

A third-degree polynomial equation was found suitable to correlate the variation of flash point (FP) with biodiesel content at any blend. The $R^2$ of 0.999 reveal that over 99.9 % of the measured FP was captured.

Polynomial regression equation and third-degree equation were found suitable for the respective cloud point and pour point variation with biodiesel percentage. The high $R^2$ (0.999) and $R^2$ (0.995) resulting from the pour point regression model and cloud point polynomial, respectively indicate that not less than 99 % of the experiment data were captured for the cloud and pour points measured..

The second degree model equation was found adequate to correlate the variation of sulphur content and WCOME–diesel fuel blends. The high $R^2$ (0.9999) indicates that 99.9 % of the experiment was captured by the sulphur content model equation.

**Table 6** Model for predicting fuel properties for WCOME-diesel fuel blends

| Fuel properties | Regression Model | $R^2$ |
|---|---|---|
| Density (Kg/m3) | Y = -0.000x2 + 0.260x + 860.6 | 0.996 |
| Kinematic viscosity ($mm^2/s$) | $Y = -0.00009x^2 + 0.013x + 4.691$ | 0.978 |
| Flash point ($^0C$) | $Y=0.00007x^2-0.002+0.309+71.77$ | 0.999 |
| Cloud point ($^0C$) | $Y= -0.000x^2 + 0.176x – 8.766$ | 0.995 |
| Pour point ($^0C$) | $Y= 0.00004x^3 - 0.003x^2 + 0.149x - 15.04$ | 0.999 |
| Sulphur content (m/m %) | $Y= 0.000001x^2 - 0.003x + 0.292$ | 0.999 |

Y= Fuel property; x= Percentage of WCOME in the blend

### 4.7 Degradation of Aluminium Coupon and Deterioration of Fuel Types

The corrosion rate of aluminium upon exposure to diesel and WCOME blends is depicted in Fig. 5 while the variation of the corrosion rates for the fuel types with the regression model is detailed in Table 7. The degradation of aluminium exposed to the fuel types for 960 hours were assessed by investigating changes in hardness and tensile strength and showed in Figs. 6 and 7, respectively. Before the commencement and after the exposure of the coupon to the fuel types, the density, viscosity and total acid number (TAN) were determined and presented in Figs. 8-10. The morphological structure of the aluminium prior exposure to the fuel types are presented in Plate 1a while those of coupons after being exposed are depicted in Plates 1b-f. The corrosion rate slightly increased with advancement in biodiesel content in the blends and exposure duration as shown in Fig. 5. As presented in Table 7, corrosion rates variation with 480 and 720 hour duration of exposure are correlated using $2^{nd}$ empirical equation while those of 240 hour and 960 hour are fitted with $4^{th}$ degree model equation and $3^{rd}$ degree regression equation, respectively. The experimental corrosion rates ranges covered by the corrosion rates regression models for aluminium coupon ranged from 86.1 to 99.6%. With the increasing in biodiesel percentage in the blends, there is an increase in hardness and tensile strength (TS) of aluminium, as depicted in Figs. 6-7, respectively. The change in hardness of aluminium in WCOME (62.89%) was higher than those of B100 (62.89%), B40 (44.37%), B20 (31.71%) and B10 (11.0%). Similarly, the change in TS of aluminium coupon exposed to WCOME (62.90%) was higher than those of the conventional diesel (2.65%) and blended diesel and WCOME.

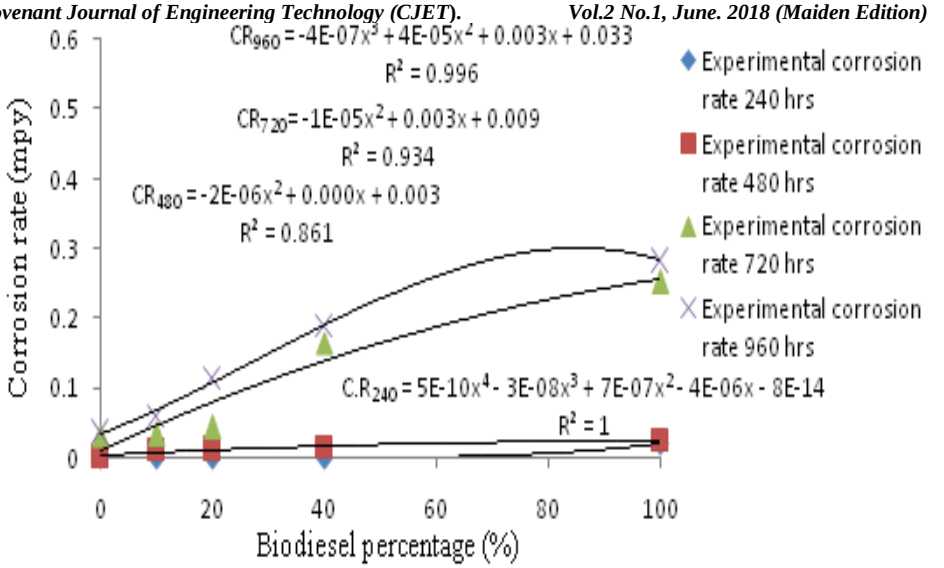


Fig. 6 Variation of corrosion rates of aluminium in waste cooking oil biodiesel -diesel blends

**Table 7** Regression models for corrosion rates of aluminium in blending ratios of waste cooking oil biodiesel

| Exposed period (hours) | Regression Models | $R^2$ |
|---|---|---|
| 240 | $CR = 0.0000000005x^4 - 0.00000003x^3 + 0.0000007x^2$ - 0.000004x -0.0000000000000008 | 1 |
| 480 | $CR = -0.000002x^2 + 0.000x + 0.003$ | 0.861 |
| 720 | $CR = -0.00005x^2 + 0.003x + 0.0009$ | 0.934 |
| 960 | $CR = 0.0000004x^3 - 0.00004x^2 + 0.003x + 0.033$ | 0.996 |

CR= corrosion rate (mil/yr); x = percentage of waste cooking oil biodiesel in the blend.

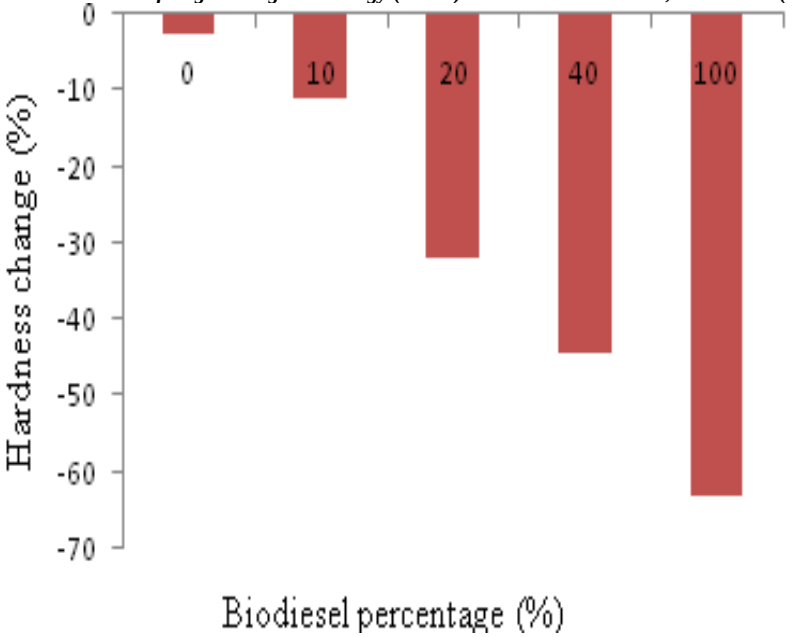


Fig. 6. Variation of hardness change and fuel types after static immersion test for 960 hours

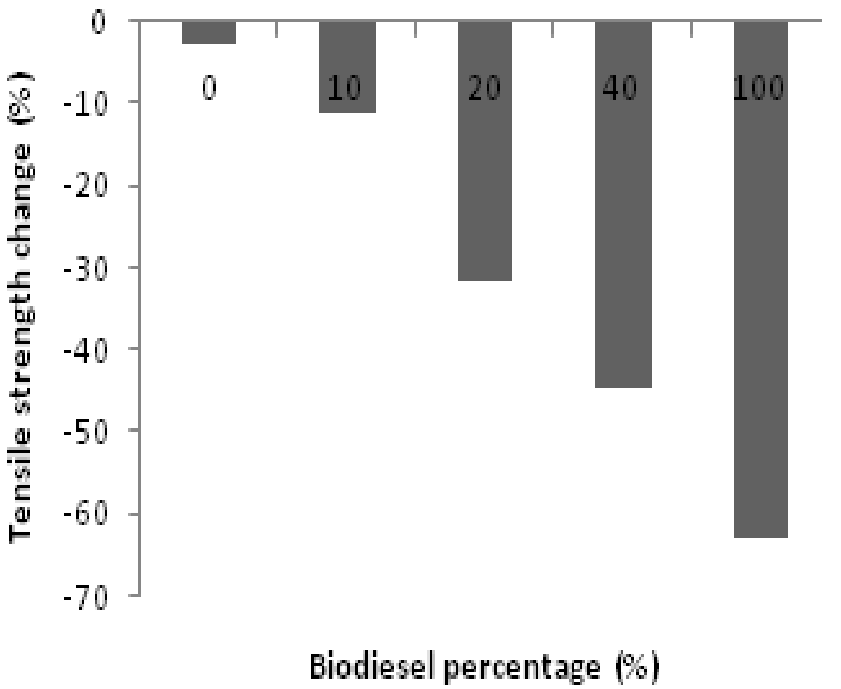


**Fig. 7.** Variation of tensile strength change and fuel types after static immersion test for 960 hours

The coupon's surface morphology of the fossil diesel (plate 1b) has less strike than those of WCOME and its blends (Plates 1c-f). The changes in the appearance of the coupon exposed to WCOME and its blends

are caused by the oxidation product which enters into the fuel, leading to fatty acid salts on the aluminium coupon. This implies that the WCOME and its blends are prone to corrosion attack than that of diesel [2]. Moreover, the micrographs show that there were slight damages to aluminium coupon exposed to biodiesel and its blends than diesel. The extents of damage are revealed by the pits on the coupon surfaces. This was further proven by deterioration of basic fuel properties such as density, viscosity and total acid number (see Figs. 8-10). This observation is in agreement with the published reports of other researchers [32-35].

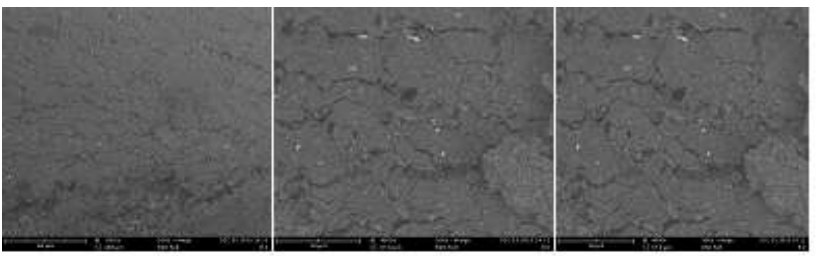

a. Aluminium before immersion b. Aluminium/B0 c. Aluminium/B10

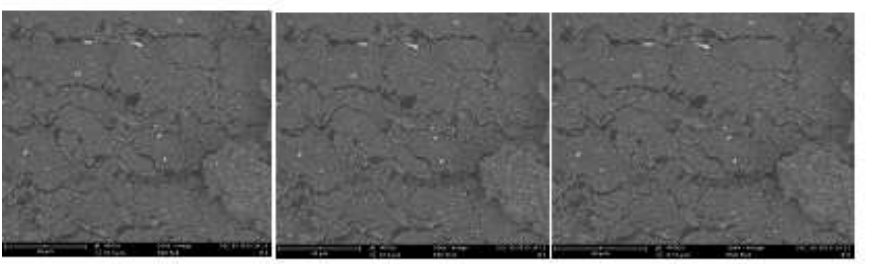

d. Aluminium/20 e. Aluminium/40 f. Aluminium/B100

u

Plate 2: SEM micrographs of aluminium (Al) surface before and after exposure to diesel (B0), B10, B20, B40 and B100 at room temperature for 960 h.

The investigated density, kinematic viscosity (KV) and total acid number (TAN) before and after exposure to different fuel types are depicted in Figs. 8-10, respectively. The density, KV and TAN were observed to increase with biodiesel content in the blends after being exposed. However, the density and KV are within the standards of density and viscosity of European Union (EN 14214) ASTM D671 specifications. Degradation of metallic component and compositional variation has been indicated for the changes [36-39].

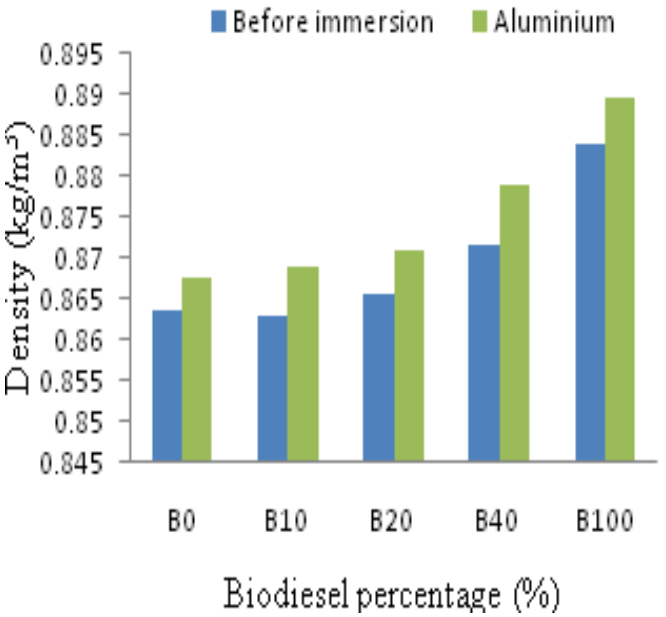


**Fig. 8** Variation of density with biodiesel fraction, before and after 960 h of exposure to coupons

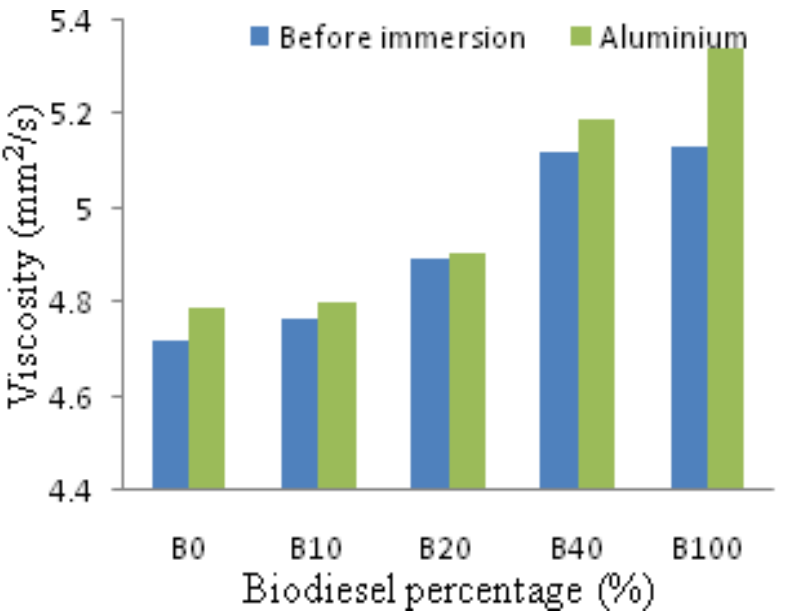


**Fig. 9** Variation of kinematic viscosity with biodiesel fraction, before and after 960 h of exposure to coupons

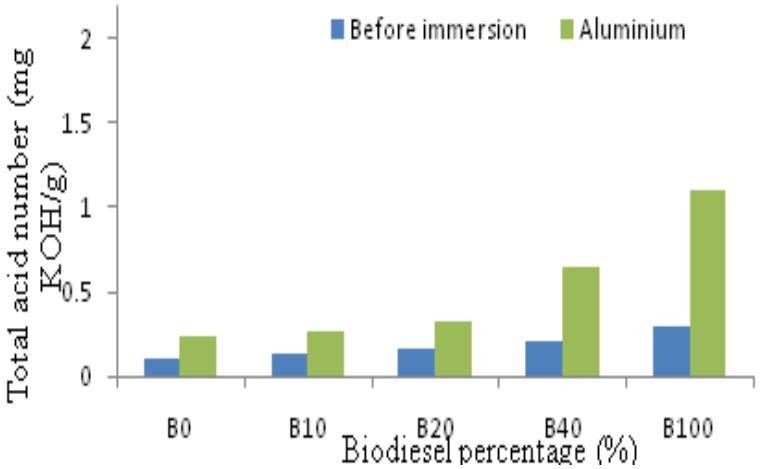


**Fig. 10** Variation of TAN with biodiesel fraction, before and after 960 h of exposure to coupons

## 5. Conclusions

Based on the corrosion study of aluminium coupons exposed to optimized waste cooking oil methyl ester (WCOME) and automotive gas oil blends, the following conclusion can be deduced:

- Maximum 97.1% WCOME yield was obtained with 1.1 wt.% KOH and 5.99 oil/methanol molar ratio at 60 oC for 78 min.
- Basic properties of WCOME met the specification of the ASTM D6751 and EN14214 standards.
- Sulphur content decreased while those of other key properties increased with the increased in the content of the blend of WCOME.
- Corrosion rates of aluminium increased with biodiesel fraction and duration of exposure
- Hardness and tensile strength of aluminium increased with biodiesel fraction
- Results showed that high blending ratios can degrade aluminium coupon in comparison with that of B0. It was observed that the 10% WCOME (B10) as a blend ratio operated close to B0 with respect to Brillness hardness and tensile strength, and the reductions in cold flow properties which make B10 a viable substitute to fossil diesel in cold and artic regions.

**Acknowledgment**

The financial assistance received from the Tertiary Educational Trust Fund for the project and assistance rendered by Pastor Akinola Omotayo in the production of biodiesel from waste cooking oil are gratefully appreciated by the authors.

## References

[1] Verma, P. ,Sharma, M.P., "Comparative analysis of effect of methanol and ethanol on Karanja biodiesel production and its optimisation, *Fuel, 180*, pp. 164-174, (2016).

[2] Cursaru, D.L, Brănoiu, G., Ramadan, I., Miculescu, F.,"Degradation of automotive materials upon exposure to

sunflower biodiesel", *Industrial Crops and Products*, (54), pp. 149-158, ( 2014).

[3] Moser, B.R., " Biodiesel production, properties, and feedstocks", *In vitro Cell Biol. Plant*, 45, pp. 229-266, (2009).

[4] Zuleta, E.C., Baena, L., Rios, L.A., Calderón, J.A., "The oxidative stability of biodiesel and its impact on the deterioration of metallic and polymeric materials: a review", *Journal of the Brazilian Chemical Society*, *23*(12), pp. 2159-2175, (2012).

[5] Singh, B., Korstad, J., Sharma, Y.C., "A critical review on corrosion of compression ignition (CI) engine parts by biodiesel and biodiesel blends and its inhibition", *Renewable and Sustainable Energy Reviews*, *16*(5), pp. 3401-3408, (2012).

[6] Chew, K.V., Haseeb, A.S.M.A., Masjuki, H.H., Fazal, M.A., Gupta, M., "Corrosion of magnesium and aluminum in palm biodiesel: A comparative evaluation", *Energy*, 57, pp. 478-483, (2013).

[7] Akhabue, C.E., Aisien, F.A., Ojo, C.O., "The effect of Jatropha oil biodiesel on the corrosion rates of aluminium and mild carbon steel", *Biofuels*, *5*(5), pp.545-550, (2014).

[8] Norouzi, S., Eslami, F., Wyszynski, M. L., Tsolakis, A. , "Corrosion effects of RME in blends with ULSD on aluminium and copper", *Fuel processing technology*, *104*, pp. 204-210, (2012)

[9] Samuel, O.D., *Characteriation and performance evaluation of waste cooking oil biodiesel-diesel fuel blends in diesel engines*, Ph.D. Thesis, Federal University of Agriculture, Abeokuta, Ogun State, Nigeria , (2016).

[10] Chuckwumenogor, O., *Characterization and corrosion behaviour of copper, aluminium and brass exposed to waste cooking oil biodiesel*, B.Eng. Project, Federal University of Petroleum Resources, Effurun, Nigeria, (2016).

[11] Robert, C., *Introduction to manufacturing processes and materials*, New York

[12] El-Gendy, N.S., Deriase, S.F., Hamdy, A., "The optimization of biodiesel production from waste frying corn oil using snails shells as a catalyst" *Energy Sources, Part A: Recovery, Utilization, and Environmental Effects*, 36(6), pp.623-637, (2014).

[13] Nachid, M., Ouanji, F., Kacimi, M., Liotta, L.F., Ziyad, M., "Biodiesel from moroccan waste frying oil: the optimization of transesterification parameters impact of biodiesel on the petrodiesel lubricity and combustion", *International Journal of Green Energy*, 12(8), pp.865-872, (2015).

[14] Zhang, Y., Dube, M.A., McLean, D.D.L., Kates, M., "Biodiesel production from waste cooking oil: 1. Process design and technological assessment", *Bioresource*

*Technology*, 89(1), pp.1-16, (2003).

[15] Freedman, B., Pryde, E.H., "Fatty esters from vegetable oils for use as a diesel fuel", In: Vegetable oils fuels", *proc. of the int. conf. on plant and vegetable oils as fuels*, St. Joseph, Mich., ASAE; pp. 117–22, (1982).

[16] Atadashi, I.M., Aroua, M.K., Aziz, A.A. , Sulaiman, N.M.N., "The effects of water on biodiesel production and refining technologies: A review", *Renewable and Sustainable Energy Reviews*, 16(5), pp.3456-3470, (2012).

[17] Phan, A.N., Phan, T.M., "Biodiesel production from waste cooking oils", *Fuel*, 87(17), pp.3490-3496, (2008).

[18] Al-Hammare, Z, Yamin J., "Parametric study of the alkali catalyzed transesterification of waste frying oil for biodiesel production", *Energy Conversion and Management*, 79, pp. 246-54, (2014).

[19] Gopal, K. N., Karupparaj, R. T., "Effect of pongamia biodiesel on emission and combustion characteristics of DI compression ignition engine", *Ain Shams Engineering Journal*, *6*(1), pp. 297-305, (2015).

[20] Dwivedi,G., Sharma, M.P., "Application of Box–Behnken design in optimization of biodiesel yield from Pongamia oil and its stability analysis", *Fuel*, 145, 256–262, (2015).

[21] Ong, H.C., Masjuki, H.H., Mahlia, T.M.I, Silitonga, A.S.,, Chong W.T., Leong, K.Y. ,"Optimization of biodiesel production and engine performance from high free fatty acid Calophyllum inophyllum oil in CI diesel engine", *Energy Conversion and Management*, pp.30-40, (2014).

[22] Bora, D. K., Polly, M., Sanduja, V., "Performance evaluation and emission characteristics of a diesel engine using mahua oil methyl ester (MOME), *SAE Technical paper*, No. 2004-28-0034, (2004).

[23] Bamgboye, A.I., Oniya, O.O., "Fuel properties of loofah (Luffa cylindrica L.) biofuel blended with diesel", *African Journal of Environmental Science and Technology*, 6(9), pp.346-352, (2012).

[24] Taravus, S., Temur, H., Yartasi, A., "Alkali-catalyzed biodiesel production from mixtures of sunflower oil and beef tallow", *Energy and Fuels*, 23, pp. 4112-4115, (2009).

[25] Agarwal, A.K., Das, L.M., "Biodiesel development and characterization for use as fuel in compression ignition engines", *Journal of Engineering for Gas Turbines and Power*, 123, pp. 440-447, (2001).

[26] Rasimoglu, N., Temur, H., "Cold flow properties of biodiesel obtained from corn oil", *Energy*, 68, pp.57-60, (2014).

[27] Islam, M.M., Hassan, M.H., Kalam, M.A., Habibullah, M. and Hossain, M.M., "Improvement of cold flow properties of Cocos nucifera

and Calophyllum inophyllum biodiesel blends using polymethyl acrylate additive, *Journal of Cleaner Production*", 137, pp.322-329, (2016).

[28] Verma, P., Sharma, M.P., Dwivedi, G., "Evaluation and enhancement of cold flow properties of palm oil and its biodiesel", *Energy Reports*, 2, pp.8-13, (2016).

[29] Altaie, M.A.H., Janius, R.B., Rashid, U., Yap, Y.H.T., Yunus, R., Zakaria, R., "Cold flow and fuel properties of methyl oleate and palm-oil methyl ester blends", *Fuel*,160, pp. 238–244, (2015).

[30] Anon, "Determination of ester and linolenic acid methyl ester contents", *English version of DIN EN* 14103, (2003).

[31] Bhale, P.V., Deshpande, N.V., Thombre, S.B., "Improving the low temperature properties of biodiesel fuel", *Renew. Energy*, 34 (3), pp.794–800, (2009).

[32] Fazal, M.A., Haseeb, A.S.M.A., Masjuki, H.H., "Degradation of automotive materials in palm biodiesel", *Energy*, 40(1), pp.76-83, (2012).

[33] Hu, E., Xu, Y., Hu, X., Pan, L., Jiang, S., "Corrosion behaviors of metals in biodiesel from rapeseed oil and methanol", *Renewable Energy*, 37(1), pp.371-378, (2012).

[34] Samuel, O.D., Ashiedu, F.I., Oreko, B.U., "Analysis of coconut ethyl ester (biodiesel) and fossil diesel blending: properties and corrosion characteristics", *Nigerian Journal of Technology*, 35(1), pp.107-113, (2016).

[35] Meenakshi, H. N., Shyamala, R. , "Effect of Flow and Dissolved Oxygen on the Compatibility of Pongamia pinnata Biodiesel with Common Construction Materials Used in Storage and Transportation", *International Journal of Chemical Engineering (1687806X)*, (2015)

[36] Fazal, M.A., Haseeb, A.S.M.A., Masjuki, H.H., "Effect of temperature on the corrosion behavior of mild steel upon exposure to palm biodiesel", *Energy*, *36*(5), pp.3328-3334, (2011).

[37] Thangavelu, S.K., Chelladorai, P., Ani, F.N., "Corrosion Behaviour of Carbon Steel in Biodiesel-Diesel-Ethanol (BDE) Fuel Blend", In *MATEC Web of Conferences* (Vol. 27). EDP Sciences, (2015).

[38] Haseeb, A.S.M.A., Masjuki, H.H., Ann, L.J., Fazal, M.A., "Corrosion characteristics of copper and leaded bronze in palm biodiesel", *Fuel Processing Technology*, *91*(3), pp.329-334, (2010).

[39] Fernandes, D.M., Montes, R.H., Almeida, E.S., Nascimento, A.N., Oliveira, P.V., Richter, E.M., Muñoz, R.A., "Storage stability and corrosive character of stabilised biodiesel exposed to carbon and galvanised steels", *Fuel*, 107, pp.609-614, (2013).

**Covenant Journal of Engineering Technology (CJET) Vol. 1, No. 2, Sept. 2018**

An Open Access Journal Available Online

# Viability of Recycled Concrete Waste as Construction Material for a Sustainable Environment

**Theme: Sustainable Buildings and Cities**

**Olaoye R. A.[1], Oluremi J.R.[1], Ajamu S.O.[1] & Abiodun Y.O.[2]**

[1]Department of Civil Engineering,
Ladoke Akintola University of Technology, Ogbomoso,
Oyo State, Nigeria
[2]Department of Civil and Environmental Engineering,
University of Lagos, Akoka
jroluremi@lautech.edu.ng

***Abstract***: A major source of environmental burden in construction industries is concrete waste because its generation and accumulation start from the time fresh concrete are produced on-site or off-site till its hardens. This made concrete the largest portion of solid waste stream by weight in the construction industries. Recycling of these waste materials into new form as well as appropriate reuse could therefore conserve natural resources, reduce the space required for land filling and the cost of transportation. This paper assesses the viability of reusing aggregates obtained from concrete waste collected from four different construction sites by comparing compressive strength of concrete made with the recycled concrete waste aggregate with concrete made with natural fresh aggregate as control specimens using an aggregate size not greater than 25mm. A total of 60 cubes of size 150mm x 150mm were cast and cured for different maturity age of 7, 14, 21 and 28 days before crushing. Laboratory results revealed that there was little variation in strength as the cubes matures. Average compressive strength of concrete made with recycled concrete waste aggregates obtained from two of the site were 22.8 N/mm2 and 24.3 N/mm2 and these were almost the same with the control test cubes with average compressive strength of 24.4 N/mm2. However, test cubes obtained from the other two sites had concrete strength lower than 20 N/mm2. Hence, concrete produced with recycled concrete waste aggregate though exhibiting lower compressive strength

could be used for walkways and kerbs production in road construction, backfilling, and in concrete production for light load bearing structural components so as to achieve a sustainable environment and conserve natural resources.

***Keywords***: Environmental sustainability, Construction waste, Waste management, Waste reuse, Recycling

## 1. **Introduction**

Concrete is the leading construction material across the world and the most widely used material in civil engineering works, therefore concrete waste arising from construction and demolition works constitutes one of the largest waste streams within developing and developed countries (Kumutha and Vijai, 2010; Singh and Sharma, 2010; PWTB, 2004). Environmental and economic implications of this waste demand urgent attention and sustainable solution as the construction industry now experience more pressure now than ever before on how to manage these waste (Snehal et al., 2013; Donalson et al., 2010; Hemalatha et al., 2008). Various measures has been aimed at reducing the use of primary aggregate and increasing the recycling and reuse of concrete waste from construction industries as aggregates for technically, economically, or environmentally acceptable construction work (Otoko, 2014; Agrela et al., 2013). Assurance on the effective reuse of concrete waste requires three basic concepts: (a) safety and quality of the finished material (b) improved and sustainable environment, and (c) increased cost effectiveness of construction (Dosho, 2007). According to Bairagi, 1993, up to 50% of natural aggregate could be replaced by recycled aggregate without seriously affecting the properties of the concrete, both in the fresh and hardened states. A study conducted in South Western Nigeria by Akinkurolere and Franklin (2005) revealed that construction wastes incur additional cost to the construction project as well as reduction in the profit margin of the contractor, taking into account the cost of storing and evacuating the waste along with the loss of revenue from not reclaiming it. Concrete waste can be used for several purposes, apart from land filling, to generate lost revenue for economic reason. Demolished sandcrete blocks waste has been recycled and utilized into fine aggregate in concrete by Akaninyene (2012). Kaosol (2010) reused concrete waste as crushed stone for hollow concrete masonry units. Kenai and Debieb (2007) examined the possibility of using crushed clay bricks as coarse and fine aggregate for a new concrete material while Umoh and Kamang (2005) investigated the use of sandcrete blocks waste collected from block moulding yards as partial replacement of fine aggregate in medium grade concrete of 20N/mm2, 25N/mm2, and 30N/mm2.

Testing the suitability of both the natural and the recycled concrete waste aggregate using experimental approach is vital before opting for reuse. Research by Chan and Fong (2006) revealed that recycled aggregate and natural aggregate should have physical properties satisfying the requirement listed in Table 1. However, the major

characteristic of concrete includes the strength, durability, deformation under load and shrinkage among other properties, but the aggregate for concrete production must meet the requirements set in relevant specification for its particular use. For lower grade applications, concrete with 100% recycled coarse aggregate is allowed. Recycled fines are not allowed to be used in concrete. The target strength is specified at 20 N/mm2 and the concrete can be used in benches, stools, planter walls, concrete mass walls and other minor concrete structures. For higher grade applications (up to C35 concrete, 35 N/mm2), the current specifications allows a maximum of 20% replacement of virgin coarse aggregates by recycled aggregates and the concrete can be used for general concrete applications except in water retaining structures (Chan and Fong, 2002). Most research work had focused on demolished concrete waste from old structures or demolished blocks and bricks from old building rather than the hardened concrete waste generated on-site from on-going construction work. This paper assesses the characteristics of concrete produced with aggregates from concrete waste obtained from four construction sites in Southwestern Nigeria.

Table 1: Properties of natural and recycled aggregate

| Property | Coarse Aggregate | |
|---|---|---|
| | Natural Aggregate | Recycled Aggregate |
| Density kg/m$^3$ | 2500 | 2300 |
| Slump (mm) | 50-75 | Tolerance of ± 25 |
| Compacting factor | 0.82- 0.92 | 0.80-0.90 |
| Water absorption | 0.5 % -1.0 % | 5 % - 6 % |

Source: Poon and Chan, 2007

## 2. Methodology

### 2.1 Sample Collection and Preparation

Concrete wastes were collected from four different construction sites where concrete mixed in the right proportions are used for various concrete works: Ogbomoso (OG), Oyo (OY), Saki (S), and Ibadan (I) all within Oyo state, Nigeria. This includes left over waste from casting of column and column bases, slab and flooring processes. The collected hardened concrete wastes were crushed to a specific size to obtain the recycled aggregates free from soil, clay, wood and others debris as contaminants. Samples obtained from each site were labeled for proper identification. The natural fresh crushed stone aggregate samples were collected directly from a quarry.

### 2.2 Experimental Tests

#### 2.2.1 Sieving

BS sieves ranging from size 0.125mm to 8mm (for fine aggregate) and 4.75mm to 25mm (for coarse aggregate) were used for sieve analysis. The samples retained on each sieve were collected, weighed and recorded. Both natural and recycled concrete waste aggregates

of size not greater than 25mm were used for concrete production.

### 2.2.2 Water Absorption Test

This test was performed to determine the amount of water (in percent) absorbed by aggregates and hence the porosity and soundness of the aggregates. The effective water absorption (EA) was calculated as the amount of water required to bring an aggregate in a concrete from the air-dry state (AD) to the saturated–surface dry (SSD) weight. A certain mass of aggregate was wrapped in the net and immersed in the water for 24 hours, allowed to be dried and reweighed again. Water absorption capacity of the aggregate is determined from the equation 1.

$$\text{Water Absorption capacity} = \frac{\text{Final mass} - \text{Initial mass}}{\text{Initial mass}} \times 100\% \quad 1$$

*2.2.3 Casting of Concrete Cube*

Concrete mix was prepared by mixing ordinary Portland cement with fine aggregates and recycle concrete waste and the natural aggregate as coarse aggregates using mix ratio of 1:2:4. Concrete cubes test specimens were cast using 150x150x150 mm mould. Mixing, casting, compacting and curing processes were carried out using standard methods in accordance with BS 1881, Part 108 of 1997 in the Structural Laboratory of the Department of Civil Engineering, Ladoke Akintola University of Technology, Ogbomoso.

*2.2.4 Workability Tests*

Slump and Compacting factor tests were carried out in accordance to procedures described in BS 1881, Part 102, 1997 and BS 1881, Part 103, 1997 respectively to determine the workability and amount of useful work necessary to produce full Compaction. The compacting factor was evaluated using equation 2.

$$\text{Compacting factor} = \frac{\text{mass of sample}}{\text{mass of fully self compacted sample}} \quad 2$$

*2.2.5 Compressive Strength Test*

Concrete cubes were cast in triplicate and cured for 7, 14, 21 and 28 days, 24 hours after casting as shown in Plate 3 and thereafter each cube was crushed under incremental compressive load until failure occurred to obtain the maximum compressive load for 7, 14, 21 and 28 days and average compressive strength was determined for each maturing age. The development of failure was monitored on the compression machine for each of the cubes cured and the compressive strength was determined from equation 3.

$$\text{Compacting factor} = \frac{\text{mass of sample}}{\text{mass of fully self compacted sample}} \quad 2$$

*2.2.5 Compressive Strength Test*

Concrete cubes were cast in triplicate and cured for 7, 14, 21 and 28 days, 24 hours after casting as shown in Plate 3 and thereafter each cube was crushed under incremental compressive load until failure occurred to obtain the maximum compressive load for 7, 14, 21 and 28 days and average compressive strength was determined for each maturing age. The development of

failure was monitored on the compression machine for each of the cubes cured and the compressive strength was determined from equation 3.

$$\text{Compressive strength } (N/mm^2) = P/A \quad 3$$

Where:

P: Ultimate compressive crushing load of concrete (N)

A: Surface area of cube under loading ($mm^2$)

The density of the cubes was also determined according to the relation in equation 4

$$\text{Density of concrete} = \frac{\text{Weight of the cube } (kg)}{\text{Volume of the cube } (m^3)} \quad 4$$

Plate 1: Stack of Sieves

Plate 2: Compression machine

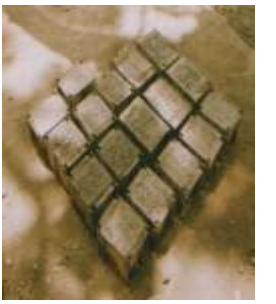

Plate 3: Cubes after casting

## 3.0 Results and Discussion

### 3.1 Aggregate gradation

The result of the sieve analysis for the fine aggregate is presented in Figure 1. The fine aggregate was found to be well graded sand which provide strong affinity for gripping with lesser binding materials. The gradation curve gave an S-Shape with effective size of 0.36 mm, coefficient of uniformity of 2.08 and coefficient of gradation of 1.12. Data from sieve analysis for the coarse natural aggregates, N and recycled concrete wastes OG, OY, S and I are presented in Table 1-5 of Appendix respectively. The gradation curve for both natural and recycled concrete waste aggregate were relatively the same as shown in Figure 2. The natural crushed stone coarse aggregate has effective size of 7.50 mm, coefficient of uniformity of 2.4 and coefficient of gradation of 1.25. The recycled concrete waste aggregate from Ogbomoso (OG) has effective size of 11 mm, coefficient of uniformity of 1.91 and coefficient of gradation of 1.25 while effective size, coefficient of uniformity and coefficient of gradation for concrete waste aggregate from Oyo (OY), Saki (S) and Ibadan (I) approach infinity respectively. Similar results were obtained from by Singh and Sharma (2010) on the use of recycled aggregates in concretes.

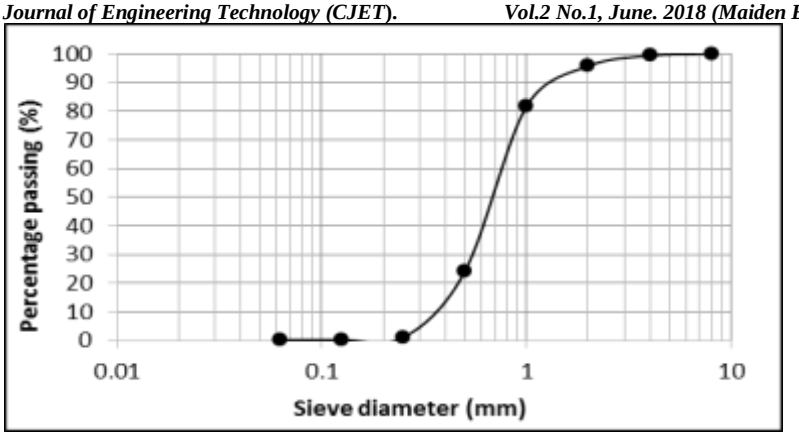


Figure 1: Gradation curve for fine aggregate

### 3.2 Workability and Consistency of Concrete

The average slump and compacting factor test result for the concrete mixes using natural and recycled concrete waste aggregate is shown in Table 2. True slump of 52 mm was obtained for concrete made from natural crushed stone aggregate which satisfies the specification for workability of such aggregate sizes. For the concretes produced with recycled concrete waste aggregates, result showed a reduction in slump value, but which remained essentially within the specified tolerances of +25mm according to BS 5328 (1990). The slump values for the four samples ranged from 25 to 35 mm hence the concrete waste aggregates still maintained the appropriate slump. The compacting factor for the concrete produced from natural crushed stone aggregate was 0.92 which is an indication of good workability and consistency properties. The compacting factor for fresh concrete produced from recycled concrete waste aggregates is low compared with natural aggregates with values ranging from 0.80 to 0.90 however, the concrete made with the four recycled concrete waste aggregates still have good workability property with consistency moving between hard to plastic.

Table 2: Average slump and compacting factor of the natural and recycled aggregates using 1:2:4 mix ratio

| Aggregate type ≤ 25mm | Slump (mm) | Compacting factor | Consistency |
|---|---|---|---|
| Natural aggregate | 52 | 0.92 | Plastic |
| OG | 26 | 0.83 | Hard |
| OY | 35 | 0.82 | Hard |
| S | 25 | 0.80 | Hard |
| I | 25 | 0.90 | Plastic |

### 3.3 Water Absorption of the Concrete Cubes

The average values of water absorption for the concrete cube produced from each of the aggregates types used are shown in Table 3. The rate of water absorption increased as the cubes matured from the $7^{th}$ day to the $28^{th}$ day. Water absorption of the concrete made from natural aggregate fell within the standard of 0.5 - 1%. For the concrete produced from recycled concrete waste aggregates, sample OG gave the highest absorption at the end of the 28days (5%), though it does not exceed the maximum value of 10% water absorption specified by Winston et al., (2002) for recycled aggregates. Results obtained indicated that recycled concrete waste aggregate absorb more water than the ordinary fresh granite due to the present of porous cement paste on the aggregates.

Table 3: Average water absorption test result for concrete cubes (%)

| | Testing days | | | |
|---|---|---|---|---|
| **Aggregate type (Water absorption %)** | 7 | 14 | 21 | 28 |
| Natural aggregate | 0.8 | 0.91 | 1.0 | 1.0 |
| Sample OG | 2.6 | 3.2 | 3.51 | 5.0 |
| Sample OY | 2.9 | 3.2 | 3.6 | 3.9 |
| Sample S | 3.0 | 3.4 | 3.6 | 3.7 |
| Sample I | 2.7 | 3.4 | 3.6 | 3.9 |

### 3.4 Density and Compressive Strength of Concrete

The average densities of concrete cubes for each curing period are presented in Table 4. According to Jackson and Dhir (1996), the most suitable concrete density usually lies between 2300kg/$m^3$ and 2500kg/$m^3$with minimum value at 2000kg/$m^3$ (Winston et al., 2002). Based on this, concrete density made from the natural aggregate, samples OY and S (recycled aggregate) are within the range of suitable concrete density at 28 days,. The other two samples gave a density value little below the specified range.

Table 4: Average Density of the Concrete Cubes

| Aggregate type | Testing days | 7 | 14 | 21 | 28 |
|---|---|---|---|---|---|
| **Natural aggregate** | Mean density of cubes (kg/$m^3$) | 2465 | 2409 | 2405 | 2406 |
| **Sample OG** | Mean density of cubes (kg/$m^3$) | 2264 | 2313 | 2243 | 2272 |
| **Sample OY** | Mean density of cubes (kg/$m^3$) | 2273 | 2254 | 2277 | 2315 |
| **Sample S** | Mean density of cubes (kg/$m^3$) | 2493 | 2488 | 2395 | 2487 |
| **Sample I** | Mean density of cubes (kg/$m^3$) | 2399 | 2318 | 2378 | 2234 |

Average compressive strengths of the concrete cubes are presented in Figure 3. Compressive strength for concrete made with natural crushed stone aggregates increased with age and the maximum strength was attained at the 28th day. The compressive strength of concrete with recycled concrete waste aggregates also increased with increase in age. The highest average compressive strength of concrete made with natural crushed stone aggregates is 24.4N/mm$^2$. The concrete made with recycled concrete waste aggregate sample OG, OY, S and I samples have maximum compressive strength of 18.0, 22.8, 24.3 and 17.5N/mm$^2$ respectively at 28th day. The compressive strengths of OY and S samples were almost equal that of natural crushed stone aggregates.

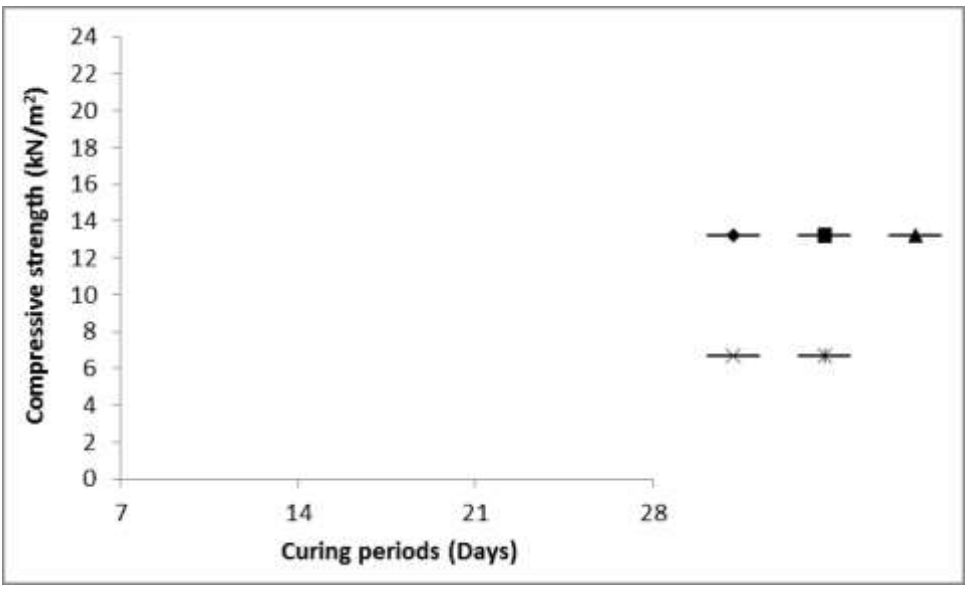


Figure 3 Variation of the compressive strength of concretes with curing days

The results are in agreement with the conclusion of (Okafor, 2010; Katz, 2003) that the strength of concrete with recycled aggregates could be only the same or lower but cannot be higher to that of concrete made from natural crushed stone aggregate. The changes might be attributed to the differences in the qualities of the materials and the concrete itself from which the recycled concrete waste aggregates are produced and which invariably governs the properties of the concrete made from recycled concrete waste aggregate.

## 4.0 Conclusions and Recommendations

In this work the potential for reclaiming and recycling hardened concrete waste from construction sites for use in value added application to maximize economic and environmental benefit has been experimented and the following conclusions were made:

i. Fresh concrete made with recycled concrete waste aggregates tends to be plastic and less workable compared to concrete made with fresh

aggregate, they exhibit higher water absorption due to previous bonding of cement paste on the aggregate surface.

ii. The compressive strength of concrete produced with recycled concrete waste aggregates increases with curing day irrespective of the aggregate type.

iii. There are variations in the compressive strength of concretes made with recycled concrete waste aggregates depending on the location of collection which ascertains the fact quality of mix and workmanship affect greatly the quality of concrete produced and hence the quality of the concrete to be produce if the concrete waste generated from those productions were to be reused as aggregates.

Based on these facts, while accepting the need to promote its usage in wider application, it must be ascertained that the aggregate for concrete application must meet the requirement set in relevant specification for its particular use because recycled concrete waste aggregate may result in higher absorption, water demand, shrinkage and creep, lower density, durability, permeability and strength. Hence concrete made from such aggregates could be used for a wide range of civil engineering works of high structural integrity if they are confirmed to be of excellent qualities otherwise while they should be used only in low strength required works like walkways and kerbs production in road construction, backfilling, low-grade concrete production, or in low-cost housing.

**References**

Agrela F., Alaejos P., De-Juan M.S (2013) Properties of concrete with recycled aggregates, *Handbook of recycled concrete and demolition waste*, Pp. 304 – 329

Akaninyene A. Umoh (2012): Recycling Demolition Waste Sandcrete Blocks as Aggregate in Concrete, *ARPN Journal of Engineering and Applied Sciences*, Vol. 7, No. 9, Pp. 1111-1118.

Akinkurolere, O.O and Franklin, S.O. (2005): Investigation into Waste Management on Construction Sites in South Western Nigeria, *American Journal of Applied Sciences*, Vol. 2 No. 5, Pp. 980-984.

Bairagi, N. K. (1993): Behaviour of concrete with different proportions of natural and recycled aggregates. *Resources, Construction and Recycling.* Vol. 9, Pp. 1-2.

BS 1881-102:1983 *Testing concrete-Part 102: Method for determination of slump*, British Standards, United Kingdom.

BS 1881-103:1993 *Testing concrete-Part 103: Method for determination of compacting factor*, British Standards, United Kingdom.

BS 1881-108: 1983 *Testing concrete-Part 103: Part 108: Method for making test cubes from fresh concrete.* British Standards, United Kingdom.

Chan, C.Y. and Fong, F.K. (2002) Management of Construction and Demolition Materials and Development of Recycling Facility in Hong Kong.

*Proceeding of International Conference on Innovation and Sustainable Development of Civil Engineering in the 21st Century*, Beijing, HKIE, July 2002.

Donalson J, Raymond C and Fazil T.N (2011): Sustainable Assessment of Recycled Concrete Aggregate (RCA) Used in Highway Construction, Proceedings of *90th Annual Meeting of the Transportation Research Board*, Washington, D.C, USA.

Dosho Yasuhiro (2007): Development of a Sustainable Concrete Waste Recycling System – Application of Recycled Aggregate Concrete Produced by Aggregate Replacing Method, *Journal of Advanced Concrete Technology*, Vol. 5, No. 1, Pp 27-42.

Hemalatha B.R, Nagendra P. and Venkata Subramanya B.V (2008): Construction and Demolition waste Recycling for sustainable growth and development, *Journal of Environmental Research and Development*, Vol. 2, No. 4, Pp759-765.

Jackson, N.J and Dhir, R.D (1996): *Civil Engineering Material,* 5th Edition, MacMillan Press Ltd., London

Kaosol T. (2010) Reuse concrete waste as crushed stone for hollow concrete masonry units, *The 3rd Technology and Innovation for Sustainable Development International Conference (TISD2010),* Faculty of Engineering, Khon Kaen University, Thailand, 4 - 6th March, 2010.

Katz .A. (2003) Properties of concrete made with recycled aggregate from partially hydrated old concrete, *Cement and Concrete Research*, Vol.33, Pp 703 - 711

Kenai S. and Debieb F. (2007): The use of coarse and fine crushed bricks as aggregates in concrete. *Construction and Building Material.*

Kumutha R. and Vijai K. (2010): Strength of concrete incorporating aggregate recycled from demolition waste. *ARPN Journal of Engineering and Applied Sciences.* Vol. 5, No. 5, Pp 64-71.

Otoko G.R. (2014) Review of the use of construction and demolition waste in concrete, *International Journal of Engineering and Technology Research*, Vol. 2, No. 4, Pp. 1 – 8.

Okofor F.O. (2010) Waste concrete as a source of aggregate for new concrete, *Nigerian Journal of Technology*, Vol. 29, No. 2, Pp 5 – 11.

Poon Chi-Sun and Dixon Chan (2007). The use of recycled aggregate in concrete in Hong Kong, *Resources, Conservation and Recycling*, Vol. 50, Pp 293-305

PWTB (Public Works Technical Bulletin) (2004): Reuse of Concrete Materials from Building Demolition, *Public Works Technical Bulletin* 200-1-27 14, September 2004

Singh S.K and Sharma P.C (2010): Use of Recycled Aggregates in concrete, A Paradigm Shift, NBM Media, Construction Information, construction portal

Senehal Anikumar, k, Anikumar G and Dadaso B.D (2013): Recycling and Reuse of Construction and Demolition Waste for Sustainable Development, *International Journal of Sustainable Development*, Vol.6, No.7, Pp. 83-92.

Umoh A. A. and Kamang E. E. J. (2005): The compressive strength of medium grade concrete made with waste sandcrete blocks aggregate, *International Journal of Environmental Issues,* Vol.3, No.1, Pp. 177-186.

Winston F.K. Fong, Jaime S.K. Yeung and C.S. Poon (2002) Hoog Kong experience of using recycled aggregates from construction and demolition materials in ready mix concrete, *International Workshop On Sustainable Development and Concrete Technology*, 267- 275.

**APPENDICES**

Table 1: Sieve analysis for natural granite N (not greater than 25mm)

| Sieve diameter (mm) | Mass retained (g) | Percentage retained % | Cumulative % passing | Percentage passing % |
|---|---|---|---|---|
| 25.00 | 0.00 | 0.00 | 0.00 | 100 |
| 19.00 | 562 | 32.77 | 32.77 | 67.23 |
| 13.20 | 5000 | 30.05 | 62.82 | 37. 18 |
| 9.50 | 1544 | 17.47 | 80.29 | 19.71 |
| 6.30 | 1368 | 15.46 | 95.75 | 4.25 |
| 4.75 | 231 | 3.18 | 98.93 | 1.07 |
| Receiver | 95 | 1.07 | 100.0 | 0 |
| Total | 8850 | 100 | | |

Table 2: Sieve analysis for sample OG (not greater than 25mm)

| Sieve diameter (mm) | Mass retained (g) | Percentage retained% | Cumulative percentage% | Percentage passing% |
|---|---|---|---|---|
| 25.00 | 0.00 | 0.00 | 0.00 | 100 |
| 19.00 | 3590 | 56.51 | 56.51 | 43.49 |
| 13.2 | 1629 | 25.64 | 82.15 | 17.85 |
| 9.5 | 690 | 10.86 | 93.01 | 6.99 |
| 6.3 | 299 | 4.71 | 97.72 | 2.28 |
| 4.75 | 35 | 0.55 | 98.27 | 1.73 |
| Receiver | 110 | 1.73 | 100 | 0.00 |
| Total | 6353 | 100 | | |

Table 3: Sieve analysis for sample OY (not greater than 25mm recycled aggregate)

| Sieve diameter (mm) | Mass retained (g) | Percentage retained% | Cumulative percentage% | Percentage passing% |
|---|---|---|---|---|
| 25.00 | 0.00 | 0.00 | 0.00 | 100 |
| 19.00 | 2161 | 31.36 | 31.36 | 68.64 |
| 13.20 | 1874 | 27.20 | 58.56 | 41.44 |
| 9.50 | 1006 | 14.60 | 73.16 | 26.84 |

| | | | | |
|---|---|---|---|---|
| 6.30 | 758 | 11.00 | 84.16 | 15.84 |
| 4.75 | 266 | 3.86 | 88.02 | 11.90 |
| Receiver | 825 | 11.97 | 100 | 0.00 |
| Total | 6890 | 100 | | |

**Table 4: Sieve analysis for sample S (not greater than 25mm recycled Aggregate)**

| **Sieve diameter (mm)** | **Mass retained (g)** | **Percentage retained%** | **Cumulative percentage%** | **Percentage passing%** |
|---|---|---|---|---|
| 25.00 | 0.00 | 0.00 | 0.00 | 100 |
| 19.00 | 2730 | 34.07 | 34.07 | 65.93 |
| 13.20 | 1752 | 21.87 | 55.94 | 44.06 |
| 9.50 | 959 | 11.97 | 67.91 | 32.09 |
| 6.30 | 764 | 9.54 | 77.45 | 22.55 |
| 4.75 | 452 | 5.64 | 83.09 | 16.91 |
| Receiver | 1354 | 16.90 | 100 | 0.00 |
| Total | 8011 | 100 | | |

Table 5: Sieve analysis for sample I (not greater than 25mm recycled Aggregate)

| Sieve diameter (mm) | Mass retained (g) | Percentage retained% | Cumulative percentage% | Percentage passing% |
|---|---|---|---|---|
| 25.00 | 0.00 | 0.00 | 0.00 | 100 |
| 19.00 | 3340 | 34.46 | 34.46 | 65.54 |
| 13.20 | 2434 | 25.12 | 59.58 | 40.42 |
| 9.50 | 1365 | 14.09 | 73.67 | 26.33 |
| 6.30 | 856 | 8.83 | 82.50 | 17.50 |
| 4.75 | 267 | 2.76 | 85.26 | 14.74 |
| Receiver | 1429 | 14.75 | 100 | 0.00 |
| Total | 9691 | 100 | | |

**Covenant Journal of Engineering Technology (CJET) Vol. 1, No. 2, Sept. 2018**

An Open Access Journal Available Online

# Use of Bamboo and Earth Materials in Construction for the Provision of Affordable Building Structures for Sustainable Development at Kuje Area Council, Abuja

**Kareem W. B[1], Okwori R. O[2], Hassan A. M[3], Mohammed B. M[4], Abubakar H. O.[5] & Dada J. A.[6]**

[1, 2, 3, 4 & 6]Department of Industrial and Technology Education,
Federal University of Technology, Minna, Niger State
[5]Department of Building Technology,
Federal Polytechnic Nassarawa, Nassarawa State.
wahabami4u@futminna.edu.ng

***Abstract***: The study was carried out on the use of bamboo and earth materials in building construction in provision of affordable housing at Kuje area council Abuja. The purpose of the study was to determine the status of the use of bamboo and earth materials in construction at Kuje area council Abuja, identifying the factors limiting the use of bamboo and earth materials in construction at Kuje area council Abuja, examine the strategies that will improve the use of bamboo and earth materials in construction at Kuje area council Abuja. Three research questions and three hypotheses were formulated to guide the study. A population of 80 respondents, comprising of 20 engineers and 60 craftsmen was used for the study. A structured questionnaire was developed by the researcher and was used as an instrument for data collection. The instrument was validated by three lecturers in the department of industrial and technology education, federal university of technology Minna. The data collected was analyzed using mean and standard deviation, while t-test statistic was used to test three hypotheses at 0.05level of significance. The findings of the study revealed that there are limitations in the use of bamboo for building construction in the Kuje Area Council. Based on the findings of the study, it was recommended that the use of bamboo and earth materials in

building construction should be introduced as part of the curriculum for construction education at both undergraduate and postgraduate levels in order to sensitize the students to their potential uses and benefits. The government should employ a policy of adapting bamboo and earth materials that require minimal amounts of capital and foreign exchange and makes use of available raw materials and skills in small-scale operations and suggestion were also made for further research works.

***Keywords*:** Bamboo, Earth Materials, Building, Sustainable, Development.

## 1. Introduction

For a long time, local materials such as bamboo have served to build the dwellings of the local houses for the human habitat, livestock and to store crops. Skills in the use of this local material are transmitted from father to son and that enabled the construction of such buildings possessed satisfaction, qualities of comfort and durability to some extent. The history of housing is inseparable from the social, economic and politics of mankind. As stated by United Nations Development Programme (UNDP), housing and sustainable human developments are closely linked together, since housing can either enhance or degrade human development. Abiola (2000) identified building material as one principal factor affecting the effective performance of Nigeria construction industry. The problem of providing affordable housing has long been a concern not only to individuals but also to government. A decent home is the basis of the possibility for obtained security, as well as other basic needs such as privacy, health and social integration. This explains the essential role that affordable housing can play in the achievement of sustainable human development.

A recent word bank report noted that two of the most critical urban development issues facing Nigeria are the financing of urban infrastructure and the institutional arrangement for housing the delivery in urban centers. The provision of basic amenity particularly housing is partly responsibility of the government which has handicapped in recent times by declining financial resources, political instability and many other factors. Local building material (bamboo, mud, etc.) are available everywhere and exists in different compositions especially in Nigeria. It is most commonly used in developing countries for housing by higher percentage of the citizens. An earth lodge is a circular building made by some of the native of North America. They have bamboo post and beam construction and are done with shaped bamboo.

Bamboo and earth materials have a long and well-established tradition as a building material throughout the world's tropical and sub-tropical regions. It is widely used for many forms of construction, in particular for housing in rural areas. Bamboo is a renewable and versatile resources, characterized by high strength and low weight, and is easily worked using simple tools. It is widely recognized as one of the most important non-timber forest resources due to the high socio-economic benefits from bamboo based products. It is estimated

million hectares area. Most of them grow in Asia, Africa and Latin America. Bamboo is the world's fastest growing woody grows three times faster than most other species. Commercially important species of bamboo usually mature in four or five years' time, after which multiple harvests are possible every second year, for up to 120 years in some species and indefinitely in others. Bamboo also excels in biomass production, giving 40 tons or more per hectare annually in managed stands. It accounts for around one-quarter of biomass produced in tropical regions and one-fifth in subtropical regions. It has been used successfully to rehabilitate soil ravaged by brick making in India, and abandoned tin- mine sites in Malaysia. It shelters top soil from the slaughter of tropical downpours, preserves many exposed areas, providing micro-climate for forest regeneration and watershed protection. It is often introduced into the banks or streams or in other vulnerable areas, for rapid control of soil erosion; one bamboo plants closely matted roots can bind up to six cubic meters of soil. The advantages of local and indigenous building materials cannot be over emphasized. It includes, light, strong, versatile, environmental friendliness, easily accessible, self renewing resource, fast growing and highly productive, which can lead to improvement of productivity (Yekini et al 2018; Azeta et al 2017).

Bamboo is used as soil stabilization, wind break, urban waste water treatment and reduction of nitrates contamination, creating a fire line in traditional forests-due to the high content of silica and Removing atmospheric carbon. The shoots are also usable for buildings and constructions in small scale and cottage industries, for handcrafts and other products. It can also be used as wood substitutes in industrial products transportation industries, for making truck bodies and railway carriages. The use of locally available and indigenous earth materials has several advantages in terms of sustainability (Nwoke et al 2017). They are: Reduction of energy costs related to transportation. Reduction of material costs due to reduced transportation costs, especially for well-established industries. Ecological balance within the region needs to be maintained while efficiently utilizing bamboo resources.

For the purpose of this study, mud bricks are as walling unit produce from rammed sand and water. It is widely used in Nigeria for walling units. The quality of earth bricks is a function of the method employed in the production and the properties of the construction materials. Earth bricks are available for construction and structure of any types. Compress earth bricks (CEB) are one of the products that Nigeria building and road research institution (NBRRI) introduce into the construction industry due to the fact that laterite is readily available in Nigeria and that it required a very small quality of cement but still compress earth bricks (CEBs) are construction bricks made with rammed clay and other stabilizing ingredient. The earth mixture is poured into a hand-operated or motorize hydraulic made, compress earth bricks are uniform in size and shape. Nowadays, improved technology induced people to use

CEB as alternatives for earth bricks in building houses because they do not require much cement for bonding, the bricks during construction thereby further reducing the building cost and their mechanical cost, with a view to ascertaining which is more applicable in building affordable houses. It is on this basis that this study aims to determine the use of bamboo and earth materials in construction for the provision of affordable building structure at Kuje area council Abuja, Nigeria.

## 2. Statement of Problem

The major factors affecting the construction industries in developing countries is the selection of good building materials (walling materials) which has been influenced by cost, physical properties and compressive strength of the walling materials. The ever increasing building cost in Nigeria is a matter of serious concern that calls for the appraisal of the conventional building processes in seeking for alternatives building materials (walling unit). Currently methods and the cost of materials and labor is continually on the increase beyond the reaches of many Nigerians, Sustainable housing development especially to the medium and low-income group of the society has become huge challenge particularly because of the huge capital outlay required to build and own a house, frequent increase in price of conventional building materials across Nigeria has reawakened serious awareness to related research to production, in the use of bamboo and earth materials as alternative for the construction of functional but low cost dwelling in rural and urban area of Nigeria. Thus, acquisition of indigenous building materials by way of compressed earth bricks (CEB) and bamboo has been suggested as a way out.

Sustainability and durability is an issue of great important for the building sector and society. Most developing nations are facing a real housing deficiency (Harrison and Sinha, 1995). Therefore, it is mandatory to construct and build houses that are more sustainable and durable at low cost. Using Bamboo and Compressed Earth Bricks (CEBs).

## 3. Objectives of the Study

The objective of this research work is to determine the use of bamboo and earth materials in construction for the provision of affordable building structure at Kuje area council Abuja.

Specifically, the study is to determine;

I. The factors of the use of bamboo and earth materials in construction at Kuje area council Abuja.
II. The factors limiting the use of bamboo and earth materials in construction at Kuje area council Abuja.
III. The strategies that will improve the use of bamboo and earth materials in construction at Kuje area council Abuja.

## 4. Research Questions

I. What are the factors associated with the use bamboo and earth materials at Kuje area council Abuja
II. What are the factors limiting the use of bamboo and earth materials in construction at Kuje area council Abuja
III. What are the strategies that will improve the use of bamboo and

earth materials in construction at Kuje area council Abuja

## 5. Hypotheses

The following null hypothesis was formulated and tested at 0.05 level of significance.

I. There is no significant difference between the mean rating of engineer and craftsmen regarding the factors associated with of the use of bamboo and earth materials in building construction at Kuje area council Abuja.

II. There is no significant difference between the mean responses of engineer and craftsmen regarding the factors limiting the use of bamboo and earth materials in building construction at Kuje area council Abuja.

III. There is no significant difference between the mean responses of engineer and craftsmen regarding the strategies that will improve the use of bamboo and earth materials in building construction at Kuje area council Abuja.

## 6. Methodology

### 6.1 Research Design

The research design used was descriptive survey because Borg & Gall (1989) describe descriptive studies as that which is aimed at finding out "what is", so observational and survey methods are frequently used to collect descriptive data. This method was successfully used by Kareem, Ma'aji, Ibrahim, Gazali and Shom (2014) in a similar research work.

### 6.2 Area of Study

This study was conducted Kuje Area Council of the Federal Capital Territory Abuja, Nigeria.

### 6.3 Population for the Study

The population of the study was eighty (80) respondents which made up of 20 engineers and (60) craftsmen who are specialists in local material in the study area. Since the population is manageable, there was no need for sampling.

### 6.4 Instrument for Data Collection

The instrument for data collection was a structured questionnaire developed by the researcher. It consisted of two parts (Part A and B); Part A indicate the Bio-data of the respondent and the part B was divided into three sections A, B and C. All items are to be responded to by indicating the appropriate perception using four point rating scale. Strongly agree = 4 points (SA), Agree (A) = 3 points, Disagree (D) = 2 points Strongly Disagree (SD) = 1 points. To ensure of the validity of the instrument, three lecturers in the department of Industrial and Technology Education, Federal University of Technology Minna validated the instrument.

Eighty (80) questionnaires were distributed twenty (20) to engineers and sixty (60) to craftsmen in building in area of study. Eighty-Three percent (83%) of the distributed questionnaire were returned and used for data analysis. The data collected were analyzed using means and standard deviation. The items mean ($\bar{x}$) and criterion mean (2.50) were computed and utilized to measure the level of agreement and or disagreement. The decision adopted was that if item mean ($\bar{x}$) is equal or more than criterion mean (2.50), the adoption is positively rated (Agree); but if otherwise, the adoption is negatively rated (Disagree).

## 7. Results

Research Question One: What are the status of the use of bamboo and earth materials at Kuje Area Council, Abuja?

**Table 1:** The current status in the use of bamboo and earth materials for building construction at Kuje area council Abuja.

| S/N | Items on the status | Mean | SD | Decision |
|---|---|---|---|---|
| 1 | Bamboo and earth materials are used because it easily absorb water in water logged areas. | 1.71 | 0.92 | Disagreed |
| **2** | Bamboo and earth materials are not used because of low level of commercialization. | 2.77 | 1.09 | Agreed |
| 3 | Bamboo and earth materials are not used because of Poor engineering design | 2.75 | 0.32 | Agreed |
| 4 | Bamboo and earth materials are used because they are largely available in our locality. | 3.29 | 0.95 | Agreed |
| 5 | Bamboo and earth materials are not used due to poor inspection of building by building inspection agency | 3.02 | 0.37 | Agreed |
| 6 | Bamboo and earth materials are not used because of low patronage of bamboo and earth materials. | 3.86 | 0.38 | Agreed |
| 7 | Bamboo and earth materials are not used due to Government lukewarm attitude towards the use of local building materials | 3.38 | 1.12 | Agreed |
| 8 | Bamboo and earth materials are used because they are easily work upon and available in abundance using simple tools. | 2.82 | 1.02 | Agreed |
| 9 | Bamboo and earth materials are not used because of discrimination in using them | 2.41 | 1.29 | Disagreed |

The data presented in Table 1 on the status of the use of bamboo and earth materials at Kuje area council Abuja, revealed that the respondent agreed with all the items with mean score ranging from 2.75 - 3.82 except items 1 and 9 which has mean score of 1.71, 2.41 respectively. This signifies that most of the respondents Agreed with the status in the use of bamboo and earth materials in building construction at Kuje area council Abuja as it is readily available.

**Research Question Two:** What are the factors limiting the use of bamboo and earth materials for building at Kuje area council Abuja?

Table 2: Identify the factors limiting the use of bamboo and earth materials for building at Kuje area council Abuja.

| S/N | Items on the factors | Mean | SD | Decision |
|---|---|---|---|---|
| 1 | Bamboo and earth materials give Poor wall finishes. | 2.57 | 1.12 | Agreed |
| 2 | Local building materials like clay suffer shrinkage and cracking. | 2.51 | 0.97 | Agreed |
| 3 | Too many quack craftsmen. | 2.84 | 0.99 | Agreed |
| 4 | Doubtful durability and longevity lifespan of Bamboo and earth materials. | 2.91 | 0.89 | Agreed |
| 5 | Early deterioration decay of bamboo | 3.16 | 1.05 | Agreed |
| 6 | Deterioration of earth buildings as a result of Absorption of moisture content | 2.69 | 1.20 | Agreed |
| 7 | Local materials such as bamboo and clay absorb Water in water logged areas | 2.59 | 1.08 | Agreed |
| 8 | Bamboo and earth materials are cheap to acquire | 2.85 | 1.15 | Agreed |
| 9 | Small scale production of bamboo and earth materials | 2.77 | 1.08 | Agreed |
| 10 | Poor road networks to transport materials to the site | 2.66 | 1.18 | Agreed |
| 11 | Bamboo and earth materials are easy to find | 2.21 | 1.18 | Disagreed |
| 12 | Lack of precise design specification | 2.34 | 1.12 | Disagreed |
| 13 | Bamboo and earth materials are easily worked on | 2.45 | 0.41 | Disagreed |

The data presented in Table 2 on the factors limiting the use of bamboo and earth materials for building at Kuje area council Abuja, reveal that the respondent agreed with all the items with mean score ranging from 2.51 - 2.91 except item 11,12 and 13 which has mean score of 2.21, 2.34 and 2.45 respectively. This signifies that most of the respondents agreed with the factors limiting the use of bamboo and earth materials for building construction at Kuje area council Abuja.

**Research Question Three:** What are the strategies that will improve the use of bamboo and earth materials for building at Kuje area council Abuja?

**Table 3:** Determine the strategies that will improve the use of bamboo and earth materials for building construction at Kuje area council Abuja

| S/N | Items on the strategies | Mean | SD | Decision |
|---|---|---|---|---|
| 1 | Reduction in development of foreign building materials in construction sectors | 3.79 | 0.89 | Agreed |
| 2 | 2 Effective mobilization of human resources | 3.42 | 0.87 | Agreed |
| 3 | Co-operative effort by government in the developing of bamboo and earth material to meet the housing need | 3.10 | 1.11 | Agreed |
| 4 | Encouragement of women in housing construction | 2.26 | | Disagreed |
| 5 | Government should increase import duties on importation of building materials that can be sourced | 2.88 | 1.14 | Agreed |

| | | | | |
|---|---|---|---|---|
| | locally | | | |
| 6 | Government should grant fiscal incentives to manufacturing of bamboo and earth materials | 3.01 | 0.97 | Agreed |
| 7 | Government should provide technical support and advice to entrepreneurs on production of bamboo and earth materials | 3.91 | 0.28 | Agreed |
| 8 | Development and propagation of indigenous technology in production of bamboo and earth materials | 3.94 | 0.28 | Agreed |
| 9 | Reduction cost of bamboo and earth materials since they are sourced locally | 3.19 | 1.11 | Agreed |
| 10 | Government should encourage large scale production of bamboo and earth materials. | 3.77 | 0.39 | Agreed |

The data presented in Table 3 on strategies that will improve the use of bamboo and earth materials for building construction at Kuje area council Abuja, reveal that the respondent agreed with all the items with mean score ranging from 2.88 - 3.94 except item 4 which has mean score of 2.26. This signifies that most of the respondents Agreed with the strategies that will improve the use of bamboo and earth materials for building construction at Kuje area council Abuja.

## 8. Discussion of the Findings

The result obtained from Table 1 revealed that all the items identified except item 1 and 9, are the status of the use of bamboo and earth materials at Kuje area council Abuja. This is in line with view of De-Boer and Baries (2000) which postulated that bamboo is widely used as a construction material around the world with an estimated 800,000 people currently living in bamboo structure. The availability is in line with the study items.

The result obtained from table 2 revealed that all the items identified except item 11,12 and 13 are the factors limiting the use of bamboo and earth materials for building at Kuje area council Abuja. This is in line with view of Anand and Ramamurthy (2003) who stated that foreign materials require high technology and energy in their production, transportation and usage.

The result obtained from table 3 revealed that all the items identified except item 4 are the strategies that will improve the use of bamboo and earth materials for building construction at Kuje area council Abuja. Harrison and Sinha (1995) corroborates this finding that sustainability and durability is an issue of great important for the building sector and society. Most developing nations are facing a real housing deficiency Therefore, it is mandatory to construct and build houses that are more sustainable and durable at low cost (Adams and Agib, 2001).

## 9. Conclusion and Recommendations

Based on the findings of the study, it was concluded that there are limitations in the use of bamboo and earth materials for building construction in the study area. This is because the water rising through clay and bamboo tends to reduce the

service span of the building, poor road networks to transport materials to the site, unavailability of skilled craftsmen, local building materials like clay suffer shrinkage and cracking. It was therefore recommended that the study of indigenous building materials should be introduced as apart of the curriclum for construction education in tertiary institutions, a sustainability knowledge in construction should be harmonized and embedded in various document, and should be developed in an integrated way across geographical boundaries and the designers should be encouraged to prepare designs that reflects an awareness of all the relationship that exists between the natural resources utilized in construction.

**References**

Abiola R. O. (2000) Management Implication of Trends in the Construction Cost in Nigeria From 1989-1999. The Quantity Surveyor, 30; 35-40

Adams, E. A. & Agib, A. R. A. (2001). Compressed Stabilized Earth Block Manufacture in Sudan. Printed by Graphorin for United Nations Educational Scientific and Culture Organization. France, Paris, UNESCO.

Anand, K. B. & Ramamurthy, K. (2003): Laboratory-based Productivity Study on Alternative Masonry System. *Journal of Construction Engineering and Management*, 241.

Azeta, J., Okokpujie, K. O., Okokpujie, I. P., Osemwegie, O., & Chibuzor, A. (2016). A Plan for Igniting Nigeria's Industrial Revolution. *International Journal of Scientific & Engineering Research*, *7*(11), 489.

Borg C. A. & Gall F. (1989). "Analysis of the method of research topics in a sample of the Brazililan distance education publications"

De-Boer, D. & Barieis, K. (2002). "Bamboo". In Elizabeth, Lynne; Adams, Cassandra (Eds.) "*Alternative Construction,: Contemporary Natural Building Method*". John Willy and Sons, New York, New York, USA.

Harrison, S. W. & Sinha, B.P. (1995) A study of alternative building materials and technologies for housing in Bangalore, *India Construction and Building Materials*, 9(4), 211-217(7).

Kareem, W. B, Ma'aji, S. A. Ibrahim, D. Gazali, S. A. and Shom, G. E. (2014). Investigation Of The Causes Of Building Failures In Nasarawa State, Nigeria. *Journal of Information, Education, Science and Technology (JIEST)*, 1(1); 195-204

Nwoke, O. N., Okokpujie, I. P., & Ekenyem, S. C. (2017). Investigation of Creep Responses of Selected Engineering Materials. *Journal of Science, Engineering Development, Environmen and Technology (JOSEDET)*, *7*(1), 1-15.

YEKINI, S. E., Okokpujie, I. P., Afolalu, S. A., Ajayi, O. O., & Azeta, J. (2018). Investigation of production output for improvement. *International Journal of Mechanical and Production Engineering Research and Development*, *8*(1), 915-922.